The Dissertation Committee for Lin Qu Certifies that this is the approved version of the following dissertation:

Evasion of RIG-I/MDA5 and TLR3-Mediated Innate Immunity by Hepatitis A Virus

Committee:

Stanley M. Lemon, M.D., Supervisor

Robert A. Davey, Ph.D.

Richard E. Lloyd, Ph.D.

Shinji Makino, D.V.M., Ph.D.

Steven A. Weinman, M.D., Ph.D.

_____

Dean, Graduate School

Evasion of RIG-I/MDA5 and TLR3-Mediated Innate Immunity by Hepatitis A Virus

by

Lin Qu

Dissertation

Presented to the Faculty of the Graduate School of

The University of Texas Medical Branch

in Partial Fulfillment

of the Requirements

for the Degree of

Doctor of Philosophy

The University of Texas Medical Branch

August, 2010

Acknowledgements

I first want to thank my supervisor Dr. Stanley Lemon for all his support, guidance and patience. His insightful advice and the research freedom I have enjoyed in his lab are essential for my development from a student to a scientist.

I would also like to thank Drs. Robert Davey, Richard Lloyd, Shinji Makino and Steven Weinman for serving on my supervisory committee and for their valuable input to my research.

I am grateful to the past and current members of the Lemon Lab, especially Dr. Yan Yang for initiating the MAVS project, Yuqiong Liang for many technical helps and know-how, and Dr. Zongdi Feng for collaboration on some of my projects. I would like to thank Drs, Kui Li, Minkyung Yi, David McGivern, Hisashi Ishida, Meital Guy-Tanamy, Seungtaek Kim, Tetsuro Shimakami, Hiromichi Dansako, and Daisuke Yamane for help with techniques and reagents and discussion on my research. I want to thank Teri Chapa for lab maintenance and Yinghong Ma for technical assistance. I also want to thank my fellow Ph.D. students in the Lemon Lab, Rohit Jangra, Carolyn Spaniel, and Gowri Devaraj, for sharing their graduate school experience with me.

I also want to thank the faculty, staffs and students at the Department of Microbiology and Immunology and Galveston National Laboratory that have helped me in my study and research.

I dedicate this work to my family for their spiritual support. I especially thank my wife Yipeng Wang, whose love and care sustained me through the years of my pursuit of Ph.D. This journey was marked by her cheers at every milestone I passed, and her encouragement at every setback I encountered. Now the finish line in sight, I am grateful to have her by my side and know that her love and trust will carry me to the next step.

Evasion of RIG-I/MDA5 and TLR3-mediated Innate Immunity by Hepatitis A Virus

Publication No._____

Lin Qu, Ph.D.

The University of Texas Medical Branch, 2010

Supervisor: Stanley M. Lemon

Since the identification of several families of pattern recognition receptors (PRRs), their roles in the innate immune system and how they are regulated by the invading pathogens have been the subjects of extensive research. Cellular helicases RIG-I and MDA5, and Toll-like receptor 3 (TLR3) are PRRs that detect virus-specific double stranded RNA (dsRNA). Activation of these PRRs by dsRNA lead to their interaction with adaptor proteins, which engage downstream kinases to activate two critical transcription factors, NF-κB and IRF3, in the induction of type I interferons (IFNs) and IFN-stimulated genes (ISGs) that ultimately establish an antiviral state. These signaling pathways are central to host antiviral defense and thus become targets for viral interference. Hepatitis A virus (HAV), a hepatotropic picornavirus, is capable of blocking IRF3 activation and type I IFN expression in cell culture, but the exact mechanism(s) remains undefined. Our studies revealed that HAV disrupts RIG-I/MDA5-mediated induction of type I IFN through proteolysis of MAVS, a mitochondrial-localized adaptor of RIG-I and MDA5, by the viral 3ABC protease precursor. The 3ABC cleavage of

MAVS requires both the protease activity of 3Cpro and a transmembrane domain in 3A that directs 3ABC to mitochondria. The signaling ability of MAVS depends on its mitochondrial localization; cleavage of MAVS by 3ABC removes MAVS from mitochondia, thus abolishing its adaptor function. We also demonstrated that the parallel, yet independent, TLR3 signaling pathway is also inhibited by HAV through cleavage of the adaptor protein TRIF by the 3CD protease-polymerase precursor. Cleavage of TRIF by 3CD requires both the protease activity of 3Cpro and the 3Dpol moiety, but not the 3Dpol polymerase activity, in an "*in cis*" manner. This research also revealed a unique order of processing in the 3CD cleavage of TRIF, and an unexpected role of the 3Dpol domain in modulating the substrate specificity of 3CD that allows it to cleave non-canonical 3Cpro cleavage sites within TRIF. The data generated in this dissertation provide two major mechanisms by which HAV evades innate immune responses, and extend our understanding of the signaling pathways of the innate immune system.

Table of Contents

List of Figures

Chapter 1: Introduction

1.1 Pattern Recognition Receptors (PRRs) and Adaptors in Antiviral Immunity

The ability of an organism to defend against invasion of pathogens depends on a functional immune system. The immune system of vertebrates consists of two arms, innate and adaptive, that work together to combat disease and infection. The innate immune system is quick acting and represents the first line of defense against invading pathogens. It is the major host defense against pathogens in nearly all living organisms. In contrast, the adaptive immune system is unique to vertebrates and is composed of highly specialized, systemic cells with the ability to remember specific pathogens in an antigen-specific fashion and mount stronger attack each time the pathogen is encountered. The innate immune system used to be considered ancient, non-specific, and overshadowed by the robustness and specificity of the adaptive immune system. However, recent research has revealed a broad spectrum of cellular receptors and their pathogen-associated ligands that demonstrate that innate immunity is just as specific and complex.

The innate immune system relies on several families of pattern recognition receptors (PRRs) that are capable of recognizing specific pathogen-associated molecular patterns (PAMPs) (4, 21, 47, 55, 75, 79). PAMPs range from bacterial and viral components to fungal and protozoal molecules, most of which are highly conserved and essential to pathogen replication and/or virulence. Recognition of PAMPs by PRRs triggers signaling pathways that emanate from these receptors and ultimately leads to the transcription of interferons and inflammatory cytokines involved in host defense. There are three major PRR families: the cytoplasmic RIG-I-like helicases (RIG-I and MDA5) (79, 194), Toll-like receptors (TLRs) (4, 55, 75), and the nucleotide-binding domain and

leucine-rich repeat (NLR) proteins (21, 47). Here I will review more in detail RIG-I, MDA5, TLR3 and their signaling pathways, as they are the main focus of my Ph.D. studies.

RIG-I-like helicases. The RIG-I-like RNA helicases represent a family of PRRs that survey the cytoplasm of cells and sense viral infection by the detection of double-strand RNA (dsRNA). This family of strictly intracellular PRRs consists of three members: retinoic acid inducible gene I (RIG-I), melanoma differentiation associated gene 5 (MDA5), and laboratory of genetics and physiology 2 (LGP2) (76, 85, 147, 193). All three of these proteins contain a DExD/H box RNA helicase domain that binds and unwinds dsRNA in an ATP-dependent manner (194). RIG-I and MDA5 also contain caspase recruitment domains, or CARD domains (7, 193-194) (Fig. 1.1). Often found in proteins involved in inflammation and apoptosis, CARD domains mediate the formation of large protein complexes via direct interactions between individual CARDs (72). Activation of RIG-I also requires the CARD domain to be polyubiquitinated through lysine 61 (K61) of ubiquitin (197). Binding of RIG-I or MDA5 with dsRNA sets off signaling cascade that culminates in the induction of type I interferons (IFNs), such as IFN-α and IFN-β (76, 193-194). *In vitro* studies showed that RIG-I prefers RNA that has triphosphate at the 5' end and dsRNA that is relatively short (65, 77, 132, 146, 148), whereas MDA5 recognizes long dsRNA but does not discern 5' triphosphate (53, 77, 146). This distinct ligand preference seems to correlate with specific recognition of individual viruses. Analysis of the corresponding knockout mice revealed that RIG-I is activated by certain flaviviruses, vescular stomatitis virus (VSV), Sendai virus and influenza A virus (78, 102, 163), whereas MDA5 mediates innate responses to picornaviruses and caliciviruses (53, 111).

The third member of the family, LGP2, does not contain CARD domain and was originally identified as a negative regulator of RIG-I signaling (147, 193). However, studies on LGP2 knockout mice showed that LGP2 is required for MDA5 response to picornaviruses (151, 176). Thus it may play a dual role in regulating the functions of RIG-I and MDA5.

MAVS: the adaptor of RIG-I and MDA5. In 2005 four independent groups simultaneously discovered a CARD-containing protein that serves as the adaptor of RIG-I/MDA5 signaling (80, 115, 156, 184). It was named the mitochondrial antiviral signaling protein (MAVS), also known as IPS-1, VISA or Cardif. In addition to an N-terminal CARD domain, MAVS also contains a proline-rich region and a C-terminal transmembrane (TM) domain (156) (Fig. 1.1). Upon viral challenge, the CARD of MAVS associates with the CARDs of RIG-I or MDA5. MAVS localizes to mitochondrial outer membrane via its C-terminal TM domain (96, 156). For an yet unknown reason, this location is essential for the signaling ability of MAVS, as deletion of the TM domain or re-targeting of MAVS to other cellular membranes such as the endoplasmic reticulum (ER) completely abolished RIG-I/MDA5 signaling (156). This discovery, for the first time, linked mitochondria to antiviral IFN responses and identified a new intracellular surface for the assembly of cytoplasmic RIG-I/MDA5 signaling complexes. The role of mitochondria in RIG-I signaling was further supported by a recent study showing that RIG-I signaling pathway can be reconstituted in a system composed of RIG-I, 5' triphosphate RNA, cytosol and mitochondria (197).

MAVS-dependent signaling requires the tumor necrosis factor (TNF) receptor-associated factor (TRAF) family members. Proteins of this family are defined by a TRAF domain responsible for interaction with TNF family receptors and other adaptors and kinases (177). MAVS contains a binding site for TRAF6 (184). TRAF6 is a RING

domain ubiquitin ligase involved in activation of the canonical IκB kinase (IKK) complex consisting of IKKα, IKKβ and IKKγ (also known as NEMO), leading to phosphorylation and degradation of the inhibitor of NF-kB (IκB), which releases NF-kB and allows its nuclear translocation (26, 34, 90). The proline-rich region of MAVS also contains a TRAF3-binding site that is essential for association with TRAF3 and TRAF3-mediated activation of non-canonical IKKs, including TBK-1 and IKKi, leading to phosphorylation, dimerization, and nuclear translocation of interferon regulatory factor 3 (IRF3) (125, 166). Thus, the RIG-I/MDA5-mediated signal is bifurcated by MAVS into parallel pathways activating NF-κB and IRF3, two critical transcription factors for the full induction of type I IFNs.

Toll-like receptor 3 (TLR3). TLRs were the first family of receptors identified that fit the PRR model. Toll was originally discovered in fruit fly *Drosophila melanogaster* as a protein that proved to be involved in both early development and insect immunity (6). This led to the search of TLRs in other species. To date, 10 TLRs have been identified in the human genome (30-31, 37, 113, 143, 170). TLRs are characterized as type I transmembrane proteins with an extracellular leucine-rich repeat (LRR) domain, a transmembrane region, and an intracellular Toll/IL-1 receptor (TIR) domain (1-3). The LRRs act as the ligand recognition domain, while the TIR domain mediates signal transduction via interaction with TIR domain-containing adaptors (1-3). In contrast to the cytoplasmic RIG-I-like helicases, TLRs are located at the cell surface or within endosomal compartments (48, 110). TLRs are activated in response to a broad variety of pathogen-associated molecular patterns including: lipopeptide by TLR1 (171), lipoarabinomannan by TLR2 (154, 168, 195), dsRNA by TLR3 (5, 112), lipopolysaccharide by TLR4 (66, 98, 133), flagellin by TLR5 (60), lipoprotein by TLR6

(169), ssDNA by TLR7 and TLR8 (36, 61, 106), CpG-rich DNA by TLR9 (62), and many more.

TLR3 recognizes viral double-stranded RNA (dsRNA) (5, 112). During replication of RNA viruses, dsRNA is produced as a replication intermediate or part of the viral RNA genome (67). DNA viruses may also produce RNA transcripts that engage TLR3, as macrophages lacking the TLR3 adaptor protein TRIF (see review below) are more susceptible to vaccinia virus (63). Poly(I:C) is a stable, synthetic dsRNA analogue that is often used as a surrogate TLR3 ligand to mimic viral infection. TLR3-deficient mice showed reduced production of inflammatory cytokines in response to poly(I:C) and were resistant to lethal doses of poly(I:C) (5). TLR3 has been implicated in clearance of virus and protection of host from pathological development of the infection, while in other cases it contributes to the debilitating effects of a host inflammatory response (38, 165). For example, TLR3-deficient mice infected with influenza A virus showed higher virus production in the lungs, but had a better survival rate than wild-type mice due to reduced inflammation (91). Whether TLR3 plays a protective or detrimental role in viral infection and disease seems to depend on factors such as the type of virus, stage of infection and the cell type that is infected.

Like all other members of the TLR family, TLR3 is a type I transmembrane protein (Fig. 1.1). Its extracellular domain consists of 23 LRRs forming a horseshoe-shaped structure that is heavily glycosylated (11, 28). Its cytoplasmic TIR domain contains a highly conserved BB loop that is described for all TLRs to interact with adaptor molecules (185). Although TLR3 is monomeric in solution, it readily forms a dimer when embedded in membrane and undergoes multimerization upon binding with dsRNA (10-11). Consistent with this, studies using different lengths of poly(I:C) indicated that longer poly(I:C) induces stronger TLR3 signaling (33, 126).

TRIF: the adaptor of TLR3. The TLRs mediate their signals via adaptor proteins of which there are five, namely MyD88, MyD88-adaptor like (Mal, also known as TIRAP), TIR domain-containing adaptor inducing IFN-β (TRIF, also known as TICAM-1), TRIF-related adaptor molecule (TRAM, also known as TICAM-2), and sterile α and armadillo motif-containing protein (SARM) (123-124). Each of these molecules contains a TIR domain and interacts with defined TLRs via TIR-TIR interaction (18). MyD88 is the central adapter molecule interacting with all TLRs except TLR3 (167, 186). Upon ligand activation, MyD88 recruits members of the IRAK family and TRAF6, leading to activation of NF-κB and production of pro-inflammatory cytokines including IL-1β, TNF-α and IL-18 (121-122, 178). The second adaptor molecule, Mal, is believed to act as a bridging adaptor between TLR4, TLR1/2, TLR2/6 and MyD88 (46, 187). TRIF mediates TLR3 and MyD88-independent TLR4 signaling (127, 186). Whereas TRAM is thought to act as a bridging adaptor between TRIF and TLR4 (144, 188), TRIF interacts directly with TLR3 (127, 186). Activated TRIF recruits kinases TBK1 and IKKi, which mediate IRF3 phosphorylation, dimerisation and nuclear translocation leading to type I IFN induction (59, 150). TRIF also interacts with TRAF6 and receptor-interacting protein 1 (RIP1) which mediate NF-κB activation (114, 150). The fifth adaptor, SARM, is a negative regulator of TRIF (22).

TRIF is a cytoplasmic protein composed of an N-terminal region that contains binding sites for TBK-1 and TRAF2, 3 and 6, a central TIR domain that interacts with the TIR domain of TLR3, and a C-terminal RIP homotypic interaction motif (RHIM) (127, 149-150). These domains play essential roles in TRIF-mediated activation of two distinct transcription factors, IRF3 and NF-κB, in the induction of type I IFN and IFN-stimulated genes (ISGs) (74, 127, 149-150). Activation of IRF3 requires both the N-terminal region and the TIR domain, whereas activation of NF-κB can be accomplished by two

independent mechanisms: one through the N-terminal region and the TIR domain, or alternatively through the C-terminal region including the RHIM domain (49, 74, 150). Studies showed that TRIF-mediated activation of IRF3 and NF-κB depends on homo-oligomerization of TRIF, which is mediated independently by two regions of TRIF: the TIR domain and the C-terminal region (49). This may partially explain why NF-κB can be activated by two independent regions of TRIF. Again, by a mechanism analogous to the RIG-I/MDA5-MAVS axis, TRIF mediates the divergence of TLR3 signal into independent pathways leading to activation of IRF3 and NF-κB (71).

TRIF also induces apoptosis, a unique capacity among the five TLR adaptor molecules (59, 74). The apoptotic potential of TRIF was mapped to the C-terminal RHIM domain, which interacts with the RHIM-containing receptor interacting protein 1 (RIP1) and RIP3, two members of the RIP kinase family (74, 116). Although RHIM is also involved in NF-κB activation, its ability to induce apoptosis is not directly linked to NF-κB, as an IκBα-super suppressor (SR) blocked RHIM-dependent NF-κB activation without preventing apoptosis (74). RIP1, but not RIP3, contains a death domain (DD) that can complex with FADD and activate the FADD-caspase 8 extrinsic apoptosis pathway (as opposed to the mitochondrial intrinsic apoptosis pathway) (58, 164). Although both RIP1 and RIP3 interact with TRIF through the RHIM domain, RIP1 is essential for TRIF-mediated NF-κB activation, whereas RIP3 suppresses this function (114). Whether this is also the case for TRIF-induced apoptosis, or RIP3 blocking of NF-κB activation is required for RIP1 to switch to induction of apoptosis remains to be investigated.

1.2 Viral Evasion of PRR-Mediated Innate Immunity

RIG-I/MDA5 and TLR3-mediated signaling pathways leading to the induction of type I IFNs and IFN-stimulated genes (ISGs) are essential to the establishment of a host antiviral state, and therefore not surprisingly become the target of interference by viruses.

The various counteracting mechanisms developed by viruses attest to the importance of these signaling pathways in innate antiviral response. Almost every step of the signaling pathways leading to activation of NF-κB and IRF3 can be blocked by various viruses as a means of escaping the host innate immunity. The following are some examples of these immune evasion mechanisms.

Paramyxovirus V proteins bind MDA5, but not RIG-I. Members of the Paramyxoviridae family include single, negative-strand RNA viruses such as measles, mumps, parainflunza viruses (PIV) of human, Newcastle disease virus (NDV) of birds, Sendai virus (SeV) of rodents, and simian virus 5 (SV5) that infect monkeys, dogs, pigs and human. Some of these viruses do not block the pathways leading to induction of IFN-α/β, but rather disrupt the IFN signaling pathway, also known as the JAK/STAT pathway (56). The SV5 V protein targets the signal transducer and activator of transcription 1 (STAT1) for degradation (35), whereas the SeV C protein interferes with STAT phosphorylation or stability (51-52). Two recent studies showed that the V proteins from some paramyxoviruses such as SV5, PIV2, mumps virus, SeV, and Handra virus bind MDA5 and inhibit its ability to induce IFN-β (7, 27). The interaction occurs between the cysteine-rich C-terminal domains of the V proteins and the DExD/H RNA helicase domain of MDA5, thereby blocking the binding of MDA5 with its RNA ligand (7). These V proteins, however, do not bind or inhibit the structurally and functionally related helicase RIG-I (27). These findings implicated MDA5 in the containment of paramyxovirus infection, which was later confirmed by an *in vivo* study using MDA5 knockout mice (54).

Respiratory syncytial virus NS2 protein targets RIG-I. The nonstructural NS1 and NS2 proteins of respiratory syncytial virus (RSV), also a member of the paramyxovirus family, have been shown to block IFN signaling by mediating

proteasome-dependent degradation of STAT2 (101, 138-139). In addition, RSV mutants lacking NS1 or NS2 induce more IFN than wild-type virus in infected cells (159), indicating that NS1 and NS2 also inhibit induction of IFN. A recent study showed that NS2 does so by interacting with RIG-I (99). Unlike the V proteins from other paramyxoviruses that bind to the helicase domain of MDA5 (7), NS2 binds to the CARD domain of RIG-I and inhibits its interaction with the CARD of the downstream adaptor protein MAVS (99). NS2 is thus a multifunctional IFN inhibitor that targets specific components of both IFN induction and IFN signaling pathways.

The TIR domain-containing protein A46R of vaccinia virus targets TLR adaptors. Vaccinia virus (VV), a DNA virus classified in the poxvirus family and used to vaccinate against smallpox, encodes a range of proteins that antagonize important components of the host antiviral response. The A46R protein of VV contains a TIR domain and is the only viral member of the TIR family identified to date (160). Through homotypic TIR interaction, A46R interact with four TLR adaptors, namely MyD88, Mal, TRIF and TRAM, and thereby interferes with downstream activation of NF-κB (17, 160). A46R particularly associates with TRIF and disrupts TRIF-mediated activation of IRF3 by either TLR3 or TLR4 pathway (160). Interestingly, A46R does not interact with the fifth TLR adaptor protein, SARM, which is a negative regulator of TRIF (22, 160). A46R is expressed early during infection (160) and its ability to antagonize TLR adaptors suggests a role in evasion of host initial antiviral responses. A VV deletion mutant lacking the A46R gene was attenuated in an animal model, further confirming the importance of A46R in blunting the host immune system (160).

Hepatitis C virus NS3/4A protease cleaves MAVS and TRIF. Hepatitis C virus (HCV) is a positive-strand RNA virus belonging to the Flaviviridae family. HCV infects over 170 million people worldwide and ~75% of infected individuals develop chronic

infection (140). Chronic hepatitis due to HCV is associated with cirrhosis and liver cancer, and is the leading cause of liver transplantation in the U.S. (137). The tendency of HCV to establish persistent infection is unique among positive-strand RNA viruses. Although HCV persistence is a result of multiple factors, the ability of the virus to evade early innate immune responses is believed to be particularly important (136). The viral-encoded NS3/4A serine protease plays an essential role in processing of the HCV polyprotein and viral RNA replication (16, 88). Recent studies showed that NS3/4A also proteolytically cleaves MAVS and TRIF, the adaptors of RIG-I/MDA5 and TLR3, respectively (44, 95-96, 103, 115) (Fig. 1.1). Cleavage of MAVS by NS3/4A occurs close to the transmembrane domain, resulting in the release of MAVS from the mitochondrial membrane, a location that is essential for MAVS to be able to assemble the signaling complex (96, 103, 115). This results in blocking of the downstream activation of IRF3 and NF-κB (96, 115). Similarly, cleavage of TRIF by NS3/4A destroys the link between TLR3 and kinases responsible for IRF3 and NF-κB activation (44, 95). HCV thus disrupts both RIG-I/MDA5 and TLR3 signaling pathways by targeting the adaptor proteins for proteolysis, a strategy that I have later found to be shared by hepatitis A virus (HAV), another hepatotropic positive-strand RNA virus (see Chapters 2 and 3).

IRF3 is targeted by different viral proteins. The transcription factor IRF3 plays a central role in the induction of type I IFN and ISGs. Thus, inhibition of IRF3 activation is an efficient way to disrupt IFN responses. In this respect, many viruses have evolved mechanisms that directly target IRF3. The Npro proteins from pestiviruses such as classical swine fever virus (CSFV) and bovine viral diarrhea virus (BVDV) interact with IRF3 and induce its ubiquitination and proteasomal degradation (9, 25, 89). As opposed to degradation, ubiquitination of IRF3 is also required for its nuclear translocation (199). The nonstructural protein NSP3 of mouse hepatitis virus A59 (MHV-A59), which

contains a papain-like protease domain 2 (PLP2) with deubiquitinase (DUB) function, binds to IRF3 and causes its de-ubiquitination to prevent its nuclear translocation, thereby inhibiting type I IFN production (199). Some viral proteins, such as the V proteins of mumps virus, human parainfluenza virus 2 (hPIV2) and parainfluenza virus 5 (PIV5), do not directly interact with IRF3, but act as alternative substrates that compete with IRF3 in its phosphorylation by kinases IKKi and TBK-1 (105). As these V proteins also target the JAK/STAT signaling pathway and interact with MDA5 (7, 56, 94), they seem to be multifunctional IFN antagonists that interfere with different steps of the MDA5 pathway leading to IRF3 activation.

1.3 Hepatitis A Virus (HAV)

Hepatitis A virus (HAV) is a small, non-enveloped, positive-strand RNA virus classified in the Hepatovirus genus of the Picornaviridae family. The same family also includes other important human and animal pathogens such as poliovirus, rhinovirus, and foot-and-mouth disease virus (FMDV). HAV is transmitted via the fecal-oral route and causes acute viral hepatitis (45). The host range of HAV is limited to human and certain nonhuman primates. Symptoms may range from a mild illness to a severely disabling disease, and often include fever, nausea and abdominal discomfort, followed within a few days by jaundice (82). HAV infection is more common throughout the developing world than in developed countries, but community-wide outbreaks still occur in some areas of the United States (81).

Natural infection with HAV usually follows oral exposure to contaminated food or water (45). The early phase of infection prior to the entry into liver is poorly understood. HAV enters the hepatocytes via membrane proteins including the hepatitis A virus cellular receptor 1 (HAVCR1) and TIM-3 (42, 158, 162, 175), although the exact mechanism is still not fully characterized. The natural ligand of HAVCR1 is

immunoglobin A (IgA), and the association of IgA with HAVCR1 enhances HAV-receptor interactions (172). Viral replication takes place during a clinically silent period of 3-5 weeks following initial infection. This period is characterized by the presence of large quantities of virus in the bile and feces, and a low level of viremia, prior to the appearance of HAV-specific antibodies, hepatic inflammation accompanied by elevation of serum ALT (alanine aminotransferase), and infiltration of immune cells into the liver (92). It is generally believed that liver damage is more the result of host immune response than the direct cytopathic effect of HAV on hepatocytes. Except for rare cases of fulminant hepatitis, the vast majority of patients with hepatitis A have a self-limited infection that resolve completely, resulting in life long immunity. Unlike HBV and HCV, HAV never progresses to chronic infection.

HAV genome and polyprotein processing. HAV is believed to replicate by mechanisms similar to those of other picornaviruses (108). The genome of HAV is about 7,500 nucleotides in length, possesses a Vpg peptide covalently linked to the 5' terminal nucleotide and terminates with a poly(A) tail (Fig. 1.2). The genome encodes a single long open reading frame flanked by 5' and 3' nontranslated regions (NTRs) (20). The positive-strand RNA genome initially serves as messenger RNA for translation. Translation is cap-independent and mediated by an internal ribosome entry site (IRES) in the 5' NTR (20, 23). The resulting polyprotein is processed by a cascade of proteolytic cleavages that first give rise to three large polypeptide segments, P1-2A, P2 and P3, which are further processed into individual proteins (73, 86, 135, 153, 173). The P1-2A segment encodes structural proteins VP4, VP2, VP3, and VP1-2A, which form the virus particle via intrinsic packaging signals located within VP4 and 2A (107, 134). The P2 segment encodes proteins 2B and 2C, of which 2C contains motifs characteristic of an NTPase, while 2B and the precursor 2BC may be involved in directing rearrangement of

intracellular membranes essential for viral RNA replication (69, 174). Mutations in 2B and 2C are involved in adaptation of HAV to growth in cell culture (40-41, 192). The P3 segment encodes proteins 3A, 3B, 3C, and 3D. Among them, 3A is the membrane anchor that attaches 3B and associated proteins to the membrane (13, 32, 131). 3B, also known as VPg, functions as peptide primer for viral RNA synthesis and is covalently linked to the 5' end of genomic RNA (180). 3Cpro is the only viral-encoded cysteine protease and is responsible for most cleavages within the polyprotein (68, 86, 135, 153, 173), except for the VP1/2A which is catalyzed by an unknown cellular protease (107), and the VP4/VP2 "maturation cleavage" which is not well understood but believed to be RNA-dependent (15). 3Dpol is the RNA-dependent RNA polymerase (83, 173). The nonstructural proteins from the P2 and P3 regions are believed to form the RNA replication complex which synthesizes a negative-strand RNA based on the viral genome and uses it as a template to produce viral genome progenies (191). The newly synthesized viral RNA genomes are assembled with structural proteins into virus particles, secreted from the infected hepatocytes, and transported to the intestine via the bile (108).

As a common feature of picornaviruses, incomplete processing of the polyprotein results in an array of intermediate precursors in addition to the mature products (Fig. 1.2). These intermediate precursors often have functions distinct from their mature products and play important roles in viral replication and virus-host interaction. For example, the poliovirus 3CD protein functions as a protease with much higher activity than the mature 3Cpro in most polyprotein processing cases and is involved in RNA replication (128-129, 196). The enhanced protease activity of poliovirus 3CD is due to modulation by the 3Dpol domain (128) In the case of HAV 3AB precursor, 3A, which contains a transmembrane domain, tethers the 3B (Vpg) peptide to the intracellular membrane where it serves as the primer for RNA synthesis (32, 87). Other precursors, such as 3ABC

and 3CD, have distinct functions from the mature 3Cpro protease (190) and are the focus of this research.

HAV and HCV. HAV and HCV both have strong tropism for the liver and both cause acute viral hepatitis, but only HCV has the ability to develop chronic infection. Both viruses are positive-strand RNA viruses with genomes encoding a single large polyprotein that is processed by viral or host proteases into structural and nonstructural proteins. Despite a number of important differences, HAV and HCV share a similar genome structure (Fig. 1.3) and have many features in common in their replication cycles. Both viruses utilize an IRES in the 5' nontranslated region to drive translation of the polyprotein, and both replicate their RNA within cytoplasmic, membrane-bound replication complexes. In contrast to HCV, HAV lacks a lipid envelope, and 5' nucleotide of its RNA genome is covalently linked to a small viral pepetide 3B (also known as Vpg) (180), as opposed to the 5' triphosphate of HCV genome. The presence of 5' Vpg in the genomes of HAV and other picornaviruses suggests that they are not likely to be sensed by the cellular helicase RIG-I, which recognizes 5' triphosphate RNA such as that of HCV (65, 77, 132, 146, 148). Instead, picornaviruses and the related caliciviruses (also contain 5' Vpg) are believed to be recognized by the related helicase MDA5 (53, 111).

In contrast to HAV which only causes acute infection, HCV establishes long-term persistent infections in the majority of infected individuals that have normal immune systems. The mechanisms of HCV persistency have not been fully understood, but are believed to involve both innate and adaptive immunity malfunctions. In the case of HAV infection, T cell responses are believed to be the main force of viral clearance, while B cell responses are responsible for maintaining a life-long immunity after the recovery. For HCV infection, T cell responses are critical in determining whether an acute infection becomes cleared or persistent. This is supported by studies showing that if chimpanzees

that had successfully cleared a previous HCV infection were depleted of memory CD4+ helper or CD8+ cytotoxic T cells and re-challenged with the same virus, they developed persistent infection (57, 157). The role of B cell immunity in HCV infection is less understood, and clearly less important than in HAV infection.

Given the many common features between HAV and HCV, and their sharp differences in clinical outcomes, we believe that an in depth comparison of the innate and adaptive immune responses to HAV and HCV should provide insights into why HCV can establish persistent infection, while HAV is always cleared after acute infection. We are particularly interested in the innate signaling pathways, which are important for early induction of type I interferons and also shape the outcomes of subsequent adaptive T and B cell immunity. As reviewed above, HCV is known to disrupt both RIG-I and MDA5 signaling pathways by cleavage of the adaptor proteins MAVS and TRIF, respectively (44, 95-96, 103, 115). It remains unclear how HAV interacts with these signaling pathways.

Although HAV is always cleared by the host immune system, its ability to replicate efficiently within the liver and produce large amount of viral progenies prior to the onset of immune responses suggests that it may be capable of evading the early innate immunity. Indeed, two recent studies demonstrated that HAV is also capable of blocking RIG-I-mediated IRF3 activation and IFN-β expression in cell culture (19, 43). In particular, HAV disrupts signal transduction between RIG-I/MDA5 and the downstream kinases (43), most likely at the level of MAVS which is the adaptor of RIG-I and MDA5. However, evidence is needed to prove this hypothesis. HAV was also shown to partially block IFN-β expression induced by overexpression of TRIF, the adaptor of TLR3, in FRhK-4 cells (43). Since FRhK-4 is TLR3-deficient and overexpression of TRIF is an indirect way to activate TLR3 pathway, whether HAV can block TLR3 signaling remains

unclear. These incomplete data and unanswered questions set the stage for my research to uncover the mechanisms by which HAV evades the RIG-I/MDA5 and TLR3-mediated innate immunity.

Figure 1.1: Sensing of viral dsRNA by RIG-I/MDA5 and TLR3.[1]

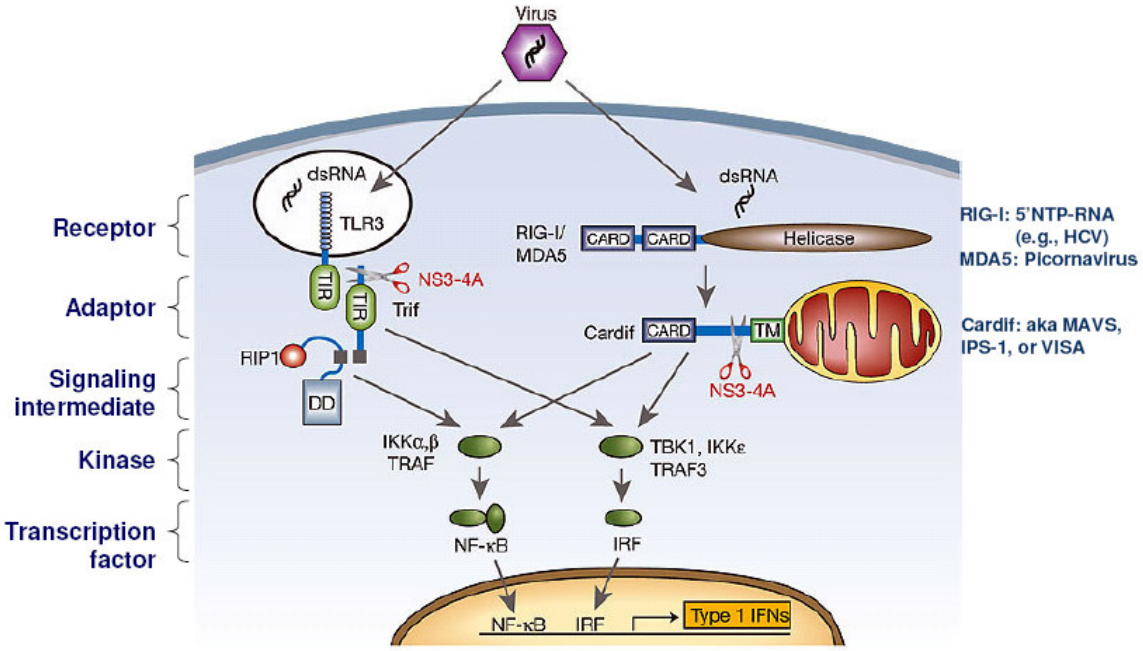

Adapted from Meylan, Nature, 2006

[1] Adapted by permission from Macmillan Publishers Ltd: Intracellular pattern recognition receptors in the host response. Meylan E, Tschopp J, Karin M. Nature. 2006 Jul 6;442(7098):39-44. Copyright (2006). Reference (118). Permission granted through a License Agreement between Lin Qu and Nature Publishing Group (License Number 2463281021290. License date Jul 6, 2010).

Figure 1.2: HAV genome and polyprotein processing.

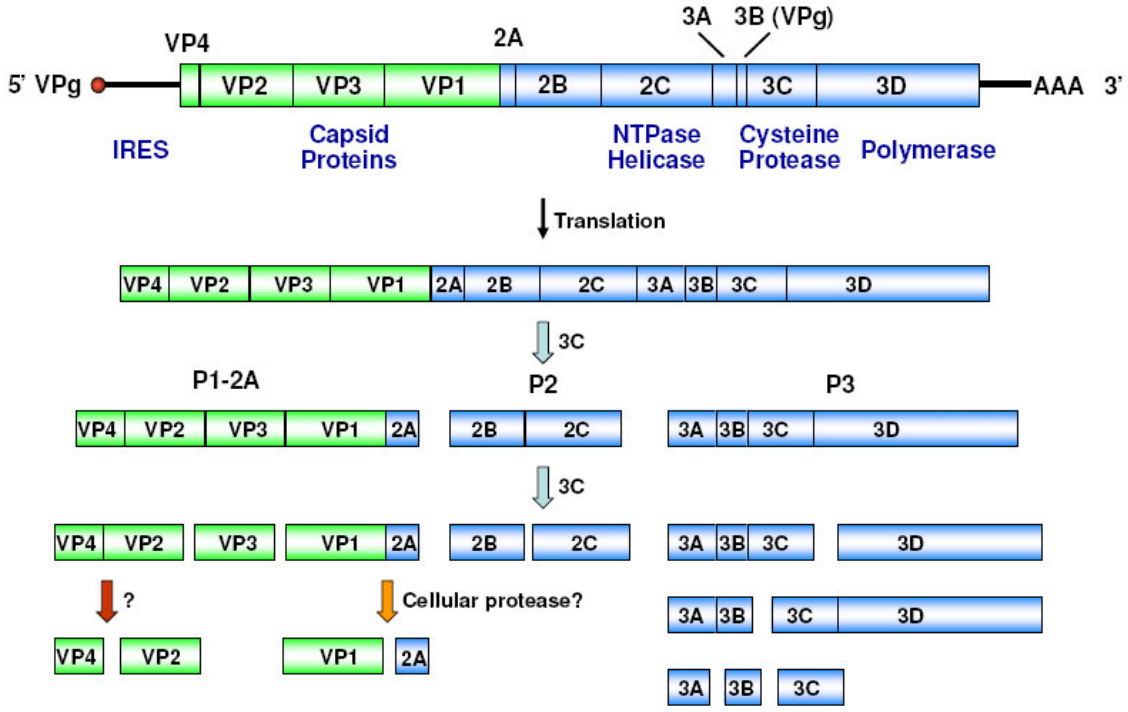

Figure 1.3: Comparison of HAV and HCV genome structures.

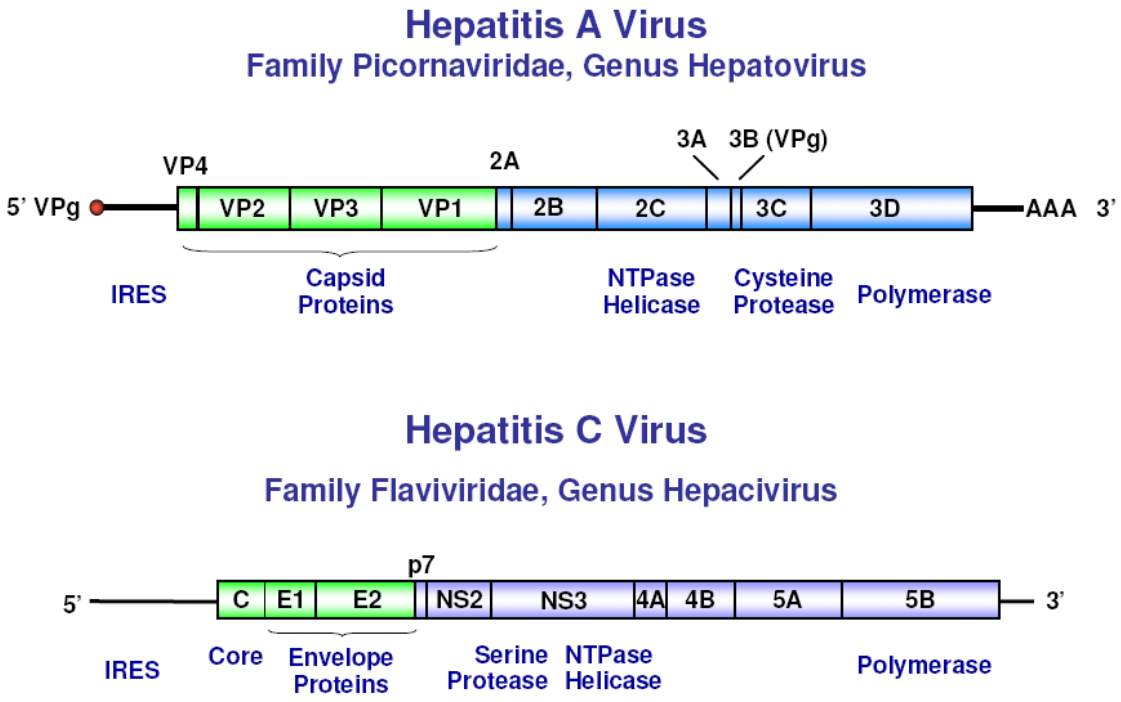

Chapter 2: Disruption of Innate Immunity due to Mitochondrial Targeting of a Picornaviral Protease Precursor[2]

2.1 Abstract

Mitochondrial antiviral signaling protein (MAVS) is an essential component of virus-activated signaling pathways that induce protective interferon responses. Its localization to the outer mitochondrial membrane suggests an important yet unexplained role for mitochondria in innate immunity. Here, we show that hepatitis A virus (HAV), a hepatotropic picornavirus, ablates type 1 interferon responses by targeting the 3ABC precursor of its 3Cpro cysteine protease to mitochondria where it colocalizes with and cleaves MAVS, thereby disrupting activation of IRF3 through the MDA5 pathway. The 3ABC cleavage of MAVS requires both the protease activity of 3Cpro and a transmembrane domain in 3A that directs 3ABC to mitochondria. Lacking this domain, mature 3Cpro protease is incapable of MAVS proteolysis. HAV thus disrupts host signaling by a mechanism that closely parallels that of the serine NS3/4A protease of hepatitis C virus, but differs in its use of a stable, catalytically active processing intermediate. Moreover, the unique requirement for mitochondrial localization of 3ABC underscores the importance of mitochondria to host control of virus infections within the liver.

[2] Part of this chapter was published on the Proceedings of the National Academy of Science of the United States of America: Disruption of innate immunity due to mitochondrial targeting of a picornaviral protease precursor. Yang Y, liang Y, Qu L, Chen Z, Yi M, Li K, Lemon SM. Proc Natl Acad Sci U S A. 2007 Apr 24; 104(17): 7253-7258. Epub 2007 Apr 16. Reference (190). PNAS authors need not obtain permission to include their papers as part of their dissertations (http://www.pnas.org/site/misc/rightperm.shtml) (2010).

2.2 Introduction

Mammalian cells have evolved complex and effective mechanisms to sense and defend against invading viruses. Toll-like receptor 3 (TLR3), retinoic acid-inducible gene I (RIG-I), and melanoma differentiation-associated gene 5 (MDA5) are pathogen-associated pattern recognition receptors that sense the presence of RNA viruses and stimulate signaling pathways that lead to induction of an antiviral state (117). The engagement of RIG-I and MDA5, caspase-recruitment domain (CARD)-containing DExD/H RNA helicases (7, 193-194), by viral RNA leads to complex formation with mitochondrial antiviral signaling protein (MAVS, also known as IPS-1, VISA or Cardif) (80, 115, 156, 184). MAVS is a unique adaptor protein that is localized to the outer mitochondrial membrane through a C-terminal transmembrane domain (156). For unknown reasons, this membrane association is crucial to its ability to signal to downstream kinases, IKKε and Tank-binding kinase 1 (TBK1), responsible for the phosphorylation and activation of interferon regulatory factor 3 (IRF3). The phosphorylation of IRF3, a constitutively-expressed latent cytoplasmic transcription factor, leads to its dimerization and relocalization to the nucleus where it induces interferon (IFN)-β transcription in association with the transcription factors p300/CBP and NF-κB (64).

IRF3 is central to type 1 IFN responses, and many viruses have evolved mechanisms that disrupt its activation. Hepatitis C virus (HCV), an hepatotropic human flavivirus, expresses a serine protease, NS3/4A, that disrupts the virus activation of IRF3 by proteolytically targeting MAVS, preventing signaling to IRF3 from the RIG-I receptor (96, 103, 115). This block at a proximal point in the signaling pathway also inhibits activation of NK-κB. NS3/4A also cleaves the TLR3 adaptor protein, TRIF, disrupting dsRNA signaling to IRF3 and NF-κB through this pathway as well (95). While the role of

TLR3 signaling remains uncertain, RIG-I appears to be the major pathogen recognition receptor for intracellular HCV RNA (163). The disruption of RIG-I signaling by HCV may significantly attenuate host innate responses, and has been suggested to contribute to the unique capacity of HCV to establish persistent infections (50).

Hepatitis A virus (HAV) provides a striking contrast to HCV in terms of its natural history. Also a positive-strand RNA virus, but classified within the family Picornaviridae rather than the Flaviviridae, HAV, like HCV, has strong tropism for the human hepatocyte. However, HAV is incapable of establishing persistent infection and is always eliminated by host defenses. Nonetheless, recent reports indicate that HAV also is capable of blocking RIG-I mediated IRF3 activation and IFN-β expression (19, 43). However, the mechanism underlying this interference with innate immune signaling has not been defined. We show here that HAV infection strongly down-regulates the expression of MAVS, ablating signaling through the MDA5 pathway. In a remarkable parallel to HCV, a stable intermediate product of HAV polyprotein processing, 3ABC, targets MAVS for proteolysis. MAVS cleavage requires a transmembrane domain in 3A that directs 3ABC to mitochondria, a surprising feature of the 3ABC protease that is unique to HAV among picornaviruses.

2.3 Materials and Methods

Cells and Viruses Fetal rhesus monkey kidney cells (FRhK-4), human embryonic kidney (HEK) 293, Huh7 human hepatoma cells, and Huh7-derived HAV-Bla, and Bla-C cells were cultured in DMEM with 10% FBS. The HAV-Bla cell line harboring the subgenomic HAV replicon RNA was established by electroporation of Huh7 cells with RNA transcribed in vitri from pHAV-Bla, followed by selection with 2 μg/ml blasticidin. These cells were subsequently maintained in media containing 2 μg/ml blasticidin, but blasticidin-free medium was used for all transfection experiments. Bla-C is a cell line

derived from HAV-Bla cells in which the HAV replicon was eliminated by treatment with IFN-α 2b (Sigma), 500 unites/ml for 4 wks, in the absence of blasticidin. These cells do not contain detectable HAV RNA, and none survive when cultured in the presence of blasticidin. HM175/18f, a cell culture-adapted, cytopathic variant of the HM175 strain of HAV was propagated in FRhK-4 cells and infectivity quantified by an immunofocus assay (93). Sendai virus was purchased from Charles River Laboratories.

Plasmids pHAV-Bla contains a cDNA copy of a subgenomic HAV replicon in which an in-frame substitution of most of the P1 (capsid protein-coding) sequence of pHM175/18f (GenBank accession M59808) (198) has been replaced with sequence encoding blasticidin. It was constructed by an approach similar to that described for pHAV-Luc (192). Briefly, a unique *Stu*I restriction site was engineered into pHM175/18f at nt 843, and a PCR-amplified segment encoding the blasticidin resistance gene flanked by the relevant restriction sites was inserted in-frame between the *Stu*I site and *Sac*I site existing within the VP1 region.

The cDNA sequences of HAV proteins and protein precursors were amplified by PCR from the plasmid pHM175/18f (198) and cloned into the pCMV-4a (Stratagene) and pCMV-HA (Clontech) expression plasmids such that the carboxyl-terminal Flag and amino-terminal HA tags, repectively, were fused in-frame to the HAV proteins. 3ABCD cDNA was also cloned into pcDNA3.1/V5-His TOPO (Invitrogen) with the V5-tag fused in-frame to the carboxyl terminus of 3ABCD. Expression vectors for human MAVS and GFP-MAVS have been described previously (156), as have pcDNA6-NS3/4A and the related pcDNA-NS3/4A-S139A mutant (95). Other plasmids were generous gifts: pIFN-β-Luc from Rongtuan Lin (McGill University); p(PRDIII-I)4-Luc from Christina Ehrhardt (Heinrich-Heine-Universitat); pEFTak IPS-1, pISG56-Luc and pPRD-II-Luc from Michael Gale (UT Southwestern Medical Center); pEF-Flag-N-RIG and pEF-Flag-

MDA5-N from Takashi Fujita (Kyoto University); pCDNA3-FlagIKKε from Tom Maniatis (Harvard University). pRL-CMV, pRL-TK (Promega) or pCMV-βGal (Clontech) were used as transfection controls.

Plasmids expressing 3ABC and MAVS mutants were generated by site-directed mutagenesis using the QuickChange kit (Stratagene) according to the manufacturer's instructions. In the 3ABC-C172A mutant, the active site nucleophile, Cys-172 in the 3Cpro sequence, was substituted with Ala (TGT with GCC). The 3ABC-ΔTM mutant contains an in-frame deletion of the trans-membrane domain between residues 39 and 59 of 3A. In the 3AC mutant, the carboxyl-terminal 4 residues of 3A and residues 1 to 19 of 3B were deleted in frame, leaving the carboxyl-terminal 4 residues of 3B to maintain a functional 3Cpro cleavage site between 3A and 3Cpro. Two MAVS mutants, MAVS-Q428A and MAVS-E463A, were similarly generated by creating Ala substitutions at Gln-428 and Glu-463 of the MAVS sequence, respectively. All mutations were confirmed by DNA sequencing.

Promoter Reporter Assay Transfections were carried out with either Lipofectamine 2000 (Invitrogen) or FuGENE 6 (Roche) as recommended by the manufacturers. Promoter reporter luciferase assays utilized the Dual-Luciferase Reporter Assay System (Promega) with firefly luciferase activities (pIFN-β-luc, pISG56-Luc or PRDII-Luc) normalized to *Renilla* luciferase activities (pRL-CMV or pRL-TK) and measured with a TD-20/20 luminometer (Turner). In some experiments, pCMV-βGal was used to normalize transfection efficiency, as previously described (94). Each experiment was carried out in triplicate. Where indicated, cells were infected with 100 hemagglutinin units/ml of Sendai virus (Charles River Laboratories) 24 hrs following transfection, and harvested 16 hr later for luciferase reporter assays and/or immunoblot analysis.

Immunoblots Cells were lysed in lysis buffer (20 mM Tris-HCl, pH 7.5, 150 mM NaCl, 10 mM EDTA-2Na, 1% [vol/vol] Nonidet P-40, 10% [vol/vol] glycerol, and 2 mM DTT, supplemented with complete protease inhibitor cocktail [Roche]). Lysates were cleared by centrifugation at 14,000 rpm for 15 min prior to being resolved by SDS-PAGE and transferred to membranes. Immunoblots were carried out using the following primary antibodies: anti-MAVS (Zhijian Chen, UT Southwestern Medical Center), anti-Flag (Sigma), anti-V5 (Invitrogen), anti-IRF3 (Michael David, UCSD), anti-IRF3 P396 (John Hiscott, McGill University), anti-ISG15 (Arthur Haas, Medical College of Wisconsin), anti-SenV (Ilkka Julkunen, National Public Health Institute, Finland), anti-GFP (Roche), IgG purified from the serum of a patient convalescing from acute hepatitis A, anti-GAPDH (Ambion), and anti-actin (Sigma). Membranes were washed and subsequently probed with appropriate secondary antibodies conjugated with horseradish peroxidase (HRP), and visualized using ECL reagents (Amersham Pharmacia Biosciences) and exposure to x-ray films.

Confocal Imaging Cells were cultured on Labtek chamber slides (Nunc) and fixed in 4% paraformaldehyde in PBS for 30 min. Cells were permeabilized with Triton X-100 (0.2%) for 15 min and blocked with 10% normal goat serum at room temperature for 1 hr. Slides were incubated with appropriate dilutions of primary antibodies for 1 hr at room temperature: rabbit anti-IRF3 (Michael David, UCSD), human polyclonal anti-HAV IgG, rabbit anti-MAVS (Zhijian Chen, UT Southwestern Medical Center), or rabbit anti-Flag (Sigma). Slides were washed and incubated for an additional hr with appropriate secondary antibodies. Mitochondria were labeled with MitoTracker (Invitrogen). Slides were counterstained with 4'-6-diamidino-2-phenylindole (DAPI) and mounted with Vectashield mounting medium (Vector Laboratories). Slides were sealed

and examined with a Zeiss LSM-510 laser scanning confocal microscope within the Infectious Disease and Toxicology Optical Imaging Core, UTMB, Galveston.

Protein Expression and Purification from *E. coli* The 3Cpro and 3ABC coding sequences from HM175/18f were cloned into the expression vector pGEX-4T3 (Amersham), fused in-frame with an amino-terminal GST tag. For protein expression, an overnight culture of *E. coli* strain BL21(DE) (Novagen) containing the expression construct was diluted 10-fold and cultured at 37˚C for 2 hours. Expression was induced by addition of 0.1 mM IPTG and continued culture at 25˚C for 3 hours. Bacterial cells were lysed in BugBuster solution (Novagen) containing 37.5 U/ml Benzonase (Novagen), 15 KU/ml recombinant lysozyme (Novagen) and 2 mM DTT. GST-3Cpro and GST-3ABC fusion proteins were purified from the bacterial lysate by affinity chromatography using the GST MicroSpin Purification Module (Amersham) according to the manufacturer's instructions.

***In vitro* Cleavage Assay** MAVS and MAVS mutants were synthesized *in vitro* and labeled with [^{35}S]-Met using the TNT T7 Coupled Transcription/Translation System (Promega) according to the manufacturer's instructions. Cleavage assays were performed in a 10-µl mixture containing 1 µl TNT product and purified protease at indicated concentrations in a buffer containing 50 mM Tris-HCl pH 8.0, 2.5 mM EDTA and 2mM DTT. Reactions were carried out overnight at 37˚C and stopped by addition of an equal volume of 2X SDS sample buffer. Cleavage products were analyzed by SDS-PAGE followed by autoradiography.

Northern Blot Analysis mRNA was extracted from cells using the Micropoly(A) Purification Kit (Ambion), and RNA concentrations determined by spectrometry at 260 nm. mRNA (1 µg) was applied to a 1% denaturing agarose-formaldehyde gel, subjected to electrophoresis, and transferred to a positively-charged nylon membrane using the

NorthernMax kit (Ambion) according to the manufacturer's instructions. Transferred RNAs were immobilized by UV cross-linking (Stratagene). HAV RNA and MAVS mRNA were hybridized to biotinylated DNA probes specific for HM175/18f genomic RNA and human MAVS, respectively. Bound probes were detected with a streptavidin-alkaline phosphatase conjugate, followed by reaction with CSPD (Roche) and exposure to x-ray film.

Real-time Quantitative RT-PCR Quantitative RT-PCR assays were carried out using TaqMan chemistry on a PRISM 7700 instrument (ABI). For quantification of HAV RNA in HAV-Bla cells treated with IFN-α, we used forward and reverse primers specific for HAV HM175/18f genomic RNA (93). Primers used to quantify IL-6 mRNA in extracts of cells prepared following SenV infection were IL6AFP, CACACAGACAGCCACTCA; and IL6ARP, GTTACATGTCTCCTTTCTCAG; the probe was IL6P, (FAM)-CAAATTCGGTACATCCTCGACGGCA. Results were normalized to the copy number of cellular GAPDH mRNA detected in a similar real-time RT-PCR assay using reagents provided with the TaqMan GAPDH Control Reagents (Human) (Applied Biosystems).

Subcellular fractionation The preparation of subcellular fractions for determining the localization of 3ABC was carried out as described previously (156).

2.3 Results

Virus activation of IRF3 is blocked by autonomous replication of a subgenomic HAV RNA. Recent reports suggest that HAV infection blocks induction of interferon-β synthesis through the RIG-I pathway by preventing activation of IRF3 (19, 43). To confirm this, we studied fetal rhesus kidney (FRhK-4) cells infected with a cell culture-adapted variant of HAV, HM175/18f (93). We found that HAV infection blocked induction of IFN-β and ISG56 promoters by Sendai virus (SenV), a well-characterized

stimulator of the RIG-I signaling pathway (194) (Fig. 2.6*A*). Although previous studies suggest that HAV infection activates NF-κB-dependent promoters (43), we found no stimulation of the basal activity of the PRD-II promoter (an NF-κB-dependent element of the interferon-β promoter). Instead, we observed complete inhibition of SenV-activation of this promoter (Fig. 2.6*B*). Because HAV infection did not interfere with SenV protein expression (Fig. 2.6*D*), we conclude that HAV disrupts RIG-I signaling at a proximal point in the pathway, before its bifurcation to IRF3 and NF-κB.

To better understand this interference with RIG-I signaling, we studied a stable cell line containing an autonomously replicating subgenomic HAV RNA. Although we previously reported transient replication of subgenomic HAV replicons in Huh7 human hepatoma cells (192), stable cell lines supporting replication of HAV replicons have not been described. The HAV-Bla replicon contains an in-frame substitution of most of the P1 (capsid protein-coding) sequence of HM175/18f virus with sequence encoding the selectable marker blasticidin (Fig. 2.1*A*). Blasticidin treatment of transfected Huh7 cells selected a single, stable cell line (HAV-Bla) that both expresses HAV antigen (Fig. 2.1*B Left*) and contains HAV RNA (Fig. 2.7). To confirm that this subgenomic RNA replicates autonomously in HAV-Bla cells, and to provide a clonally-related cell line for use as a control, we treated the cells with IFN-β in the absence of blasticidin, thereby eliminating the replicon RNA. The cured cells (Bla-C) no longer expressed HAV antigen (Fig. 2.1*B Right*) or detectable viral RNA, and none survived when blasticidin was added back to the culture media.

SenV-induced activation of the IFN-β promoter was profoundly blocked in the HAV-Bla replicon cells compared with their cured Bla-C progeny (Fig. 2.1*C*). We also observed a marked reduction in SenV-induced dimerization of IRF3 (Fig. 2.1*D*), suggesting that SenV activation of IRF3 is compromised by the HAV replicon. SenV

infection also failed to cause nuclear translocation of IRF3 in HAV-Bla cells, whereas this was readily apparent in the cured Bla-C cells (Fig. 2.1*E Lower*). The induction of IFN stimulated gene-15 (ISG15) synthesis was also inhibited (Fig. 2.6*E*), and although SenV infection typically induces only low levels of detectable phosphoserine-396 IRF3 in normal Huh7 cells (94), this was substantially (albeit, not completely) eliminated in the replicon cells (Fig. 6*E*, compare lanes 2 and 4). Importantly, immunoblots indicated that both the cured and replicon-containing cell lines were equally permissive for SenV replication (Fig. 2.1*D Lower*). These results confirm that HAV replication and protein expression blocks activation of IRF3 through the RIG-I pathway.

RIG-I recognizes 5' triphosphates that are present on some viral RNAs (65, 130), but not HAV RNAs which are covalently linked to a small peptide, 3B (VPg), at their 5' terminus (180). MDA5 is likely to be more important for HAV; it recognizes RNA from other picornaviruses (53, 78). To determine whether MDA5 signaling is disrupted by HAV infection, we ectopically expressed constitutively-active MDA5 and RIG-I mutants representing the N-terminal CARD-like domains of these molecules (MDA5-N and N-RIG, respectively). Both mutants activated the IFN-β promoter in cured Bla-C cells, while this response was substantially blocked in the HAV-Bla cells (Fig. 2.1*F Left*). These results confirm that HAV blocks MDA5 as well as RIG-I signaling. The IFN-β response to overexpression of MAVS was also reduced, yet not ablated, in HAV-Bla compared with Bla-C cells, while expression of the kinase IKKε, which phosphorylates IRF3 in response to dsRNA signaling, activated the IFN- β promoter equally in both cell lines (Fig. 2.1*F*). Collectively, these results suggest that HAV disrupts signaling between MDA5/RIG-I and the downstream kinases, most likely at the level of MAVS, which serves as an essential adaptor for both RIG-I and MDA5 (80, 115, 156). Since MAVS is required for RIG-I signaling to both IRF3 and NF-κB (156), this interpretation is

consistent with the block in NF-κB activation that we noted in HAV-infected FRhK-4 cells (Fig. 2.6), and a profound suppression of SenV-induced IL-6 transcription in HAV-Bla cells (Fig. 2.8).

HAV disrupts MDA5 signaling by post-transcriptional down-regulation of MAVS expression. To better understand how HAV might block MDA5 signaling, we analyzed MAVS expression in the replicon cells. Remarkably, immunoblots demonstrated an absence of MAVS expression in these cells, compared to the cured Bla-C cells or parental Huh7 cells (Fig. 2.2*A*). This was accompanied by the presence of a novel MAVS-immunoreactive protein species (asterisk in Fig. 2.2*A*), a possible degradation product, that migrated with an apparent molecular mass slightly greater than that of the minor MAVS species normally detected in these blots. Interestingly, a similar protein was observed in HAV-Bla cells, but not Bla-C cells overexpressing MAVS (asterisk in Fig. 2.1*F Right*). Confocal microscopy confirmed a marked loss of endogenous MAVS in HAV-Bla versus Bla-C cells (Fig. 2.2*B*). We also found a striking reduction in the abundance of MAVS in HAV-infected FRhK-4 cells compared with adjacent non-infected cells (Fig. 2.2*C*). Immunoblotting confirmed that a HAV infection causes a profound down-regulation of MAVS in both FRhK-4 and Huh7 cells (Fig. 2.3*D*). Although the greater molecular mass of MAVS in uninfected FRhK-4 cells compared with Huh7 cells suggests a species (rhesus vs. human) difference, HAV infection of either cell type completely eliminated MAVS expression.

Northern blots indicated no differences in the abundance of MAVS-specific mRNA in the HAV-Bla vs. cured Bla-C cells (Fig. 2.2*E*). Also, when we cultured HAV-Bla cells in the presence of MG-115, a potent inhibitor of the proteasome, there was no increase in MAVS abundance (data not shown). We conclude that HAV infection causes

profound post-transcriptional down-regulation of MAVS expression by a proteasome-independent mechanism.

The HAV 3ABC protease precursor down-regulates MAVS. Primary cleavage of the HAV polyprotein occurs between 2A and 2B, and is catalyzed by 3Cpro, a cysteine protease which is the only protease expressed by HAV (Fig. 2.1*A*) (107, 153). 3Cpro subsequently directs other processing events within the polyprotein, excluding VP1/2A cleavage which is catalyzed by an unknown cellular protease, and VP4/VP2 cleavage which occurs late in viral assembly. Thus, there are 7 distinct nonstructural proteins and several intermediate precursors expressed by the HAV-Bla replicon (Fig. 2.3*A*) (135). To determine which might down-regulate MAVS, we co-transfected Huh7 cells with vectors expressing an N-terminal GFP-MAVS fusion protein and N-terminally HA-tagged nonstructural proteins and polyprotein processing intermediates shown in Fig. 2.3*A*. A reproducible reduction in GFP-MAVS abundance was observed only with co-expression of 3ABC or 3ABCD (Fig. 2.3*B Top*), and in both cases this was accompanied by appearance of a lower mass (~95 kDa) protein reactive with anti-GFP (asterisk in Fig. 2.3*B*). In contrast, there was no reduction in the abundance of GFP when it was co-expressed with 3ABC or 3ABCD, nor any change in the ratio of GFP-MAVS to GFP abundance when both were co-expressed with 3AB or 3BC (data not shown). Because 3ABC is known to be a stable, catalytically active precursor of 3Cpro (135), we suspected that the 95-kDa protein might result from proteolysis within the MAVS sequence. Immunoblots demonstrated autoprocessing of 3ABCD to 3ABC (Fig. 2.3*B Middle*), confirming both the catalytic activity of the 3Cpro sequence in these constructs and the stability of 3ABC. Importantly, there was no evidence for MAVS cleavage in cells expressing the mature 3Cpro protease (Fig. 2.3*B Top*), even though 3Cpro was efficiently expressed (Fig. 2.3*B Middle*, lane 10). In contrast, 3CD was not detected,

possibly due to the presence of a ubiquitination signal within the 3Dpol sequence (104), preventing any conclusions about its ability to cleave MAVS. Parallel expression of the HCV NS3/4 protease resulted in a slight reduction in the mass of GFP-MAVS, as expected for cleavage near its C-terminus (Fig. 2.3*B Middle*, lane 1) (96, 115).

Confocal microscopy showed GFP-MAVS co-localized with MitoTracker, a fluorescent dye taken up specifically by mitochondria (Fig. 2.9 *Left*). This finding is consistent with the mitochondrial localization of MAVS (156). However, in cells expressing 3ABC (but not 3Cpro), the subcellular distribution of GFP-MAVS was altered to a diffuse, cytoplasmic pattern, indicating disruption of its mitochondrial association (Fig. 2.9 *Right*). To determine whether 3ABC also targets endogenous MAVS, we transfected Huh7 cells with vectors expressing C-terminally Flag-tagged 3ABC and other HAV proteins. We also expressed the HCV NS3/4A protease that is known to cleave MAVS near its carboxyl terminus. 3ABC expression caused a severe reduction in the abundance of endogenous MAVS (Fig. 2.3*C Left*, compare lanes 3 and 2), confirming that 3ABC is responsible for down-regulation of MAVS. In contrast, there was no reduction in MAVS abundance associated with ectopic expression of 3Cpro, 3BC, or a mixture of 3A and 3BC (Fig. 2.3*C Left*). Immunoblotting confirmed abundant expression of 3Cpro (Fig. 2.3*C*, right panel), indicating that the failure of 3Cpro to reduce MAVS abundance was not due to insufficient expression. A low abundance of 3Cpro was present in cells expressing 3ABC (Fig. 2.3*C*, lane 1, arrow), confirming the activity of the cysteine protease as well as the stability of the 3ABC intermediate (135).

MAVS is targeted for proteolysis by the cysteine protease activity of 3ABC. To confirm that 3ABC-mediated proteolysis causes the down-regulation of MAVS, we constructed a 3ABC mutant in which the active site cysteine nucleophile, 3C-Cys-172, was substituted with Ala (3ABC-C172A). This substitution is known to eliminate the

protease activity of 3Cpro (14). The absence of auto-protease activity in 3ABC-C172A stabilized the expression product, resulting in a greater abundance of the mutant compared with the wild-type 3ABC in transfected Huh7 cells (Fig. 2.4*A Right*, compare lanes 2 and 1). Nonetheless, in contrast to 3ABC, there was no cleavage of GFP-MAVS, nor any cleavage of endogenous MAVS in cells expressing 3ABC-C172A (Fig. 2.4*A*, and data not shown). These results confirm that the cysteine protease activity of 3ABC is responsible for the degradation of MAVS.

We next examined the sequence of MAVS for a potential 3Cpro cleavage site. With the exception of the 3A/3B cleavage, each of the 3Cpro cleavage sites within the HAV polyprotein possess a P1 glutamine residue and the consensus sequence (L/V/I)x(T/S)Q↓x (155). Such a consensus 3Cpro cleavage sequence exists at Gln-428 of human MAVS (Fig. 2.4*B*), 80 residues upstream of the HCV NS3/4A cleavage site, Cys-508 (Fig. 2.4*D*) (95). The P-side residues at this potential cleavage site, LASQ, are similar to the 2A/2B and 2C/3A cleavage sites, LFSQ and LWSQ, respectively. To determine whether MAVS is cleaved by 3ABC at Gln-428, we substituted Gln-428 with Ala in a C-terminally Flag-tagged MAVS expression vector (MAVS-Q428A). We also made a second mutant, MAVS-E463A, eliminating a Glu-Gly di-peptide sequence with weak homology to the 3A/3B cleavage site (Fig. 2.4*B*). Although we observed cleavage of wild-type MAVS and the E463A mutant in HAV-Bla replicon cells, this did not occur with the Q428A mutant (Fig. 2.4*C*). As expected, none of these proteins was cleaved in the cured Bla-C cells (lanes 4-6). Confirming these results, ectopic expression of the MAVS-Q428A mutant led to equivalent levels of IFN-β promoter activation in the HAV-Bla and cured Bla-C cells (Fig. 2.10*C*), whereas the response to wild-type MAVS was partially blocked in replicon-containing cells (Fig. 2.1*F*).

These results were further confirmed by *in vitro* cleavage assays incorporating bacterially expressed GST-3Cpro and GST-3ABC fusion proteins and [^{35}S]-labeled MAVS substrates produced *in vitro* in a coupled transcription/translation reaction. These experiments demonstrated that MAVS was partially cleaved overnight by GST-3ABC at a concentration of 100 nM, but was barely cleaved by GST-3Cpro at the same concentration (Fig. 2.11*A*). The MAVS substrate was also partially cleaved by an equal concentration of a maltose-binding protein fusion with a single-chain NS3 protease (MBP-scNS3) derived from HCV (95) (Fig. 2.11*A*). Consistent with the results shown in Fig. 2.4C, the Q428A substitution in MAVS significantly reduced but did not eliminate cleavage by GST-3ABC, whereas the E463A mutation had no effect on the GST-3ABC cleavage or on MBP-scNS3 cleavage of MAVS (Fig. 2.11*B*). We conclude from these results that the 3Cpro cysteine protease activity of 3ABC directs proteolysis of MAVS at Gln-428 (Fig. 2.4*D*).

Mitochondrial targeting of 3ABC is essential for MAVS proteolysis. 3ABC contains a hydrophobic transmembrane domain in 3A (amino acid residues 39-59, Fig. 2.6*A*) (12). To determine whether this domain is required to direct the association of the protease with membranes in order to catalyze the cleavage of MAVS, we created an in-frame deletion within the 3ABC expression vector, removing the 3A transmembrane domain (Fig. 2.6*B*, 3ABC-ΔTM). Ectopic expression of 3ABC-ΔTM failed to cause cleavage of GFP-MAVS, while a similar 3B-deletion mutant (Fig. 2.6*B*, 3AC) was able to do so (Fig. 2.6*C*, compare lane 2 with lanes 1 and 3). Co-transfection of vectors expressing 3A and 3BC did not result in cleavage of endogenous MAVS (Fig. 2.4*C Left*, lane 6), indicating that 3A must be expressed *in cis* with 3Cpro to cause the cleavage. Together, these data suggest strongly that membrane association of 3ABC, determined by the transmembrane domain within 3A, is required for MAVS cleavage.

The transmembrane domains of picornaviral 3A proteins anchor the viral replicase to intracellular membranes on which viral RNA synthesis occurs (see Discussion). Although mitochondrial membranes have not been implicated in picornaviral replication, there is limited homology between the HAV domain and the carboxyl-terminal transmembrane domain of MAVS which anchors MAVS specifically to the outer mitochondrial membrane (Fig. 2.5*A*) (156). Surprisingly, 3ABC co-localized strongly with MitoTracker in transfected cells, suggesting a specific mitochondrial localization (Fig. 2.5*D*). 3AC also co-localized with MitoTracker, but not 3ABC-ΔTM, which appeared to localize to the nucleus, or the mature protease, 3Cpro, which showed a diffuse staining pattern consistent with the absence of membrane binding. Cell fractionation studies confirmed these results, as 3ABC, 3ABC-C172A, and 3A were found exclusively in a crude mitochondrial cell fraction (P5 pellet), co-segregating with MAVS and the 39-kDa subunit of cytochrome C oxidase I (CI-39) (Fig. 2.5*E*, lanes 1, 7 and 10). These HAV proteins were not detectable in an S15 fraction enriched for ER membranes (lanes 3, 9, and 12). In contrast, 3ABC-ΔTM was not detected in either fraction (lanes 4 and 6), consistent with its nuclear localization suggested in Fig. 2.6*D*.

Additional confocal microscopic studies confirmed these results. Co-expression of 3ABC and GFP-MAVS led to a diffuse staining pattern for GFP, due to cleavage and release of GFP-MAVS from the mitochondrial outer membrane, and mitochondrial localization of the protease (Fig. 2.10*A*). Such cells demonstrated only partial co-localization of the proteins. In contrast, co-expression of 3ABC-ΔTM and GFP-MAVS, led to a diffuse staining pattern for the mutated 3ABC and largely unaltered mitochondrial localization of GFP-MAVS, while co-expression of the catalytically-inactive 3ABC-C172A mutant (which retains the 3A transmembrane domain) led to strong co-localization of the protease precursor and GFP-MAVS, in a pattern consistent

with the localization of both proteins to the mitochondrial membrane. Consistent with these results, ectopic expression of 3ABC, but not 3ABC-ΔTM, 3ABC-C172A, or 3Cpro, effectively blocked SenV activation of the IRF3-dependent PRD-III-I promoter in FRhK-4 cells (Fig. 2.10*B*).

2.4 Discussion

Both HAV and HCV are positive-strand RNA viruses that share a tropism for the liver in humans. Nonetheless, they have important differences in genome structure and replication strategy. Viral RNAs produced during the replication of these viruses are also likely to be sensed differently by the host. The 5' nucleotides of both positive- and negative-strand HAV RNA are linked covalently to 3B (otherwise known as VPg) (180). Such RNAs are unlikely to be recognized by RIG-I (65, 130). Presumably, their presence is detected by MDA5, a related CARD-domain containing DExH/D helicase that senses RNA derived from other picornaviruses (53, 78). In contrast, HCV appears to activate IRF3 by engaging RIG-I (163). Nonetheless, both RIG-I and MDA5 share MAVS as a common adaptor, the integrity and mitochondrial location of which is essential to activation of both IRF3 and NF-κB (156). The targeting of MAVS by both the cysteine protease of HAV and the serine protease of HCV thus represents a remarkable example of convergent virus evolution, and provides strong albeit indirect evidence for the importance of MAVS to host control of virus infections within the liver.

While multiple lines of evidence suggest that disruption of RIG-I signaling could limit the ability of the cell to restrict HCV replication (50, 163), its importance in the pathogenesis of hepatitis C is controversial (182). Unlike HCV, HAV is incapable of establishing long-term persistent infections. Thus, our results show that virus-mediated proteolysis of MAVS is not, by itself, sufficient for persistent infection with a positive-strand RNA virus. HAV infection is nonetheless clinically silent for 3-5 weeks following

infection, despite extensive replication within the liver (92). 3ABC-mediated proteolysis of MAVS may contribute to this clinically quiescent phase of the infection. It may also facilitate the ability of the virus to establish persistent non-cytopathic infections in cultured cells, a feature that typifies HAV despite its sensitivity to interferon.

Despite similarity in the mechanisms by which HAV and HCV disrupt signaling through the MDA5/RIG-I pathways, there are marked contrasts. In the case of HCV and the distantly related flavivirus, GB virus B (named after the surgeon, G. Barker, who fell ill in 1966 with a hepatitis virus) (142), it is the fully mature, assembled NS3/4A protease complex that cleaves MAVS (24, 115). In the case of HAV, we have shown here that it is a stable processing intermediate, 3ABC, that directs the proteolysis of MAVS (Fig. 2.3*C*). Unlike 3ABC, the mature protease, 3Cpro, is unable to cleave MAVS. 3ABC is directed to the mitochondrial where it co-localizes with MAVS and attacks it proteolytically. This subcellular localization, not described previously for any picornavirus, is dependent upon the transmembrane domain of 3A, which has homology with the transmembrane domain of MAVS (Fig. 2.5*A*). Deletion of the transmembrane domain in 3ABC resulted in the loss of MAVS cleavage (Fig. 2.5*C*), as did a substitution of the active site cysteine of 3Cpro with alanine (Fig. 2.4*A*). Thus, destruction of MAVS requires both the mitochondrial targeting properties of 3A and the cysteine protease activity of 3Cpro. The HCV NS3/4A protease also co-localizes with MAVS (96), but is not directed specifically to mitochondrial membranes.

The specific mitochondrial localization of 3ABC is surprising. All positive-strand RNA viruses replicate their genomes on the surface of intracellular membranes, but mitochondrial membranes have not been implicated in picornaviral replication. The 2C protein of poliovirus, a well-studied picornavirus, is responsible for reorganizing intracellular membranes that support RNA replication; evidence suggests these are

derived from the ER and the cellular anterograde membrane traffic system (39, 145). Although not as well studied, HAV 2C also induces rearrangement of intracellular membranes, which have been presumed to be ER-derived and the site of RNA synthesis (174). Among other functions, picornaviral 3A proteins fulfill a central role in *cis* assembly of the replicase complex, as the transmembrane domains of 3A tether 3AB and associated viral and cellular proteins to the membrane (161, 183). Thus, the mitochondrial-specific targeting of 3ABC suggests the possibility that HAV RNA replication may occur on mitochondrial membranes, and not membranes of the ER as long suspected. Although requiring investigation, this would not be without precedent among positive-strand RNA viruses. Nodavirus RNA replication occurs on outer mitochondrial membranes in insect cells (119). This may have consequences pathologically, as mitochondrial abnormalities were observed in early ultrastructural studies of acute hepatitis A in chimpanzees; a finding not observed in acute hepatitis B (152).

Our results and those of others suggest that the accessory functions of 3A vary among different picornaviruses. The 3A protein of enteroviruses is directed to ER membranes, as described above, and contains an amino-terminal domain that disrupts ER-to-Golgi traffic (29, 181). This function is not essential for RNA replication, and may contribute to immune evasion by reducing secretion of IFN-β and pro-inflammatory cytokines, as well as by limiting movement of class I molecules to the plasma membrane (29). As we have shown here, the 3A protein of HAV also contributes to immune evasion, but through a very different mechanism.

Figure 2.1: HAV blocks activation of IRF3 at the level of MAVS.

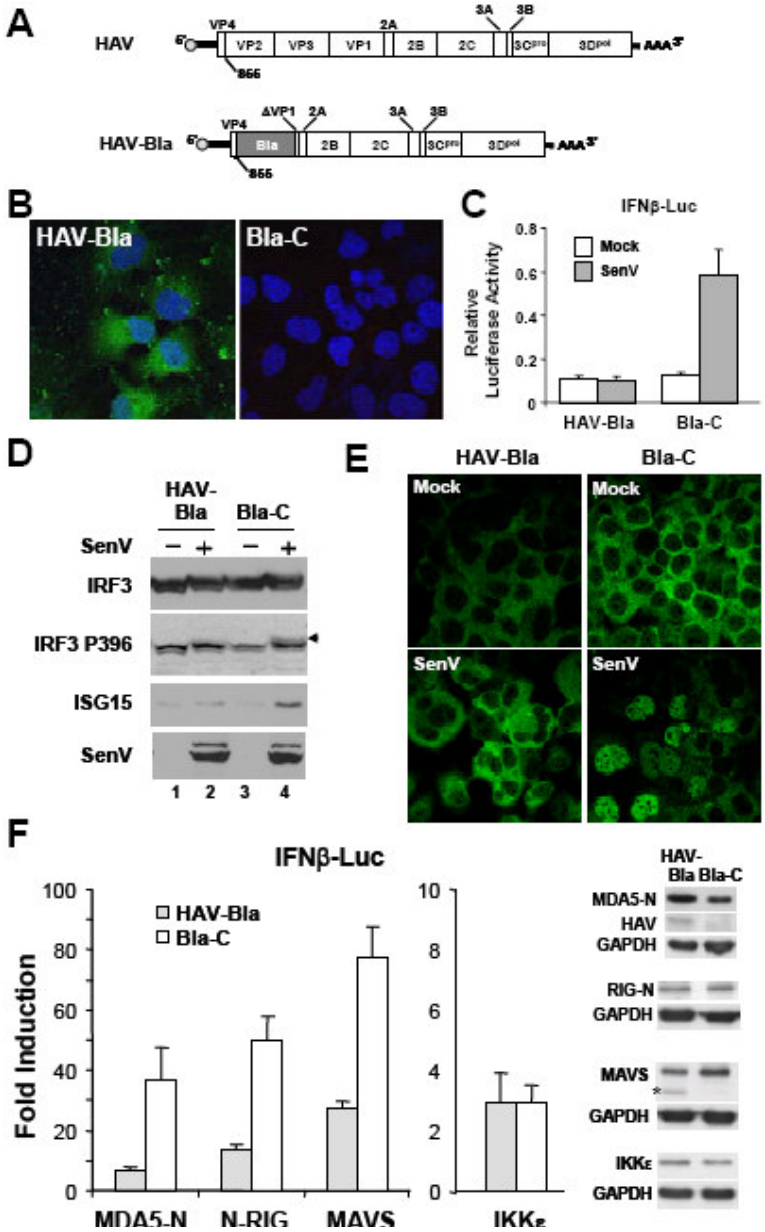

(A) Organization of (top) the wild-type HAV genome and (bottom) the subgenomic HAV-Bla replicon in which most of the P1 sequence of HM175/18f is replaced with blasticidin sequence (shaded box, Bla). **(B)** Detection of HAV antigen by immunofluorescence labeling with human anti-HAV IgG in (left) HAV-Bla replicon cells and (right) IFN-cured Bla-C cells. Nuclei were visualized with DAPI. **(C)** Reporter assays

showing that SenV-induced activation of the IFN-β promoter is blocked in HAV-Bla replicon cells compared to cured Bla-C cells. **(D)** Immunoblot analysis of IRF3, phospho-S396 IRF3, and ISG15 abundance in HAV-Bla and Bla-C cell extracts prepared 16 hrs after SenV infection vs. mock infection. The arrowhead indicates the phospho-S396 band migrating immediately above the major IRF3 species (present only in lane 4). The bottom panel demonstrates equivalent expression of SenV proteins in both cell types. **(E)** Cellular localization of IRF3 in (left panels) HAV-Bla and (right panels) Bla-C cells following (top panels) mock versus (bottom panels) SenV challenge. **(F)** IFN-β promoter assays of HAV-Bla and Bla-C cells expressing MDA5-N and N-RIG, MAVS, and IKKε. To the right are immunoblots showing the expression levels of these proteins. A unique rapidly-migrating MAVS-reactive protein in HAV-Bla cells is indicated by (*). GAPDH served as a loading control.

Figure 2.2: MAVS is down-regulated post-transcriptionally by HAV.

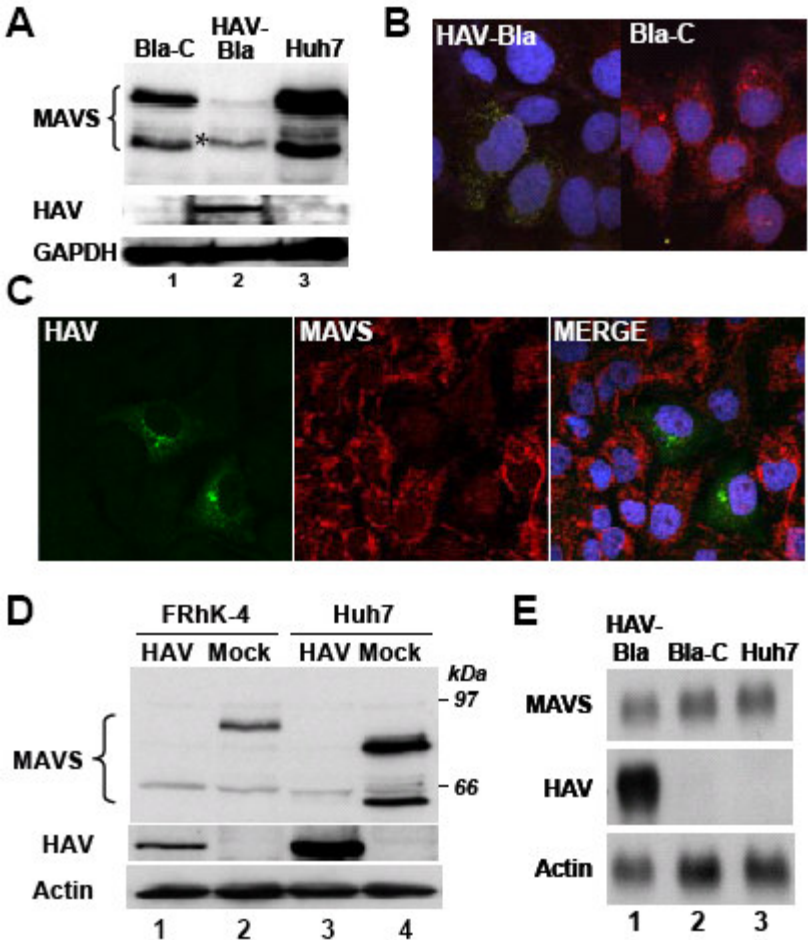

(A) Immunoblot showing (top) endogenous MAVS, (middle) an HAV protein, and (bottom) GAPDH in extracts from HAV-Bla, Bla-C, and normal Huh7 cells. **(B)** Confocal microscopic images of (left) HAV-Bla and (right) Bla-C cells labeled with human anti-HAV (green) and rabbit anti-MAVS (red). **(C)** Down-regulation of MAVS in HAV-infected FRhK-4 cells. Cells were infected with HM175/18f virus at low m.o.i. (~0.01) 3 days prior to labeling with anti-HAV (green) and anti-MAVS (red). Two HAV-infected cells are evident, both of which show marked suppression of MAVS expression. **(D)** Immunoblots showing (top panel) MAVS, a ~97 kDa HAV protein, and actin loading controls in extracts of FRhK-4 (lanes 1 and 2) and Huh7 (lane 3 and 4) cells prepared 3 days following mock (lanes 2 and 4) or high m.o.i. HAV infection (m.o.i = 2, lanes 1 and 3). **(E)** Northern blots of MAVS and actin mRNAs and HAV RNA.

Figure 2.3: HAV 3ABC, but not 3Cpro, down-regulates MAVS.

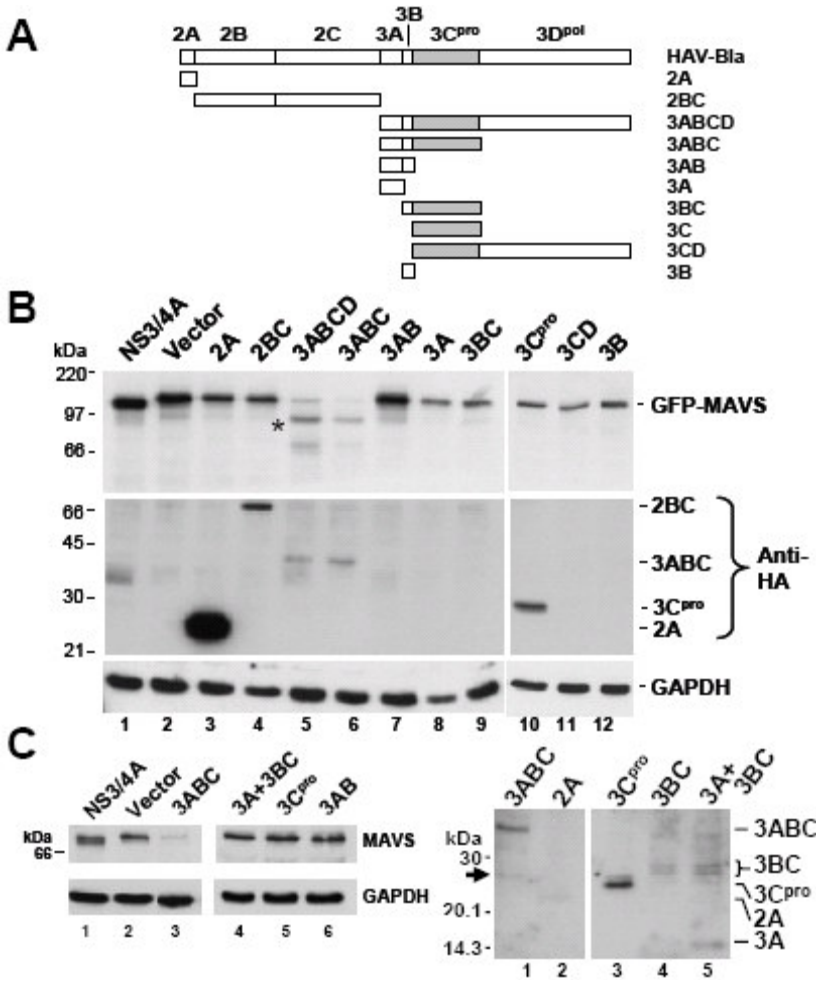

(A) Schematic showing HAV proteins and processing intermediates. **(B)** (top panels) Immunoblots showing GFP-MAVS labeled with anti-GFP in extracts of Huh7 cells co-transfected with vectors expressing GFP-MAVS and N-terminally HA-tagged HAV proteins as indicated (lanes 3-12), HCV NS3/4A (lane 1), or empty vector (lane 2). A rapidly migrating GFP-MAVS species (*) was detected only in cells expressing 3ABC and 3ABCD (lanes 5 and 6). (middle panels) Immunoblots of ectopically expressed HAV proteins, detected with anti-HA. (bottom panels) GAPDH loading controls. **(C)** (left) Immunoblots showing (top panels) endogenous MAVS and (bottom panels) GAPDH loading controls in extracts of Huh7 cells expressing C-terminally Flag-tagged HAV proteins (lanes 3-6), HCV NS3/4A (lane 1), or empty vector (lane 2). (right) Immunoblot showing expression levels of Flag-tagged 3ABC, $3C^{pro}$, 3A and 3BC. The arrowhead marks the $3C^{pro}$ processing product of 3ABC.

Figure 2.4: The cysteine protease activity of 3ABC is responsible for MAVS cleavage.

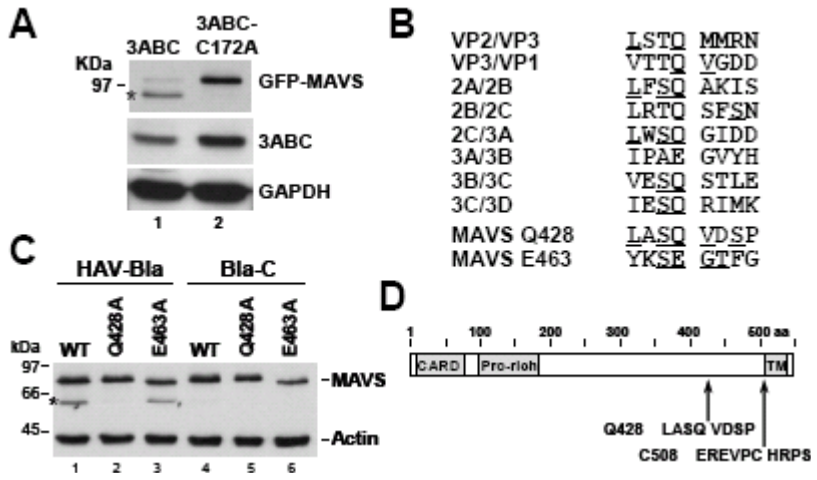

(A) Immunoblots of (top) GFP-MAVS, (middle) 3ABC, and (bottom) GAPDH in extracts of Huh7 cells co-transfected with GFP-MAVS and either 3ABC or 3ABC-C172A vectors; a cleavage product was detected only in cells expressing wild-type 3ABC (lane 1, *). **(B)** Alignment of the sequences surrounding $3C^{pro}$-catalyzed cleavages in the HAV polyprotein, and possible cleavage sites, Q428 and E463, in MAVS. Underlined residues in MAVS sequences are those found at the same position relative to any site of scission in the polyprotein. **(C)** Immunoblot showing GFP-MAVS and actin loading controls in HAV-Bla (lanes 1-3) and Bla-C (lanes 4-6) cells expressing MAVS-Flag (lanes 1 and 4) or Q428A (lanes 2 and 5) and E463A (lanes 3 and 6) MAVS-Flag mutants. Cleavage was eliminated by the Q428A mutation. **(D)** Schematic of MAVS showing the location of the CARD-like, proline-rich domains, and C-terminal transmembrane (TM) domains, and the positions of HAV 3ABC cleavage at Q428 and HCV NS3/4A cleavage at C508.

Figure 2.5: The 3A transmembrane domain targets 3ABC to mitochondria and is essential for 3ABC cleavage of MAVS.

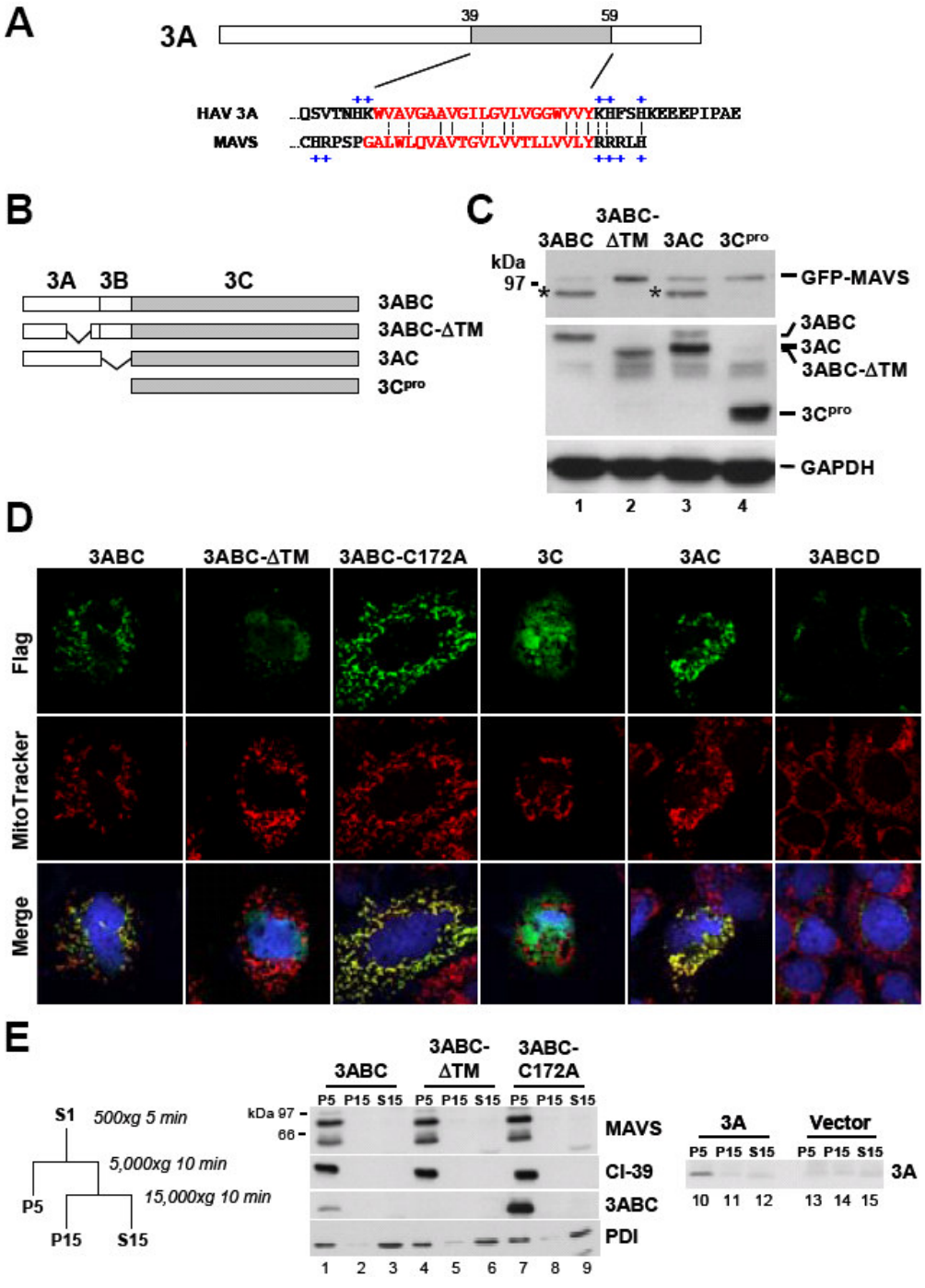

(A) Schematic of the HAV 3A polypeptide showing location and sequence of the transmembrane domain aligned with that of MAVS (residues in red). **(B)** Schematic of C-terminally Flag-tagged HAV P3 expression constructs. **(C)** Immunoblots of (top) GFP-MAVS, (middle) 3ABC expression products, and (bottom) GAPDH loading control in extracts of co-transfected Huh7 cells. Asterisk marks GFP-MAVS cleavage products (lanes 1 and 3 only). **(D)** Laser-scanning confocal microscopy images of transfected Huh7 cells showing cellular localization of (top frames) C-terminally Flag-tagged HAV P3 expression products, (middle frames) mitochondria (MitoTracker), and (bottom frames) merged images with DAPI localization of nuclei. To compensate for quantitative differences in HAV protein expression, the green channel gain was increased for 3ABC-ΔTM and decreased for 3ABC-C172A. **(E)** Ectopically expressed HA-tagged 3ABC, 3ABC-C172A, and 3A, but not 3ABC-ΔTM, are associated with mitochondria. Cell fractions were prepared according to the scheme shown to the left, as described previously (5). CI-39, complex I 39-kDa subunit (mitochondria); PDI, protein disulfide isomerase (endoplasmic reticulum).

Figure 2.6: HAV infection disrupts SenV activation of IRF3 and NF-κB responsive promoters in FRhK-4 cells.

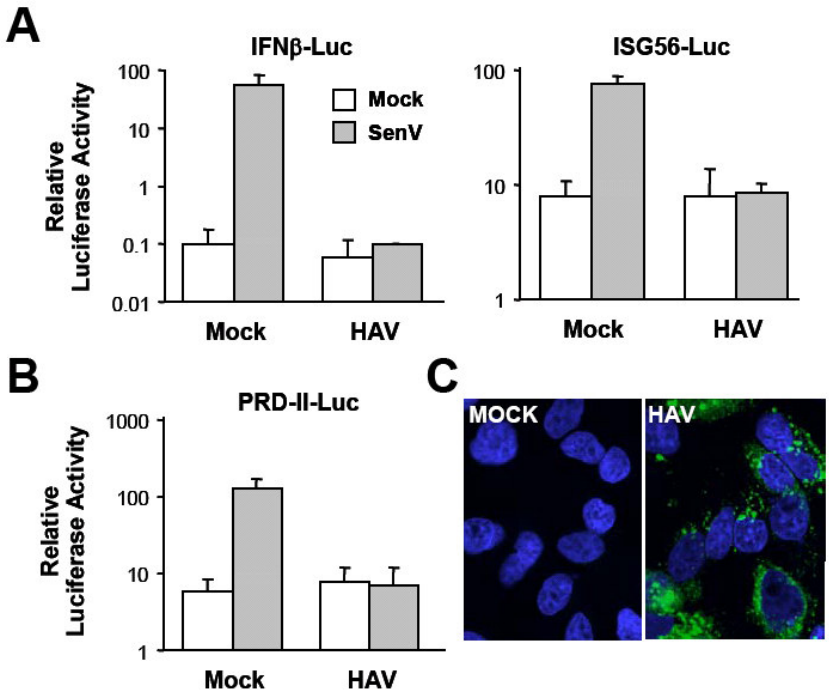

(A) Cells were infected or mock-infected with HM175/18f virus (m.o.i. ~1) 48 hrs prior to transfection with (left panel) IFN-β-Luc or (right panel) ISG-56-Luc promoter reporter plasmids. pTK-Rluc was utilized as a transfection control. Twenty-four hrs following transfection, cells were challenged with SenV, then harvested for luciferase assay 16 hrs later. Mean relative luciferase activities (firefly luciferase vs. Renilla luciferase) are shown for triplicate cultures, ± S.D. **(B).** SenV-activation of the NF-κB-responsive PRD-II promoter in HAV infected FRhK-4 cells. Cells were treated as in panel (A). **(C)** Immunofluorescence detection of HAV-specific antigens in (right panel) HM175/18f-infected and (left panel) mock-infected FRhK-4 cells. Labeling was with polyclonal human anti-HAV antibody. Nuclei were visualized with DAPI.

Figure 2.7: Replication of the HAV-Bla replicon RNA is inhibited by treatment with interferon-α 2b.

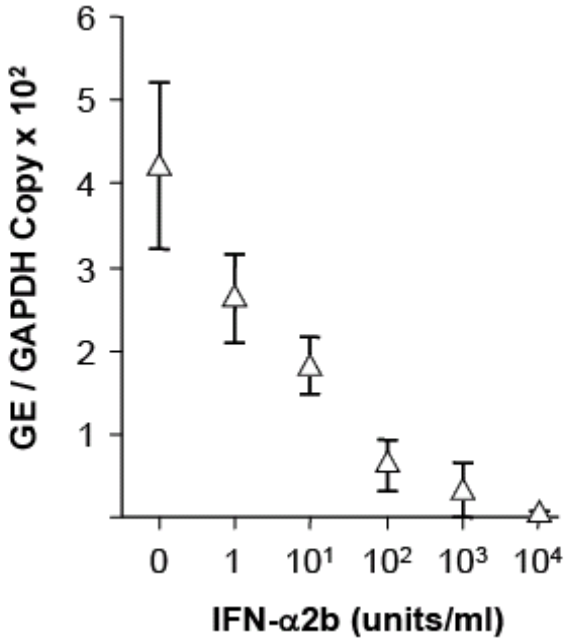

Real-time RT-PCR detection of HAV RNA (relative to GAPDH mRNA copy number) in HAV-Bla cells treated for 4 days with the indicated concentration of IFN-a. Data shown represent the mean ± S.D. from triplicate assays. GE, HAV genome equivalents.

Figure 2.8: TaqMan real-time RT-PCR detection of IL-6 mRNA in HAV-Bla and Bla-C cells following mock or SenV challenge.

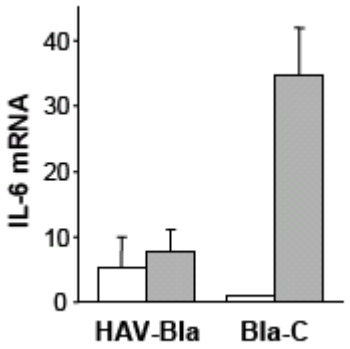

Results were normalized to the GAPDH mRNA copy number, and are displayed relative to th IL-6 mRNA abundance in mock-infected Bla-C cells.

Figure 2.9: Cleavage by 3ABC releases MAVS from mitochondria.

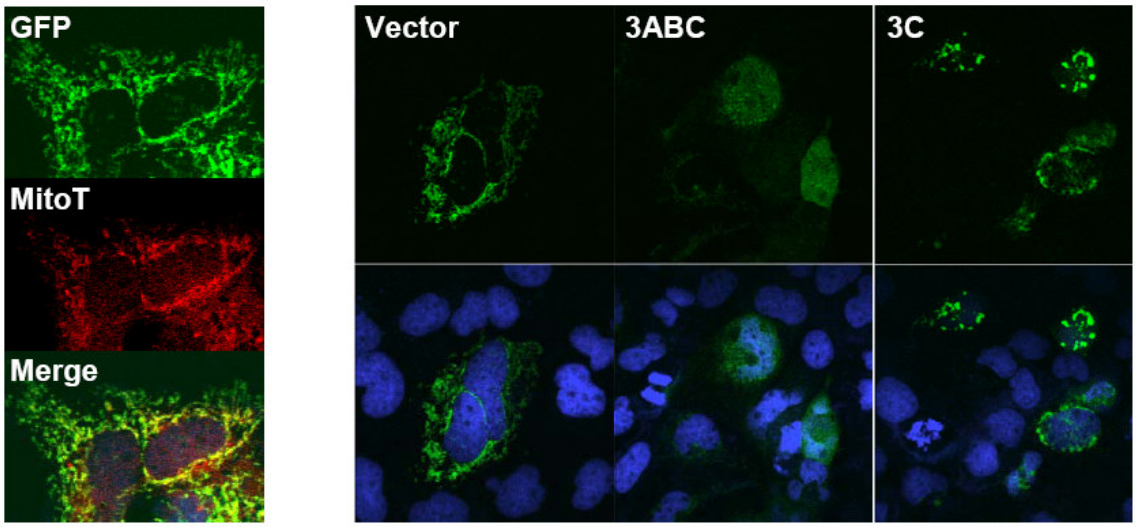

(Left panel) Confocal microscopic image showing co-localization of (top) GFP-MAVS with (middle) MitoTacker, a fluorescence dye that localizes specifically to mitochondria in transfected Huh7 cells. The bottom frame shows a merged image. (Right panel) Cellular localization of GFP (MAVS) fluorescence in Huh7 cells co-transfected with GFP-MAVS and either (left) empty vector, or vectors expressing (middle) C-terminally Flag-labeled HAV 3ABC and (right) 3C. Top frames show GFP fluorescence only, while the bottom frames show a merge of GFP and DAPI-visualized nuclei.

Figure 2.10: Mitochondrial targeting by the TM domain of 3A and the cysteine protease activity of 3Cpro are both required for 3ABC-mediated cleavage of MAVS and inhibition of IFN-β synthesis.

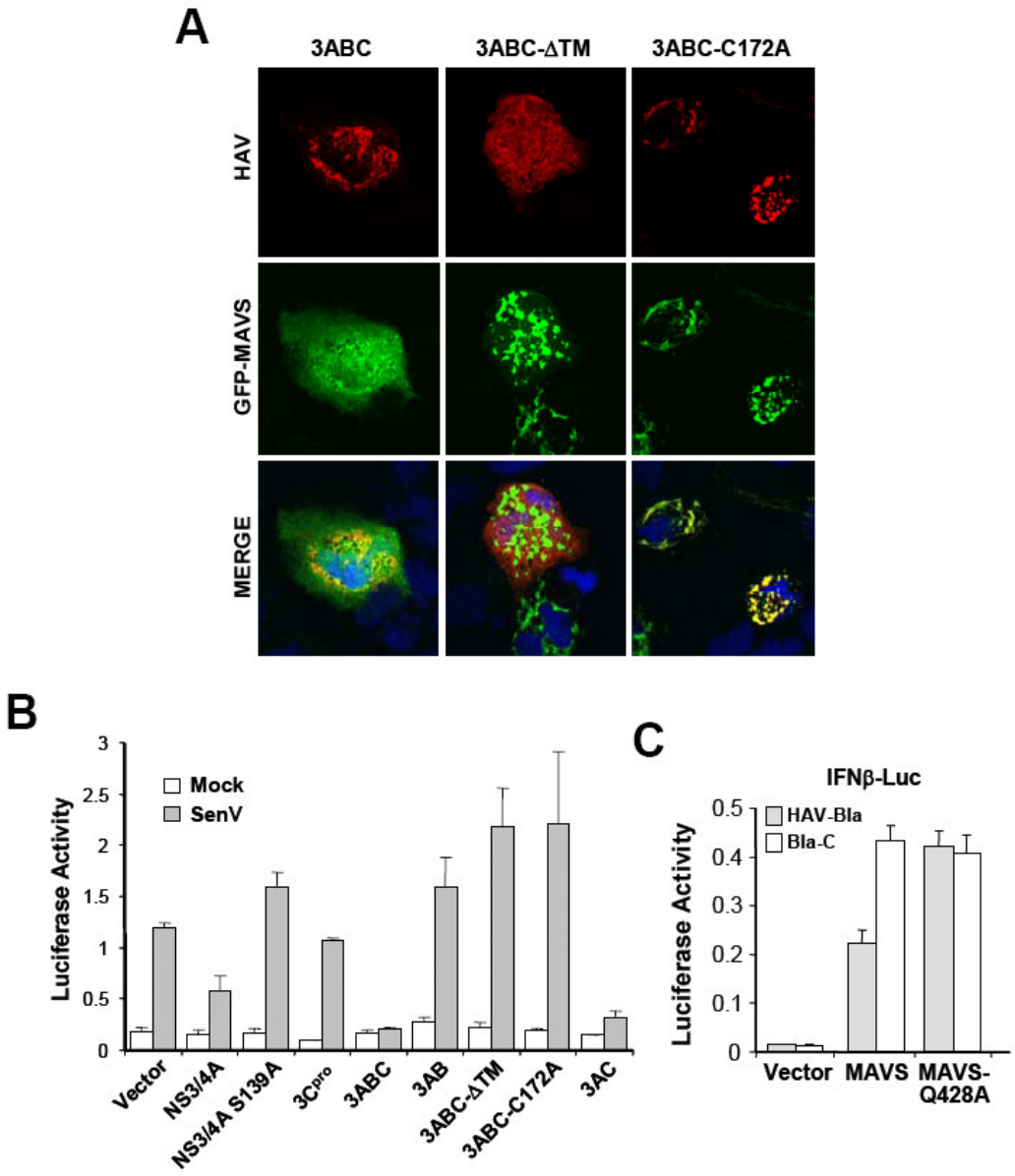

(A) Co-localization of 3ABC and MAVS. Confocal microscopic images of cells expressing 3ABC, or the mutant 3ABC-ΔTM, or 3ABC-C172A. Top frames show HAV proteins labeled with anti-Flag (red), while

the middle frames show GFP fluorescence of GFP-MAVS. **(B)** IFN-β promoter activities in transfected FRhK-4 cells expressing various segments of the HAV polyprotein, and the HCV NS3/4A protease for comparison, following infection with SenV. **(C)** The HAV replicon does not interfere with activation of the IFN-β promoter induced by overexpression of MAVS-Q428A. IFN-β promoter assays were carried out in HAV-Bla and Bla-C cells transfected with vectors expressing constitutively MAVS or the MAVS-Q428A mutant which is resistant to 3ABC-mediated cleavage.

Figure 2.11: *In vitro* cleavage of MAVS by GST-3ABC.

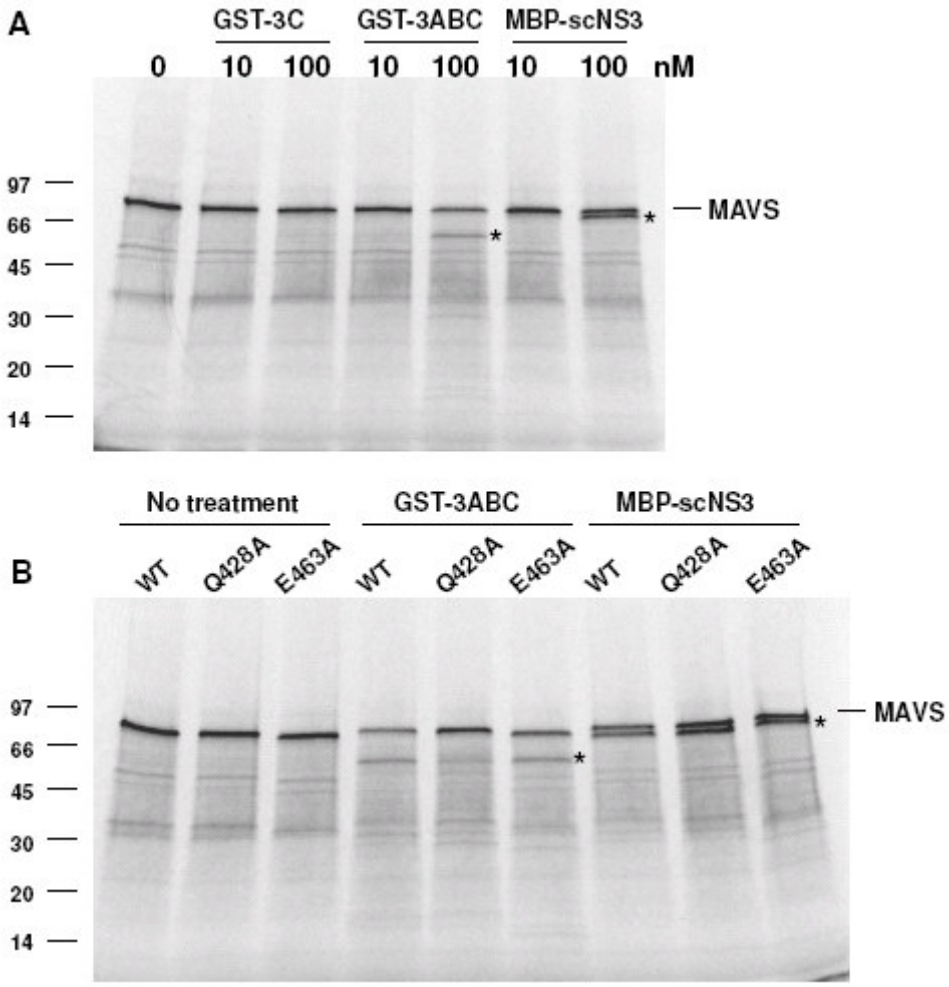

(A) Cleavage of *in vitro* translated MAVS by purified recombinant proteases. [^{35}S]-labeled MAVS was produced *in vitro* in a coupled transcription/translation reaction, and incubated with proteases at indicated concentration. Asterisks indicate cleavage products. **(B)** *In vitro* cleavage of wild-type MAVS and mutants by GST-3ABC and MBP-scNS3.

Chapter 3: Inhibition of TLR3 Signaling by a Picornaviral Protease-Polymerase Precursor through Cleavage of the Adaptor Protein TRIF

3.1 Abstract

Toll-like receptor 3 (TLR3) and RIG-I-like helicases (RIG-I and MDA5) recognize virus-derived double-stranded (ds) RNA and activate innate immune signaling pathways through the adaptor proteins TRIF and MAVS, respectively. Previously, we demonstrated that hepatitis A virus (HAV), a hepatotropic picornavirus, disrupts RIG-I/MDA5 signaling by targeting the adaptor protein MAVS for cleavage by the viral 3ABC cysteine protease precursor. Here we show that HAV also inhibits TLR3 signaling by targeting the adaptor protein TRIF for degradation through the action of a distinct viral protein, the 3CD protease-polymerase precursor. TRIF is proteolytically cleaved *in vivo* by 3CD, not by the mature 3Cpro protease or the 3ABC precursor. The 3CD cleavage of TRIF depends on both the cysteine protease activity of 3Cpro and the 3Dpol sequence, but not 3Dpol polymerase activity, in an "*in cis*" manner. 3CD cleaves TRIF at two non-canonical 3Cpro cleavage sites in an ordered process in which cleavage at Gln-554 is a prerequisite to cleavage at Gln-190. Mutagenesis data indicate that 3CD possesses altered substrate specificity, allowing it to recognize and cleave non-canonical 3Cpro cleavage sites within TRIF that are normally resistant to 3Cpro. HAV thus blocks both RIG-I/MDA5 and TLR3-dependent signaling pathways through cleavage of the adaptors by distinct protease precursors derived from a common polyprotein.

3.2 Introduction

Toll-like receptor 3 (TLR3) and RIG-I-like helicases, including retinoic acid-inducible gene I (RIG-I) and melanoma differentiation-associated gene 5 (MDA5), are

pathogen-associated pattern recognition receptors that detect virus-specific double stranded RNA (dsRNA) and activate antiviral signaling pathways (5, 117, 193-194). Upon binding with viral dsRNA, these receptors complex with adaptor proteins, which engage downstream kinases to activate two critical transcription factors, NF-κB and interferon regulatory factor 3 (IRF3), in the induction of type I interferons (IFN-α and IFN-β) and IFN-stimulated genes (ISGs) that result in the establishment of an antiviral state (117). TLR3 is a transmembrane protein with an extracellular RNA-binding domain and an intracellular Toll/IL-1 receptor (TIR) domain responsible for signaling, whereas RIG-I and MDA5 are homologous cytoplasmic caspase-recruitment domain (CARD)-containing helicases (5, 193-194). RIG-I and MDA5 share a common CARD adaptor protein, the mitochondrial antiviral signaling protein (MAVS, also known as IPS-1, VISA or Cardif) which is localized on the mitochondrial outer membrane (80, 115, 156, 184). In the parallel, but independent, TLR3 signaling pathway, TLR3 signals to downstream kinases via the TIR domain-containing adaptor inducing IFN-β (TRIF, also known as TICAM-1) (127, 189). TRIF is a multidomain protein that contains N-terminal TRAF6-binding motifs, a central TIR domain responsible for interaction with the TIR domain of TLR3, and a C-terminal RIP homotypic interaction motif (RHIM) (74, 127, 150, 189). Recent studies showed that TRIF-mediated activation of IRF3 requires both its TIR domain and N-terminal region, whereas NF-κB can be activated by two independent mechanisms: one through the TIR domain and N-terminal region, and the other through the C-terminal RHIM motif which also induces apoptosis as a distinct host defense mechanism (74, 150).

The roles of RIG-I/MDA5 and TLR3 in host antiviral responses have also made them targets for viral interference. Hepatitis C virus (HCV), a positive-strand RNA virus associated with chronic viral hepatitis and liver cancer (140), is known to disrupt both

RIG-I and TLR3 signaling pathways through cleavage of the adaptor proteins MAVS and TRIF, respectively, by the viral NS3/4A serine protease (95-96, 103, 115). This immune evasion mechanism is believed to suppress expression of multiple host defense genes and may contribute to the unique ability of HCV to establish persistent infection within the liver. Hepatitis A virus (HAV), a member of the Picornaviridae family, is also a hepatotropic positive-strand RNA virus, but unlike HCV, it only causes acute hepatitis and is incapable of persistent infection. Nonetheless, a clinically silent period of 3-5 weeks follows initial HAV infection, characterized by active viral replication and shedding with no signs of hepatic inflammation (92). This suggests that HAV may also be capable of blocking immune responses in the early infection phase. Indeed, we recently showed that like HCV, HAV also disrupts virus-induced activation of the RIG-I/MDA5 pathway by targeting the adaptor protein MAVS for proteolysis by the 3ABC cysteine protease precursor (190). Cleavage of MAVS by 3ABC requires both the protease activity of 3Cpro and a transmembrane domain in 3A that directs 3ABC to mitochondria where MAVS is localized (190). The shared ability of HAV 3ABC protease precursor and HCV NS3/4A protease to disrupt RIG-I/MDA5 signaling supports a critical role for this pathway in liver antiviral defense. However, it remains unclear whether the TLR3 signaling pathway is equally important in host control of HAV, and whether it is also regulated by HAV.

Here we show that HAV infection strongly inhibits TLR3 signaling, and that this is associated with reduced abundance of the adaptor protein TRIF. We demonstrate that TRIF is proteolytically cleaved by the viral 3CD protease-polymerase precursor, and that this requires both the cysteine protease activity of 3Cpro and the 3Dpol region in an "*in cis*" manner. Our data also reveal a unique order of processing in the 3CD cleavage of TRIF, and an unexpected role of the 3Dpol domain in modulating the substrate specificity

of 3CD that allows it to cleave non-canonical 3Cpro cleavage sites within TRIF. This study thus provides a second major mechanism by which HAV evades innate immune responses.

3.3 Materials and Methods

Cells and Viruses Human embryonic kidney (HEK) 293FT cells (Invitrogen), Huh7 human hepatoma cells, and Huh7-derived Huh7.5 and Bla-C cells (190) were cultured in DMEM with 8% FBS. The same medium supplemented with Blasticidin was used to culture Huh7 and Huh7.5 cells expressing control vector, TLR3, and TLR3 ΔTIR mutant (179), and the HAV-Bla subgenomic replicon cells (190). The cell culture-adapted HAV strain HM175/18f was amplified in Huh7 cells. Viral titers were determined in fetal rhesus kidney FRhK-4 cells.

Plasmids and Antibodies The TRIF expression vector pCDNA6-TRIF and pCMV-HA vectors expressing N-terminally HA-tagged HAV proteins were constructed as previously described (95, 190). Truncations of TRIF were generated by PCR, and point mutations within TRIF and 3CD were generated by site-directed mutagenesis (Strategene). Plasmids pIFN-β-Luc (Rongtuan Lin, McGill University), pPRD-II-Luc (Michael Gale, University of Washington), pCMV-β-gal (Clontech), pEF-Bos-TRIF (Kate Fitzgerald, University of Massachusetts) and pCDNA3-Flag-IKKi (Tom Maniatis, Harvard University) were obtained from the indicated sources. Antibodies against TLR3 (Ilkka Julkunen, National Institute for Health and Welfare, Finland), TRIF S219 (Cell Signaling Technology, used for most TRIF immunoblots unless otherwise indicated), TRIF aa 4-31 (Alexia), HAV 2A and 3C (Verena Gauss-Muller, University of Lubeck, Germany), ISG15 (Santa Cruz), HA and Actin (Sigma) were gifts or purchased from the indicated sources. Rabbit anti-TRIF antibody S537-2 was obtained by immunization of rabbits with recombinant TRIF protein expressed and purified from *E. coli* (95).

Transfection and Luciferase Reporter Assays For protein expression, cells were transfected with the indicated plasmids using Lipofectamine 2000 (Invitrogen) and after 20 hours lysed in 1% NP-40 lysis buffer. For luciferase reporter assays, expression and/or Luc reporter plasmids were transfected into cells (seeded in triplicate in 96-well format) with the internal pCMV-β-gal transfection control. At 20 hours posttransfection, when indicated, poly(I:C) (Sigma) was added to the medium and incubated for additional 6 hours. Cells were then lysed in Reporter Lysis Buffer (Promega) and equal amount of lystaes were used for luciferase and β-galactosidase assays (Promega). In the case of HAV infection, cells were infected with HAV at a MOI of 3 and cultured for 4 days prior to transfection.

Immunoprecipitation and immunoblotting For detection of endogenous TRIF, 1 mg of cell lysate was immunoprecipitated with 1 μg of rabbit anti-TRIF antibody S537-2, followed by immunoblotting with TRIF antibody from Cell Signaling Technology. A similar procedure was used to detect expression of HA-3CD constructs, except using HA antibody for immunoprecipitation and rabbit anti-3C antibody for immunoblotting.

3.3 Results

HAV inhibits TLR3 signaling by down-regulating the abundance of the adaptor protein TRIF. Recent studies demonstrated that TLR3 is expressed and functional in primary hepatocytes (179). However, the Huh7 hepatoma cell line, which supports replication of both clinically isolated and cell culture-adapted HAV strains (84), is TLR3-deficient (179). To investigate whether HAV disrupts TLR3 signaling in an hepatocyte-derived TLR3-competent cell line, we first reconstituted TLR3 expression in Huh7 cells by lentiviral transduction of TLR3 and established three isogenic cell lines: Huh7-vector, Huh7-TLR3, and Huh7-ΔTIR which contains a TIR domain-deleted TLR3 (Fig. 3.1*A*). Stimulation of Huh7-TLR3 cells with extracellularly applied poly(I:C), a

synthetic dsRNA analog, induced transcriptional activation of IFN-β promoter and expression of IFN-stimulated genes such as ISG15, which were not observed in Huh7-vector or Huh7-ΔTIR cells (Fig. 3.1*A, B*). However, infection of Huh7-TLR3 cells with a cell culture-adapted variant of HAV, HM175/18f, strongly inhibited poly(I:C) induction of IFN-β promoter and ISG15 expression (Fig. 3.1*A*, *B*). The expression levels of TLR3 and its ΔTIR mutant were not affected by HAV (Fig. 3.1*A*), suggesting that HAV disrupts TLR3 signaling not by reducing TLR3 abundance.

The TLR3 pathway can be activated by either extracellular poly(I:C) stimulation or overexpression of the adaptor protein TRIF or downstream kinases such as TBK-1 or IKKi (Fig. 3.1*C*). This allowed us to determine which step of the TLR3 signaling pathway was disrupted by HAV. Activation of IFN-β promoter by TRIF overexpression was reduced by HAV by about 50% (Fig. 3.1*C*), consistent with a previous report using rhesus monkey FRhK-4 cells (43). In contrast, HAV had no effect on activation of IFN-β promoter by the downstream kinase IKKi (Fig. 3.1*C*), suggesting that HAV disrupts TLR3 signaling at the TRIF level or upstream of TRIF. Consistent with the diminished TRIF function, the abundance of endogenous TRIF was significantly reduced in HAV-infected Huh7 cells (Fig. 3.1*D*). HAV also reduced endogenous TRIF level in the RIG-I-deficient, but TLR3-competent Huh7.5-TLR3 cells (Fig. 3.1*D*), suggesting that HAV-induced reduction of TRIF is independent of the RIG-I pathway and also does not require the TLR3 partner. The abundance of endogenous TRIF was also markedly reduced in a stable Huh7 cell line harboring an HAV subgenomic replicon (HAV-Bla), as compared to the isogenic Bla-C cell line that was cured of HAV replicon by IFN-α treatment (190) (Fig. 3.6). Collectively, these results suggest that HAV inhibits TLR3 signaling by down-regulating the abundance of the essential TRIF adaptor.

The HAV 3CD protease-polymerase precursor disrupts TLR3 signaling through cleavage of TRIF. The HAV-induced down-regulation of TRIF is reminiscent of that of the RIG-I/MDA5 signaling adaptor MAVS, which is targeted for degradation by the HAV 3ABC protease precursor (190). We thus speculated that a viral protein(s) may be responsible for reducing the abundance of TRIF, thereby disrupting TLR3 signaling. To explore this possibility, individual viral proteins and intermediate processing precursors were ectopically expressed in Huh7-TLR3 cells to determine their effects on poly(I:C)-induced, TLR3-dependent activation of IFN-β promoter. While proteins from the P1-2A structural region (P1-2A, VP0, VP3, VP1-2A) and the 2BC region (2BC, 2B, 2C) had little or no effect on TLR3 signaling, the polyprotein processing intermediate 3ABCD, and its partially processed 3CD protease-polymerase precursor, strongly blocked TLR3 signaling (Fig. 3.2*A*). Since 3ABCD is the precursor of 3CD, its inhibitory effect on TLR3 signaling is most likely through production of the 3CD effecter. The 3ABC protease precursor, which is also derived from the 3ABCD polyprotein but targets the RIG-I/MDA5 signaling adaptor MAVS (190), had no effect on TLR3 signaling (Fig. 3.2*A*). We also found no significant blocking of TLR3 signaling by the mature 3Cpro protease (Fig. 3.2*A*), although immunoblotting suggested that it was expressed at far more excessive level than other 3C-containing precursors (Fig. 3.2*B*). Since ectopic expression of individual viral proteins may cause artificial effects not found in viral infection, we next investigated whether 3CD inhibited TLR3 signaling by reducing the abundance of TRIF, as was the case in HAV-infected cells. Co-expression of TRIF with 3CD or other viral proteins in HEK 293FT cells (which express negligible amount of endogenous TRIF) showed that the level of ectopically expressed TRIF was significantly reduced by 3CD, but was not affected by other viral proteins (Fig. 3.2*C*). The reduction of full-length TRIF by 3CD was accompanied by the appearance of two

smaller TRIF fragments with apparent molecular weights of 75-kDa and 55-kDa (indicated by arrows in Fig. 3.2*C*), both detected by an antibody that recognizes residues surrounding S219 of TRIF. Since the sum of the two fragments are larger than the full-length TRIF (90-kDa), they are most likely overlapping fragments, or the 75-kDa fragment is a cleavage intermediate that is further cleaved into the 55-kDa fragment. Using a different antibody reacting to aa 4-31 of TRIF, we found another 3CD-generated TRIF fragment with an apparent molecular mass of 20-kDa, corresponding to the N-terminal region of TRIF (Fig. 3.2*D*). The accumulation of at least three different sizes of TRIF fragments indicated that 3CD induces multiple cleavage events within the TRIF protein. Since 3CD is known to be a catalytically active precursor of the 3Cpro cysteine protease (135), it is likely to directly cleave TRIF through the cysteine protease activity.

TRIF is known to be cleaved by cellular caspases at residues D281 and D289 upon pro-apoptotic stimulation, including overexpression of TRIF itself (141). However, the caspase-cleaved 38-kDa TRIF fragment was distinct from those generated by 3CD (Fig. 3.7*A*). Moreover, a D281E-D289E (DDEE) double mutant of TRIF, which was shown previously to be resistant to caspase cleavage as evidenced by the lack of 38-kDa caspase cleavage fragment (141), was still cleaved in the presence of 3CD (Fig. 3.7*A*). These data suggest that 3CD-mediated cleavage of TRIF is not through cellular caspases, but rather by its own protease activity. Interestingly, a pan-caspase inhibitor, z-VAD-fmk, also inhibited 3CD-mediated cleavage of TRIF (Fig. 3.7*B*). Although widely used as a caspase inhibitor, z-VAD-fmk is known to inhibit other cellular enzymes containing cysteine active sites (120), which may explain its inhibitory effect on the 3Cpro cysteine protease activity within 3CD.

3CD cleavage of TRIF requires 3Cpro protease activity and the 3Dpol moiety in an "*in cis*" manner. Given that TRIF is cleaved by 3CD, but not by the mature 3Cpro,

we tested whether an unprocessed 3CD or a post-processing 3C-3D complex is required to cleave TRIF. We co-expressed TRIF with either 3CD or a mixture of 3Cpro and 3Dpol in 293FT cells, along with 3Cpro or 3Dpol as negative control. Unlike 3CD, the mixture of 3Cpro and 3Dpol did not cleave TRIF (Fig. 3.3*B*), suggesting that cleavage of TRIF requires both 3Cpro and 3Dpol in a precursor form, not as a complex. To confirm this, we created both hypo- and hyper-processing mutants of 3CD by modifying the 3C/3D cleavage efficiency. The 3C/3D junction consists of a primary 3Cpro cleavage site IESQ↓R and an alternative cleavage site EFTQ↓C, separated by nine amino acids (Fig. 3.8*A*). In the 3CD hypo-processing mutant QQRR, both cleavage sites were abolished by Q-to-R mutations (Fig. 3.8*A*), thereby producing only 3CD precursor (Fig. 3.8*B*). In the 3CD hyper-processing mutant LWG, the primary 3C/3D cleavage site was optimized to LWSQ↓G, identical to the highly efficient 2C/3A cleavage site (Fig. 3.8*A*). This mutant accumulated less 3CD precursor but produced more mature 3Cpro due to enhanced 3C/3D processing (Fig. 3.8*B*). As result, TRIF was cleaved by the 3CD hypo-processing mutant QQRR, but not by the hyper-processing mutant LWG (Fig. 3.8*C*), confirming that 3CD cleavage of TRIF requires both 3Cpro and 3Dpol in an "*in cis*" manner.

We next determined if both 3Cpro protease and 3Dpol polymerase activities are required for 3CD cleavage of TRIF. An Ala substitution (C172A) of the 3Cpro active site nucleophile Cys-172 (Fig. 3.3*A*) completely abolished the ability of 3CD to cleave TRIF (Fig. 3.3*C Top*). This correlated with the loss of 3CD auto-protease activity, as evidenced by the absence of mature 3Cpro that was normally processed from the 3CD precursor (Fig. 3.3*C Lower*). These results confirmed that the 3Cpro cysteine protease activity of 3CD is responsible for cleavage of TRIF. A highly conserved GDD motif within 3Dpol (Fig. 3.3*A*) is essential for the RNA-dependent RNA polymerase activity. However, a 3CD mutant carrying a GDD-to-GAA mutation was still able to cleave TRIF (Fig. 3.3*C*

Top), suggesting that the 3Dpol polymerase activity is not required for 3CD cleavage of TRIF. This mutant also produced mature 3Cpro, albeit at reduced level (Fig. 3.3*C Lower*), confirming the cysteine protease activity. We also introduced a C486S mutation into the CDLS sequence located at the C-terminus of 3Dpol that resembles a CXXX prenylation signal (Dr. Jeffrey Glenn, personal communication) (Fig. 3.3*A*). This mutation somehow enhanced 3CD cleavage of TRIF (Fig. 3.3*C Top*), most likely due to increased 3CD expression by a yet unknown mechanism, which also resulted in more production of mature 3Cpro (Fig. 3*C Lower*). Consistent with their abilities to cleave TRIF, both 3CD GAA and 3CD C486S mutants inhibited poly(I:C)-induced activation of IFN-β promoter in Huh7-TLR3 cells as efficiently as the wild-type (WT) 3CD, whereas the 3CD C172A mutant failed to block activation of IFN-β promoter (Fig. 3.3*D*). Put together, these results suggest that 3CD cleavage of TRIF and blocking of TLR3 signaling depend on both 3Cpro protease activity and the 3Dpol moiety, but not the 3Dpol polymerase activity, in an "*in cis*" manner.

3CD cleaves TRIF at Gln-190 and Gln-554 in an ordered process. To further confirm that 3CD directly cleaves TRIF, we examined the amino acid sequence of human TRIF for potential 3Cpro cleavage sites. Previous studies based on the 3Cpro cleavage sites within HAV polyprotein revealed a strict requirement of Gln at the P1 position (except for the 3A/3B cleavage site which has a Glu in place of Gln) and a consensus sequence (L, V, I)X(S, T)Q↓X, where X can be any amino acid (155). The 3ABC cleavage site in MAVS, LASQ, is a perfect fit with this consensus sequence (190). However, TRIF does not contain sequences that completely fit the consensus 3Cpro cleavage sequence; instead, it contains several sequences that partially fit the consensus sequence. In addition to the strictly required Gln at P1 position, these sequences have either hydrophobic (or aromatic) amino acid at the P4 position or serine/thronine at the

P2 position, but not satisfying both positions, and therefore may potentially serve as non-canonical 3Cpro cleavage sites (Fig. 3.4*A Left*). Considering the sizes of 3CD-cleaved TRIF fragments (75-, 55-, and 20-kDa, see Fig. 3.2*C*, *D*), we focused on two clusters of possible cleavage sites (Fig. 3.4*A Right*) that are likely to generate such lengths of fragments. To determine which sites were actually cleaved by 3CD, we generated a series of TRIF mutants by substituting the invariant Gln at the potential cleavage sites with Arg, and examined their cleavage by 3CD. Co-expression of these TRIF mutants with 3CD showed that cleavage of TRIF was not affected by the Q211R, Q581R-Q583R, or Q612R mutation (Fig. 3.4*B*), excluding these as 3CD cleavage sites. In contrast, the Q190R mutation blocked the cleavage event that generates the 55-kDa but not the 75-kDa fragment, while the Q552R-Q554R mutation completely abolished 3CD cleavage of TRIF, eliminating both cleavage fragments (Fig. 3.4*B*). We further separated the Q552R and Q554R mutations and determined that the effect of Q552R-Q554R mutation is due to the Q554R mutation (Fig. 3.4*C*). These results established Q190 and Q554 as 3CD cleavage sites within TRIF, and clarified the identities of the observed TRIF cleavage fragments. The 75-kDa fragment thus results from cleavage at Q554 and corresponds to aa 1-554 of TRIF (Fig. 3.9*A*). This fragment is further cleaved at Q190, giving rise to the 55-kDa and 20-kDa fragments that correspond to aa 191-554 and 1-190, respectively (Fig. 3.9*A*).

The different effects of Q190R and Q554R mutations on cleavage of TRIF indicated that 3CD cleaves TRIF in an ordered process. The fact that cleavage at Q190 could not proceed when the Q554 cleavage site was blocked (Fig. 3.4*B*, *C*) suggests that cleavage at Q554 is a prerequisite to cleavage at Q190. We thus propose a "two-step" cleavage model for the 3CD cleavage of TRIF, in which the first cleavage at Q554 site

induces a conformational change that exposes the Q190 site for the second cleavage (Fig. 3.4*D*).

The N-terminal region of TRIF contains three TRAF6-binding motifs that are important for activation of transcription factors NF-κB and IRF3 in TLR3 signaling (149-150). The Q190 cleavage site is located between the first and second TRAF6-binding motifs (Fig. 3.9*A*). The Q554 cleavage site is located between the TIR domain and RHIM motif (Fig. 3.9*A*), both important for transcriptional activation of IFN-β (74). Cleavage of at these two sites could yield fragments with no or diminished signaling ability, or with dominant negative effect over the full-length TRIF. In this regard, we ectopically expressed the 3CD-generated TRIF fragments N-190 (aa 1-190), N-554 (aa 1-554), M-364 (aa 191-554) and C-158 (aa 555-712), and examined their abilities to activate IFN-β and NF-κB-specific (PRD-II) promoters by luciferase reporter assay. While the N-190 and C-158 fragments were incapable of activating IFN-β or NF-κB promoter, the N-554 and M-364 fragments were able to activate both IFN-β and NF-κB promoters (Fig. 3.9*B*). When mixed with wild-type (WT) TRIF at 1:1 ratio, the N-190 and C-158 fragments did not reduce the signaling ability of WT TRIF (Fig. 3.9*C*), indicating that they do not have dominant negative effects. Although these results suggest that some of the 3CD-generated TRIF fragments are still capable of signaling when ectopically expressed, such fragments were not detected in terms of endogenous TRIF in HAV-infected cells (Fig. 3.1*D*) or in HAV replicon cell line (Fig. 3.6*B*), probably due to rapid degradation after cleavage.

Altered substrate specificity of 3CD contributes to cleavage of TRIF. We next addressed the question of why TRIF is cleaved by 3CD but not by 3Cpro. The 3CD cleavage sites within TRIF, $DWSQ_{190}$ and $EQSQ_{554}$, are both non-canonical 3Cpro cleavage sites in that the P4 position is occupied by acidic amino acid (D or E) instead of

hydrophobic amino acid (L, I or V) in consensus 3Cpro cleavage sequence (Fig. 3.5*A*), which could explain why they can not be cleaved by 3Cpro. These sites were nonetheless efficiently cleaved by 3CD, suggesting that 3CD may possess altered substrate specificity that tolerates or prefers acidic amino acids at the P4 position. To test this possibility, we first compared 3Cpro and 3CD on a canonical substrate, the HAV P1-2A polyprotein. When co-expressed in 293FT cells, 3Cpro readily processed P1-2A into VP1-2A, whereas 3CD cleaved P1-2A very poorly (Fig. 3.5*B*). This was in striking contrast to their abilities to cleave TRIF (Fig. 3.2*C*; 3.3*B* and *C*; 3.5*D*), suggesting that unlike 3Cpro, 3CD may prefer a non-canonical substrate over a canonical substrate. If this is the case, changing the non-canonical cleavage sites within TRIF into canonical sites would allow TRIF to be cleaved by 3Cpro. To test this, we created TRIF mutants by substituting the P4 position amino acids Asp-187 and Glu-551 with 3Cpro-preferred Leu (D187L and E551L, respectively, Fig. 3.5*A*), and examined their cleavage by 3Cpro and 3CD. In contrast to WT TRIF which was cleaved by 3CD but not by 3Cpro, the D187L mutant, now carrying a LWSQ cleavage sequence, was readily cleaved by both 3Cpro and 3CD, which yielded a novel cleavage fragment with an apparent molecular mass of 70-kDa (Fig. 3.5*D*, lanes 5 and 6). This 70-kDa fragment had a same migration pattern as the TRIF C-522 fragment corresponding to aa 191-712 (Fig. 3.5*C*; Fig. 3.5*D*, lane 5 vs. 14), confirming that the cleavage occurred at the Q190 site. As expected, this fragment was not further cleaved by 3Cpro, but was further processed by 3CD at the Q554 site, generating the same 55-kDa fragment as 3CD did on WT TRIF (Fig. 3.5*D*, lane 3 vs. 6). On the other hand, the TRIF E551L mutant, now carrying a LQSQ cleavage sequence, was cleaved by 3CD in a same pattern as the WT TRIF (Fig. 3.5*D*, lane 3 vs. 9), and was only marginally cleaved by 3Cpro (Fig. 3.5*D*, lane 7 vs. 8). Nonetheless, when the two mutations were combined, the double mutant (DELL) was readily cleaved by both 3Cpro

and 3CD, generating the same 70- and 55-kDa fragments (Fig. 3.5*D*, lane 10 vs. 11 and 12), although 3Cpro seemed to be less efficient than 3CD in converting the 70-kDa fragment into 55-kDa fragment (Fig. 3.5*D*, lane 11 vs. 12). Taken together, these results demonstrated that changing the non-canonical cleavage sites within TRIF into canonical sites allows 3Cpro to cleave TRIF, confirming that the different abilities of 3CD and 3Cpro in cleavage of TRIF is at least in part due to their difference in substrate specificity.

3.4 Discussion

The importance of pattern recognition receptors in sensing of viral infection and activation of innate immunity is often reflected by the counteracting mechanisms evolved by viruses. A perfect example is the HCV NS3/4A protease, which disrupts both RIG-I and TLR3 signaling pathways by proteolytically cleaving the signaling adaptor proteins MAVS and TRIF, respectively. Unlike HCV, HAV RNAs are believed to be sensed by MDA5, since their 5' ends are covalently linked to the viral 3B(VPg) peptide, thus unlikely to be detected by RIG-I. Nonetheless, since both RIG-I and MDA5 pathways share MAVS as a common adaptor, they are similarly disrupted by 3ABC cleavage of MAVS (190). As the only known extracellular dsRNA receptor involved in innate immunity, TLR3 is presumably responsible for sensing both HAV and HCV RNAs from a cell surface or endosomal location. Here we showed that TLR3 signaling is also inhibited by HAV through cleavage of the adaptor TRIF by the 3CD protease-polymerase precursor. The targeting of RIG-I/MDA5 and TLR3 signaling pathways by both HAV and HCV proteases strongly supports the important roles of these pathways in host antiviral defense within the liver. The shared ability of HAV and HCV to disrupt both RIG-I/MDA5 and TLR3 signaling also raises a question of whether other mechanism(s)

of immune evasion may account for the high frequency of HCV persistent infection that is not observed in HAV infection.

The ability of HAV to disrupt both RIG-I/MDA5 and TLR3 signaling pathways is likely to contribute to the clinical silent period of 3-5 weeks following initial infection. This period is characterized by robust viral replication within the liver and shedding of virus into the feces, which reach their maximum just prior to the onset of hepatic inflammation and liver injury that eventually clear the virus (92). In a recent animal study, we also found little evidence of IRF3-dependent ISG expression (ISG56, ISG15) within the liver of HAV-infected chimpanzees during the first 2 weeks of infection (data not shown). Cleavage of MAVS and TRIF by 3ABC and 3CD, respectively, may deal a double blow to these two major cellular antiviral response pathways and facilitate viral replication during this clinically quiet phase of infection.

Although both HAV and HCV target TRIF for degradation, there are significant differences between the viral proteases that are involved, and the fashion in which they cleave TRIF. In the case of HCV, TRIF is cleaved by the fully processed and assembled NS3/4A protease complex (95); for HAV, it is the 3CD protease-polymerase precursor that cleaves TRIF. TRIF is not cleaved by mature 3Cpro, 3Dpol, or a mixture of 3Cpro and 3Dpol (Fig. 3.3*B*), indicating that cleavage of TRIF requires both 3Cpro and 3Dpol in an "*in cis*" manner. This is further supported by the fact that TRIF is cleaved by a 3CD hypo-processing mutant (which only produces the unprocessed 3CD precursor) but not by a 3CD hyper-processing mutant (in which the 3C/3D processing is enhanced) (Fig. 3.8). 3CD is also different from NS3/4A in the way it cleaves TRIF. NS3/4A cleaves TRIF at a single Cys-372 site (95), whereas 3CD cleaves TRIF at two sites, Gln-190 and Gln-554, in an ordered process. A Gln-to-Arg mutation blocked cleavage at Gln-190 without affecting cleavage at Gln-554, but a similar mutation at Gln-554 abolished

cleavage at both sites (Fig. 3.4*C*, *D*), suggesting that cleavage at Gln-554 is a prerequisite to cleavage at Gln-190. We thus propose a "two-step" model for 3CD cleavage of TRIF (Fig. 3.4*E*). In this model, 3CD cleaves TRIF first at Gln-554, but has no access to the Gln-190 site. Cleavage at Gln-554 then induces a conformational change (probably by removing the C-terminal 158-aa region) that exposes the Gln-190 site for the second cleavage. Therefore, our study demonstrated remarkable differences between 3CD and NS3/4A in cleavage of TRIF. Whether these differences result in different efficiency in blocking TLR3 signaling requires further investigation.

Our present work also revealed an unexpected role of the 3Dpol region in modulating the substrate specificity of 3CD. All confirmed 3Cpro cleavage sites within HAV polyprotein and MAVS contain a hydrophobic amino acid (L, I, or V) at the P4 position (155, 190), which fits into the hydrophobic S4 binding pocket within the crystal structure of 3Cpro (14). In contrast, both 3CD cleavage sites within TRIF contain an acidic amino acid (D190 and E551) at the P4 position (Fig. 3.5A), therefore are non-canonical cleavage sites. A previous study showed that a substituted peptide substrate, Ac-E<u>E</u>RTQSFS-NH2 (the E at P4 position is underlined), similar to the TRIF cleavage site $EQSQ_{554}$ in terms of P4 position, is not cleaved by 3Cpro (70). 3CD thus possesses altered substrate specificity that allows it to recognize and hydrolyze non-canonical cleavage sites within TRIF that are otherwise resistant to 3Cpro. In support of this notion, we showed that 3CD actually performs much worse than 3Cpro on a canonical 3Cpro substrate, P1-2A, in clear contrast to their abilities to cleave TRIF (Fig. 3.5*B*). We also provided evidence that changing the non-canonical cleavage sites within TRIF into canonical 3Cpro cleavage sites allows 3Cpro to cleave TRIF (Fig. 3.5*D*), further explaining that the difference between 3CD and 3Cpro in cleavage of TRIF is at least in part due to their difference in substrate specificity. Apparently the altered substrate

specificity of 3CD is conferred by the 3Dpol region, although the exact mechanism remains to be determined.

Like 3ABC, 3CD represents another sample of a common strategy used by HAV and other picornaviruses to create intermediate processing precursors that are functionally distinct from their mature products (128-129, 196). These precursors are made possible by the inefficient processing activity of 3Cpro and suboptimal cleavage sites within the polyprotein (86, 135). Our work on 3ABC (190) and 3CD demonstrated that they are not mere precursors but play indispensable roles in viral evasion of innate immune responses. Within these precursors, 3A and 3D serve as accessory molecules that extend the function of 3Cpro protease to substrates that are otherwise unaccessible (MAVS) or uncleavable (TRIF) by 3Cpro. In this regard, it is plausible that other precursors derived from the common 3ABCD polyprotein, such as 3BC, 3BCD, or 3ABCD itself, may also play discrete roles in viral replication or manipulation of cellular functions.

Figure 3.1: HAV inhibits TLR3 signaling by reducing the abundance of TRIF.

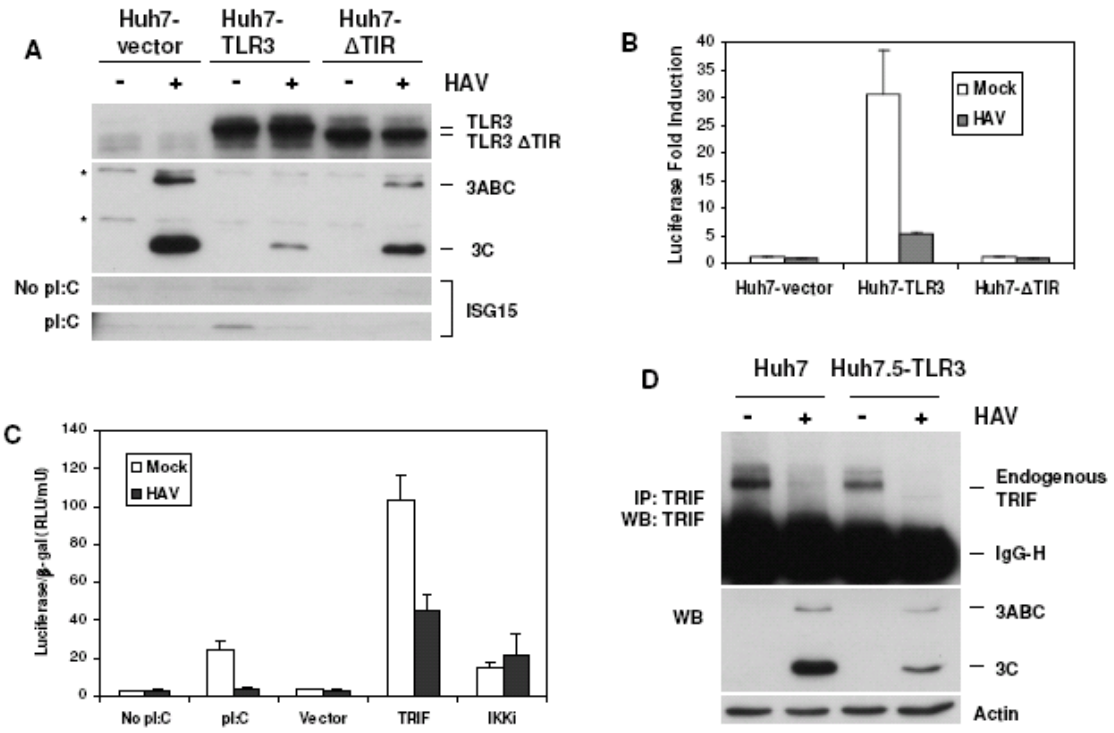

(A) Huh7 cells stably expressing vector, TLR3, or TLR3 ΔTIR mutant were infected with HAV at a MOI of 3 and cultured for 4 days prior to 6 hours of extracellular poly(I:C) stimulation. Expression of TLR3 (top), HAV proteins 3ABC and 3C (middle), and poly(I:C)-induced ISG15 (lower) in mock- and HAV-infected cells were analyzed by immunoblotting. Nonspecific bands detected by 3C antibody were marked by asterisks. **(B)** Extracellular poly(I:C)-induced activation of IFN-β-Luc promoter in the same cells as in (A). **(C)** Poly(I:C), TRIF, or IKKi-induced activation of IFN-β-Luc promoter in mock- and HAV-infected Huh7-TLR3 cells. Luciferase reporter activity was normalized by the internal β-gal transfection control. **(D)** Endogenous levels of TRIF in mock- and HAV-infected Huh7 and Huh7.5-TLR3 cells (top). Endogenous TRIF was analyzed by immunoprecipitation using a rabbit anti-TRIF antibody (95) and detected by immunoblotting with the TRIF antibody from Cell Signaling Technology. HAV infection was confirmed by immunoblot of viral proteins 3ABC and 3C (middle). Actin served as loading control (lower).

Figure 3.2: HAV 3CD disrupts TLR3 signaling through cleavage of TRIF.

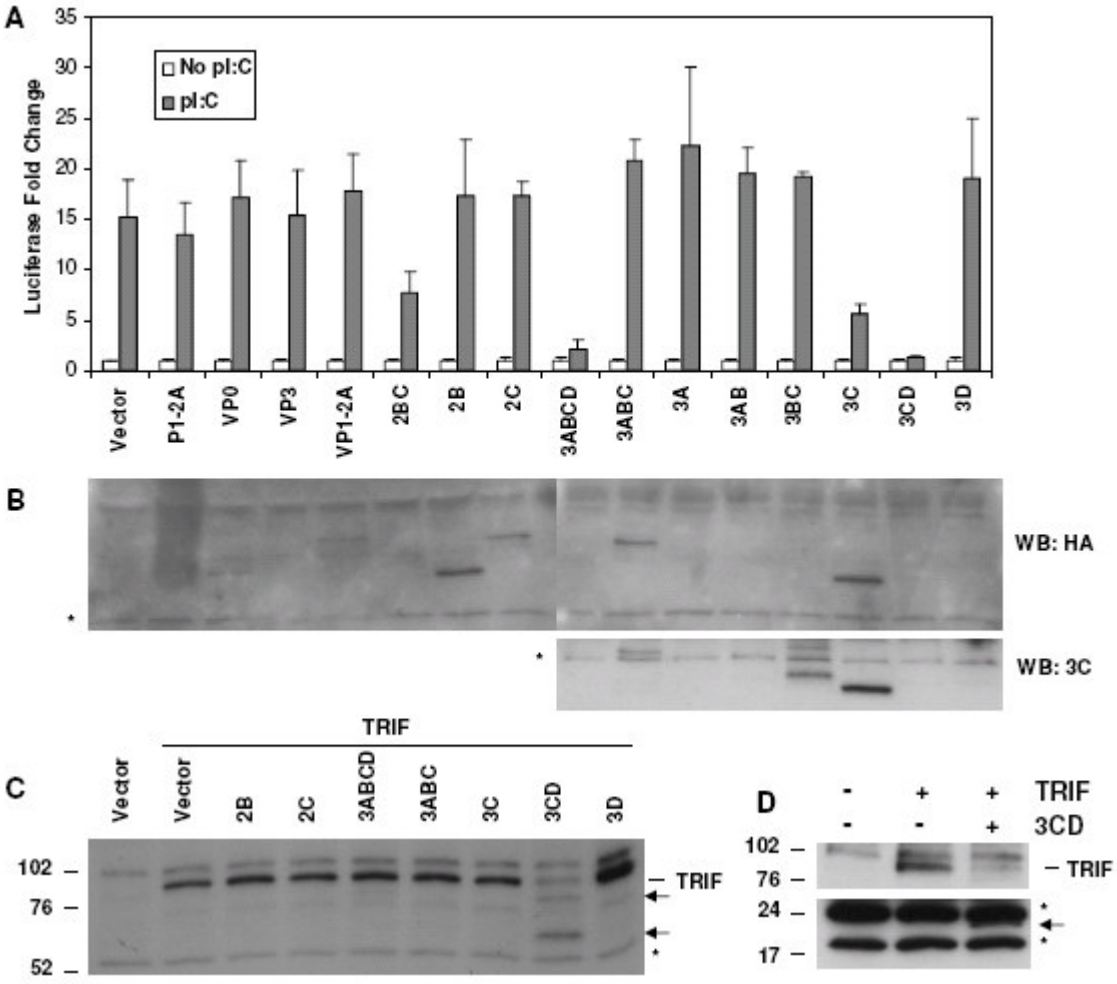

(A) IFN-β-Luc reporter assay of Huh7.5-TLR3 cells transfected with expression vectors encoding HA-tagged HAV proteins and stimulated with extracellular poly(I:C). **(B)** Huh7.5-TLR3 cells were transfected with the same set of expression vectors as in (A). Cell extracts were analyzed by immunoblotting with an HA antibody that detects the HA-tagged HAV proteins, or with the 3C antibody that detects 3C and its precursors. **(C)** HEK 293FT cells were co-transfected with vectors expressing TRIF and HAV nonstructural proteins. Cell lysates were analyzed by immunoblotting with a TRIF antibody (Cell Signaling Technology). In addition to the 90-kDa full-length TRIF, two TRIF fragments, 75- and 55-kDa in size (marked by arrows), were detected in cells expressing 3CD. **(D)** HEK 293FT cells were co-transfected with vectors expressing TRIF and 3CD. Cell lysates were analyzed by immunoblotting with a TRIF antibody

that was produced against a peptide corresponding to TRIF aa 4-31 (Alexia). In addition to the full-length TRIF, a 20-kDa TRIF-immunoreactive fragment (indicated by arrow) was detected in the presence of 3CD. Nonspecific protein bands (marked by *) detected by the antibodies in (B), (C), and (D) indicate equal loading.

Figure 3.3: 3CD cleavage of TRIF requires both the protease activity of 3Cpro and the 3Dpol region in an "*in cis*" manner.

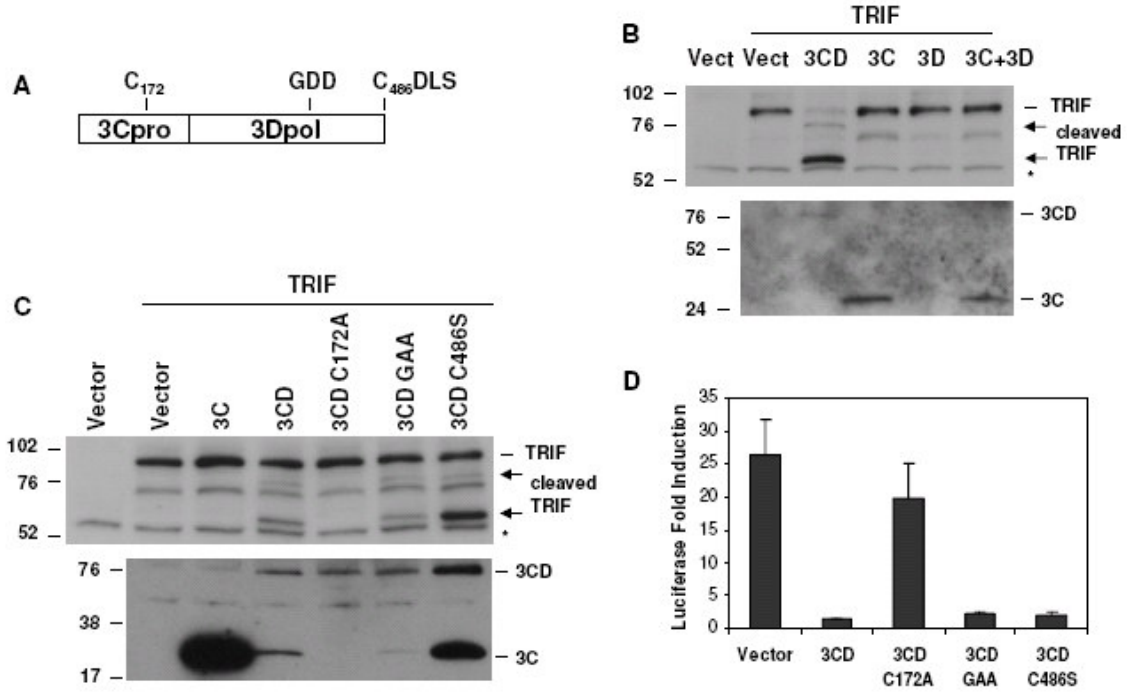

(A) Structural organization of 3CD, showing the Cys-172 residue at 3Cpro active site, GDD polymerase motif of 3Dpol, and a putative CXXX prenylation motif (CDLS) at the C-terminus of 3Dpol. **(B)** and **(C)** HEK 293FT cells were co-transfected with vectors expressing TRIF and HA-tagged 3C, 3D, or 3CD constructs as indicated. TRIF and cleavage fragments (marked by arrows) were detected by immunoblot (upper). HA-tagged 3C and 3CD were analyzed by anti-HA immunopricipation followed by anti-3C immunoblot (lower). A nonspecific protein band (marked by *) detected by TRIF antibody indicates equal loading. **(D)** Luciferase reporter assay of Huh7-TLR3 cells transfected with vectors expressing 3CD constructs and stimulated with extracellular poly(I:C).

Figure 3.4: 3CD cleaves TRIF at Gln-190 and Gln-554 in an ordered process.

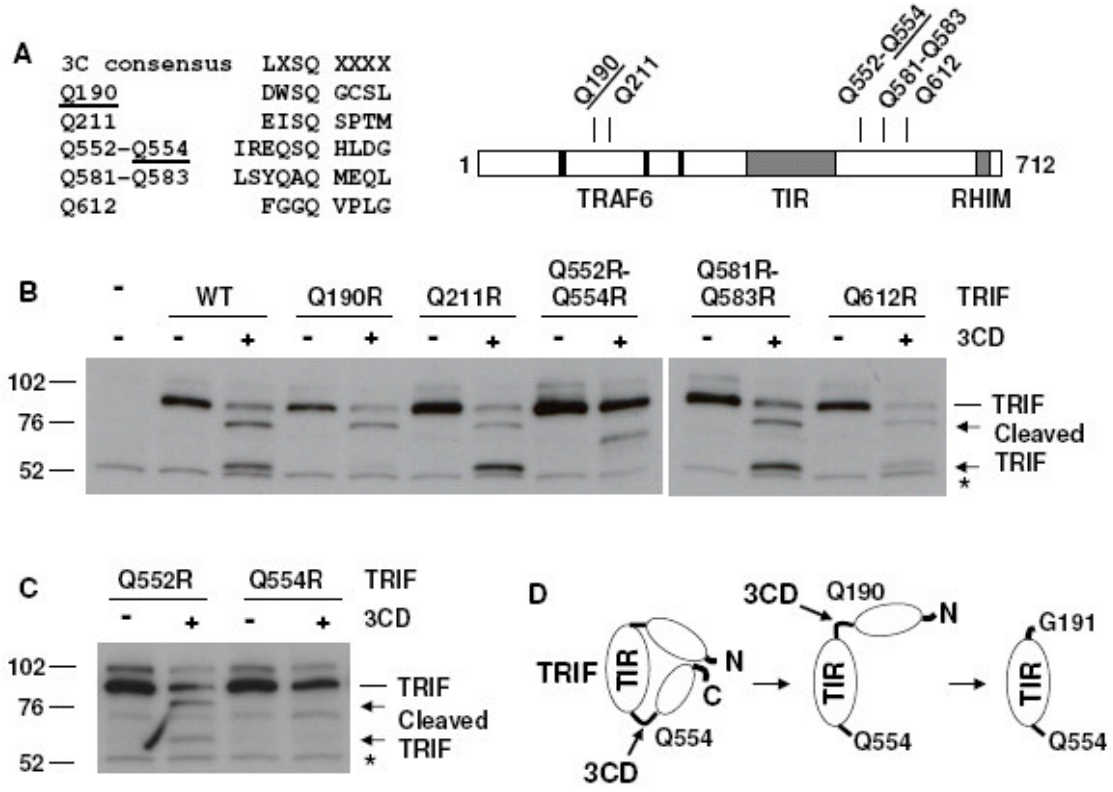

(A) Alignment of the consensus 3Cpro cleavage sequence and possible cleavage sites in TRIF (left), and locations of these sites relative to the TRAF6-binding motifs (black bars) and TIR and RHIM domains (grey boxes) within TRIF (right). Underlined were cleavage sites confirmed by mutational analysis. **(B)** and **(C)** Immunoblots showing cleavage of TRIF in HEK cells co-transfected with vectors expressing TRIF mutants and 3CD. TRIF cleavage fragments were marked by arrows. A nonspecific protein band (marked by *) detected by TRIF antibody indicates equal loading. **(D)** Model for 3CD cleavage of TRIF. Cleavage at the preferred primary Gln-554 site induces a conformational change that exposes the Gln-190 site for the second cleavage.

Figure 3.5: Changing 3CD cleavage sites in TRIF into canonical sites allows 3Cpro to cleave TRIF.

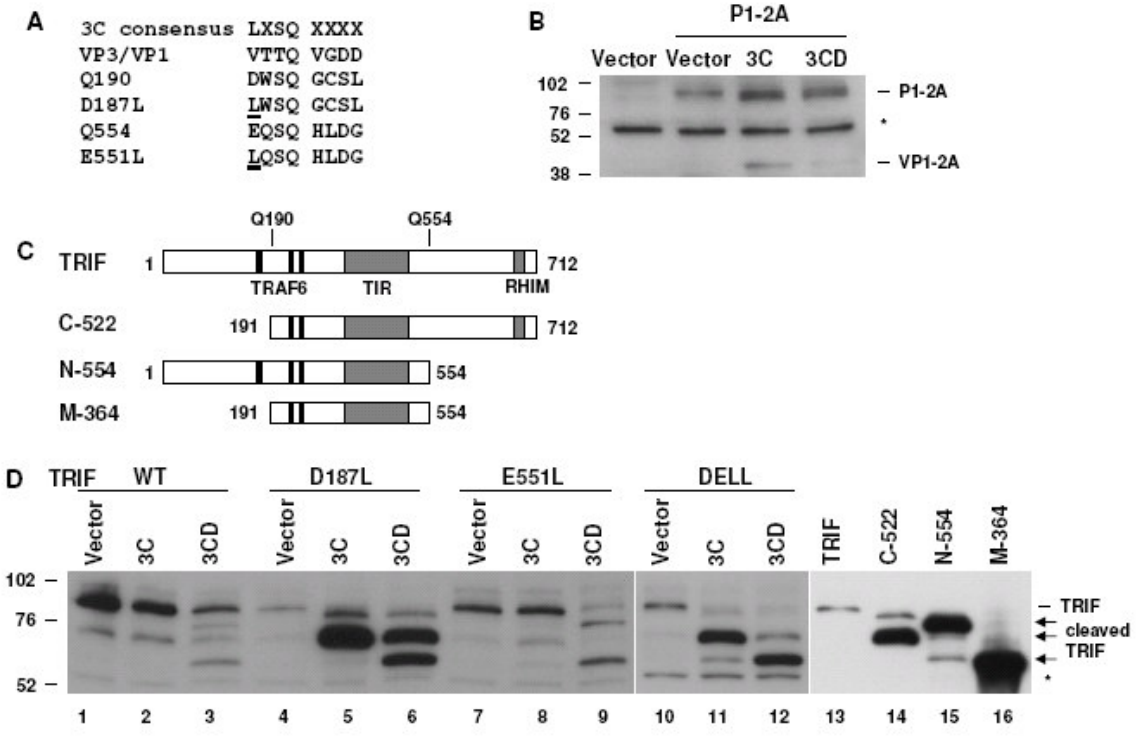

(A) Alignment of the consensus 3Cpro cleavage sequence and 3CD cleavage sites in TRIF. The VP3/VP1 cleavage sequence serves as an example of canonical 3C cleavage site. In the D187L and E551L mutants, the residues at the P4 positions of the Q190 and Q554 cleavage sites (D187 and E551, respectively) were substituted by L (underlined), a 3Cpro-preferred residue. **(B)** Cleavage of P1-2A by 3C and 3CD. HEK 293FT cells were co-transfected with vectors expressing P1-2A and 3C or 3CD. P1-2A and one of the cleavage products, VP1-2A, were detected by immunoblotting with anti-2A antibody. **(C)** Schematic of TRIF fragments resulting from 3CD cleavage at Q190 and Q554. **(D)** Cleavage of TRIF mutants by 3C and 3CD. HEK 293FT cells were co-transfected with vectors expressing TRIF constructs and 3C or 3CD (lane 1 to 12), or transfected with full-length or truncated TRIF expression constructs corresponding to 3CD-cleaved fragments (lane 13-16). TRIF and cleavage fragments (marked by arrows) in the lysates were analyzed by immunoblotting. Nonspecific protein bands (marked by *) detected by antibodies in (B) and (D) indicate equal loading.

Figure 3.6: Abundance of endogenous TRIF is reduced in HAV-Bla subgenomic replicon cells.

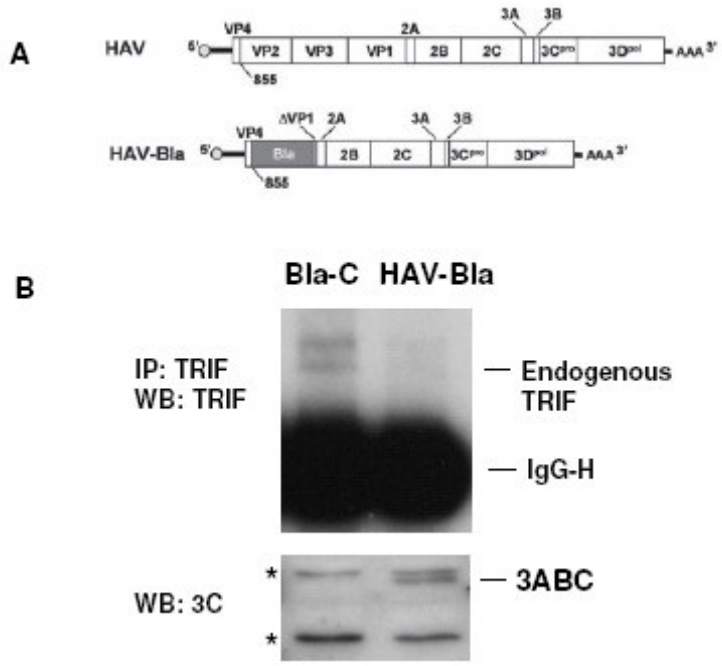

(A) Structural organization of the HAV genome (Upper) and the HAV-Bla subgenomic replicon (Lower). Details of construction of the subgenomic replicon were previously described (190). **(B)** Endogenous TRIF levels in the HAV-Bla cells and the IFN-α-cured Bla-C cells (190) were analyzed by immunoprecipitation with TRIF antibody S537-2 (95) and immunoblotting with TRIF antibody from Cell Signaling technology (Upper). HAV protein 3ABC was detected by immunoblotting with anti-3C antibody (Lower). Nonspecific protein bands (marked by *) detected by anti-3C antibody indicates equal loading.

Figure 3.7: 3CD-mediated cleavage of TRIF does not depend on caspases but is inhibited by the caspase inhibitor z-VAD-fmk.

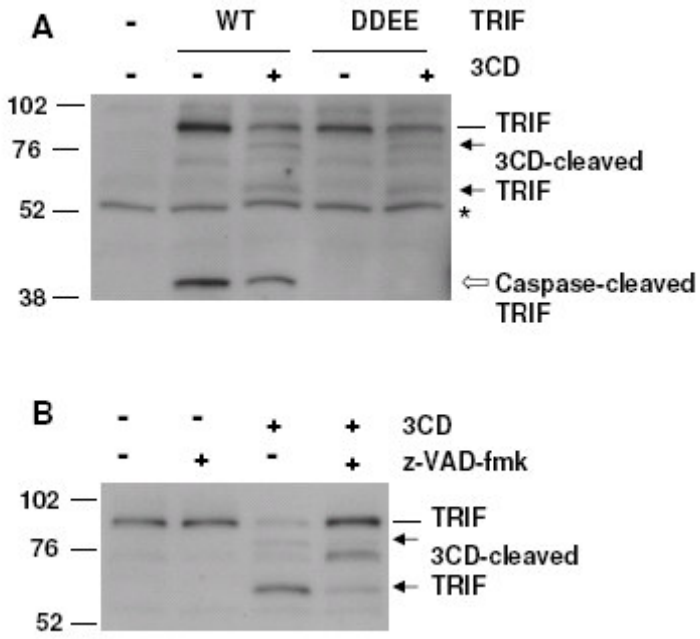

(A) 3CD-mediated cleavage of both wild-type (WT) and a caspase-resistant D281E-D289E (DDEE) mutant of TRIF. HEK 293FT cells were co-transfected with vectors expressing TRIF constructs and 3CD. TRIF and cleavage products generated by 3CD (solid arrows) or caspases (block arrow) were analyzed by immunoblotting. A nonspecific protein band (marked by *) detected by TRIF antibody serves as equal loading conntol. **(B)** z-VAD-fmk inhibits 3CD cleavage of TRIF. HEK 293FT cells were co-transfected with TRIF and 3CD expression vectors. At 4 hours posttransfection, z-VAD-fmk was added to the medium and incubated for additional 16 hours. TRIF and cleavage products (marked by arrows) were analyzed by immunblotting.

Figure 3.8: Cleavage of TRIF by 3CD hypo- or hyper-processing mutant.

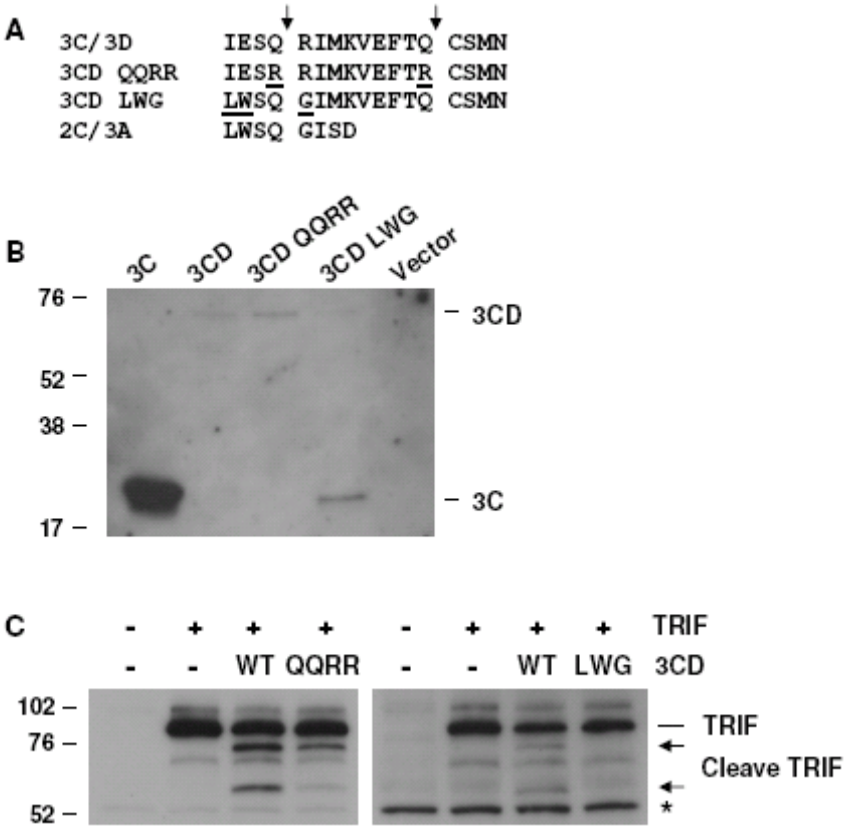

(A) Alignment of wild-type and mutated 3C/3D cleavage sequences with the primary 2C/3A cleavage sequence. Underlined are mutated residues that eliminate (QQRR) or optimize (LWG) the 3C/3D cleavage. In the LWG mutant, the P4-P2' residues of the modified 3C/3D primary cleavage site, LWGQ↓GI, are identical to those of the 2C/3A cleavage site. **(B)** The 3C/3D processing phenotypes of 3CD mutants. HEK 293FT cells were transfected with HA-tagged 3C (control) or 3CD constructs. Cell lysates were analyzed by anti-HA immunoprecipitation followed by anti-3C immunoblotting. **(C)** Cleavage of TRIF by 3CD mutants. HEK 293FT cells were co-transfected with vectors expressing TRIF and 3CD mutant constructs. TRIF and cleavage products (marked by arrows) were detected by immunoblotting. A nonspecific protein band (marked by *) detected by TRIF antibody indicates equal loading.

Figure 3.9: Signaling abilities of 3CD-cleaved TRIF fragments.

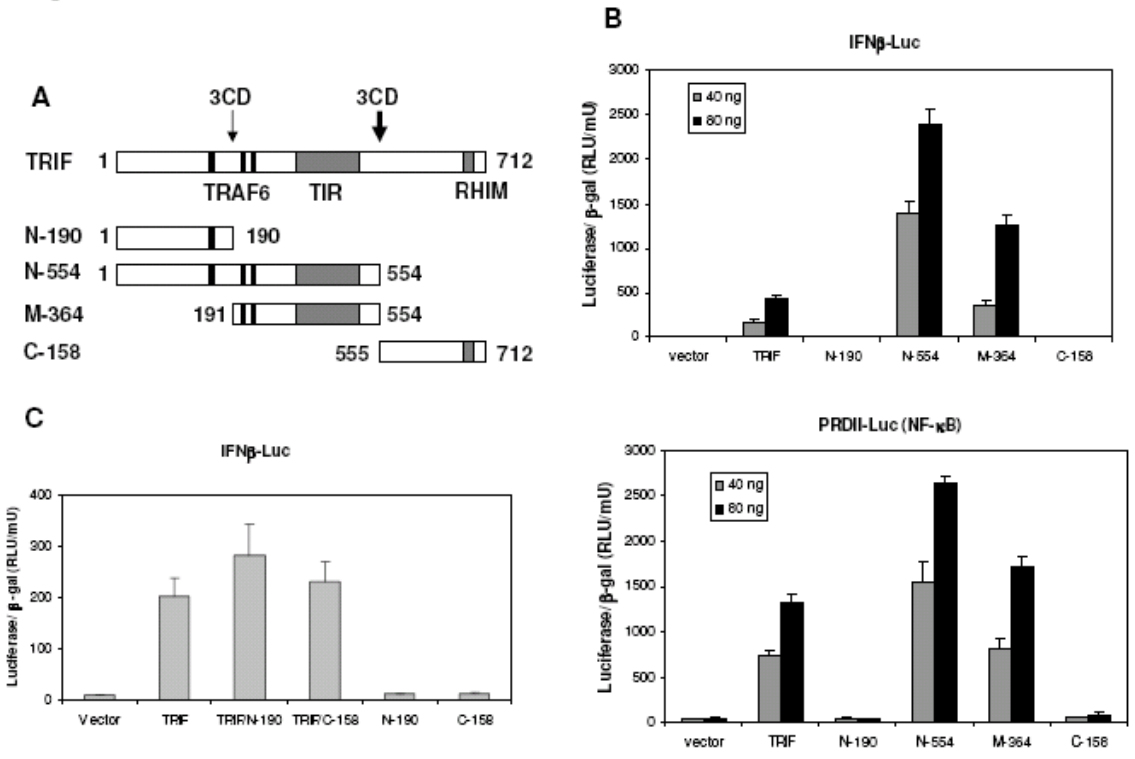

(A) Schematic of TRIF fragments resulting from 3CD cleavage. **(B)** Dose-dependent activation of IFN-β-Luc promoter (Upper) and NF-κB-specific PRDII-Luc promoter (Lower) by ectopic expression of TRIF fragments in HEK 293FT cells. **(C)** TRIF-induced activation of IFN-β-Luc promoter in HEK 293FT cells was not affected by co-expression (at a 1:1 ratio) with N-190 or C-158 fragment. Luciferase reporter activity was normalized by the internal β-gal transfection control.

Chapter 4: Discussion and Future Directions

The results of my Ph.D. studies have provided insights into viral evasion of pattern recognition receptor-mediated host innate immune responses. In particular, my work has focused on the mechanisms by which HAV, a human hepatotropic picornavirus, interfere with RIG-I/MDA5 and TLR3-mediated antiviral immunity. Chapter 2 focused on disruption of the RIG-I/MDA5 signaling pathway by HAV 3ABC protease precursor through proteolysis of the adaptor protein MAVS. Chapter 3 focused on the inhibition of the parallel, but independent, TLR3 signaling pathway by a different HAV protein, the 3CD protease-polymerase precursor, which cleaves the adaptor protein TRIF. These studies revealed two major mechanisms by which HAV evade host innate immunity, and they have one thing in common, which is to target the adaptor proteins for cleavage by viral protease precursors derived from a common 3ABCD polyprotein (Fig. 4.1). A similar strategy is used by HCV, which expresses the NS3/4A protease to cleave both MAVS and TRIF (44, 95-96, 103, 115). It appears that these two hepatotropic viruses, although recognized by different sensors (HCV is recognized by RIG-I, whereas HAV is most likely sensed by MDA5), may face similar host antiviral responses in the liver and therefore counteract in a similar manner.

The ability of HAV 3ABC to cleave MAVS depends on both its protease activity and a transmembrane domain in 3A that directs 3ABC to mitochondrial membrane where it colocalizes with MAVS. The mitochondrial targeting of 3ABC strongly supports the emerging concept that mitochondrial membrane serves as a platform for the formation of RIG-I/MDA5 signaling complex (156). Interestingly, *in vitro* cleavage assay showed that MAVS was cleaved by purified GST-3ABC, but barely by GST-3C (Fig. 2.11*A*). Since this assay did not involve mitochondria, the result suggests that in addition to

mitochondrial targeting, the presence of the TM domain in 3ABC may also alter the substrate specificity of 3Cpro. In vitro cleavage assays using purified 3AC or TM domain-deleted 3ABC are needed to further address this possibility.

3ABC cleavage of MAVS is in close parallel with cleavage of MAVS by the HCV NS3/4A protease (96, 103, 115). However, since MAVS is cleaved by NA3/4A and 3ABC at different sites resulting in different lengths of cleavage products, subtle difference may exist in the effects of the cleavage that could contribute to the difference between the viruses in their interaction with the host. In this regard, it would be interesting to compare the signaling abilities of MAVS cleavage products generated by NS3/4A and 3BAC. To date, the NS3/4A-cleaved N-terminal large fragment of MAVS is known to be non-functional (97), but the counterpart generated by 3ABC, and the membrane-associated C-terminal small fragments have not been rigorously tested.

It would also be interesting to test if targeting (not necessarily cleavage) of MAVS by viral protein(s) as an immune evasion mechanism can be extended to other picornaviruses. In particular, the avian encephalomyelitis virus (AEV) is the most closely related to HAV and is classified together with HAV in the Hepatovirus genus within the Picornaviridae family (109). Despite their differences in the internal ribosomal entry site (IRES) (8), the two viruses share high protein homology (109). Like HAV 3ABC, the VP3 protein of AEV is also localized to mitochondria (100), although whether it interferes with mitochondria-associated antiviral responses remains unclear.

Cleavage of TRIF by HAV 3CD protease-polymerase precursor provides the second means of immune evasion and is in parallel with the cleavage of MAVS by 3ABC, but through a completely different mechanism. While 3A directs 3ABC to the mitochondrial membrane where it colocalizes with and cleaves MAVS, the 3Dpol region modulates the substrate specificity of 3CD that allows it to cleave non-canonical 3Cpro

cleavage sites within TRIF. Although both 3ABC and 3CD depend on the 3Cpro protease activity to cleave their substrates, their effects on the corresponding signaling pathways do not overlap. Our studies showed that while 3ABC blocked SeV-induced, RIG-I-dependent activation of IFN-β promoter, it had no effect on poly(I:C)-induced, TLR3-mediated IFN-β induction. The opposite effects were also found true for 3CD. These results are in line with the current understanding that RIG-I/MDA5 and TLR3 mediate independent signaling pathways with little or no crosstalk (94).

Although TRIF is cleaved by both HCV NS3/4A (95) and HAV 3CD, the resulting cleavage products exhibited different signaling abilities. In the case of HCV NS3/4A cleavage, which resulted into two fragments, N-372 (aa 1-372) and C-340 (aa 373-712), neither fragment could activate the IFN-β promoter (95). Only the C-340 fragment (containing the TIR and RHIM domains) retained the ability to activate the NF-κB promoter (95), consistent with previously described deletion mutants (127, 150, 189). Neither the N-372 nor C-340 fragment showed a dominant negative effect when co-expressed with full-length TRIF (95). Cleavage of TRIF by HAV 3CD generated four fragments: N-554 and M-364 retained the ability to activate both NF-κB and IFN-β promoters, while neither N-190 nor C-158 activated the NF-κB or IFN-β promoter (Fig. 3.9*B*). N-190 and C-158 also had no dominant negative effect over full-length TRIF (Fig.3.9*C*). The abilities of N-554 and M-364 to activate the IFN-β promoter may be due to the fact that they both contain the TIR domain and either intact (N-554) or partial (M-364) N-terminal region that are required for activation of both IRF3 and NF-kB, whereas NS3/4A-generated fragments lack either the TIR domain (N-372) or the N-terminal region (C-340) (95). However, in both cases the endogenous cleavage products were difficult to detect by immunoblot (95) or immunoprecipitation (Fig. 2.1*D*), suggesting that they may be rapidly degraded after the cleavage. Although some of the cleavage

products retained the ability to activate the NF-κB or IFN-β promoter (or both) when overexpressed, and at this point we can not exclude the possibility that they could exist transiently, these cleavage products may not have the signal transduction capacity of TRIF, i.e., the ability to transduce signal from TLR3. A more thorough analysis of these cleavage products at both overexpression and endogenous levels is needed to fully understand the functional impact of NS3/4A and 3CD cleavage of TRIF.

Our study revealed a role of the 3Dpol domain in altering 3CD substrate specificity so that it tolerates or prefers acidic instead of hydrophobic amino acids in the P4 positions of the non-canonical cleavage sites within TRIF. This conclusion was based on several lines of evidence. First, TRIF was cleaved by 3CD, not the mature 3Cpro. This was not due to higher activity of 3CD than 3Cpro, because we next showed that 3CD was actually much less active than 3Cpro on a canonical substrate, the HAV P1-2A polypeptide. Third, point mutations that changed the non-canonical cleavage sites of TRIF into canonical 3Cpro cleavage sites allowed 3Cpro to cleave TRIF, proving that the inability of 3Cpro to cleave TRIF is at least due to a substrate specificity problem. However, we do not exclude other possibilities, e.g., 3Cpro may not colocalize with TRIF in the cytoplasm, and the mutations introduced into TRIF may change its intracellular localization and bring it close to 3Cpro. This may be addressed by using immunofluorescence confocal microscopy. The altered substrate specificity of 3CD can also be supported by *in vitro* protease assays that determine the efficiency of purified 3Cpro and 3CD in cleavage of wild-type and mutated TRIF substrate peptides. However, our effort in developing such assays has been hampered by the difficulty in purification of 3CD, which was totally insoluble when expressed in *E. coli* (data not shown).

Modulation of 3CD activity by the 3Dpol domain is not without precedent among picornaviruses. In the case of poliovirus 3CD, the 3Dpol domain enhances the protease

activity of 3CD in most polyprotein processing events (128). For HAV 3CD, the 3Dpol domain does not enhance the protease activity of 3CD (3CD was much less active than 3Cpro in cleavage of the HAV P1-2A polypeptide), but rather modifies its substrate specificity. Thus the roles of 3Dpol in modulation of 3CD function vary among different picornaviruses.

How does the 3Dpol domain modulate the substrate specificity of 3CD? One can envision that 3Dpol may fold with 3Cpro or have close interaction with 3Cpro so that it changes the conformation of the S4 substrate binding pocket of 3Cpro to accommodate acidic amino acid in the corresponding P4 position of the substrate. The interaction between 3Cpro and 3Dpol may be mutually important, i.e., 3Cpro may also help the folding of 3Dpol. This is supported by our observation that while 3Cpro can be readily expressed and purified from both mammalian HEK 293FT cells and *E. coli*, 3Dpol is virtually undetectable when expressed alone in HEK 293FT cells and completely insoluble when expressed in *E. coli* (data not shown). In contrast, 3CD can be detected when expressed in HEK 293FT cells, albeit at very low abundance, suggesting that 3Cpro may stabilize 3Dpol. The answer to this question may be found in the future when the solubility problem of 3CD is solved and its crystal structure becomes available.

Our studies also demonstrated that cleavage of TRIF can be modulated by changing the production of 3CD, which is achieved by blocking or enhancing the 3C/3D cleavage through point mutations at the 3C/3D junction (Fig. 3.8). It would be interesting to introduce these mutations into HAV genome to create mutant viruses by reverse genetic technology. Such mutations could be lethal due to the essential role of 3Dpol in viral replication. If the recombinant virus is viable, with either enhanced or reduced expression of 3CD, it would be interesting to test its effect on TLR3 signaling and whether the virus is more virulent or attenuated in host cells.

Another remaining question is whether HAV-induced down-regulation of MAVS and TRIF, which we demonstrated in cell culture, can be observed in HAV-infected animal models and related to the lack of IFN and ISGs during early phase of infection. This can be challenging due to the relatively low abundance of these proteins in the cell and the limitation of detection methods, but if done successfully, would make significant contribution to the study of HAV pathogenesis. It is my hope that the viral mechanisms of immune evasion that were discovered in this dissertation may fill several gaps of our understanding of the interaction between HAV and host antiviral response, and extend our knowledge of the signal transduction pathways in innate immunity.

Figure 4.1: Disruption of innate signaling pathways by HAV and HCV.

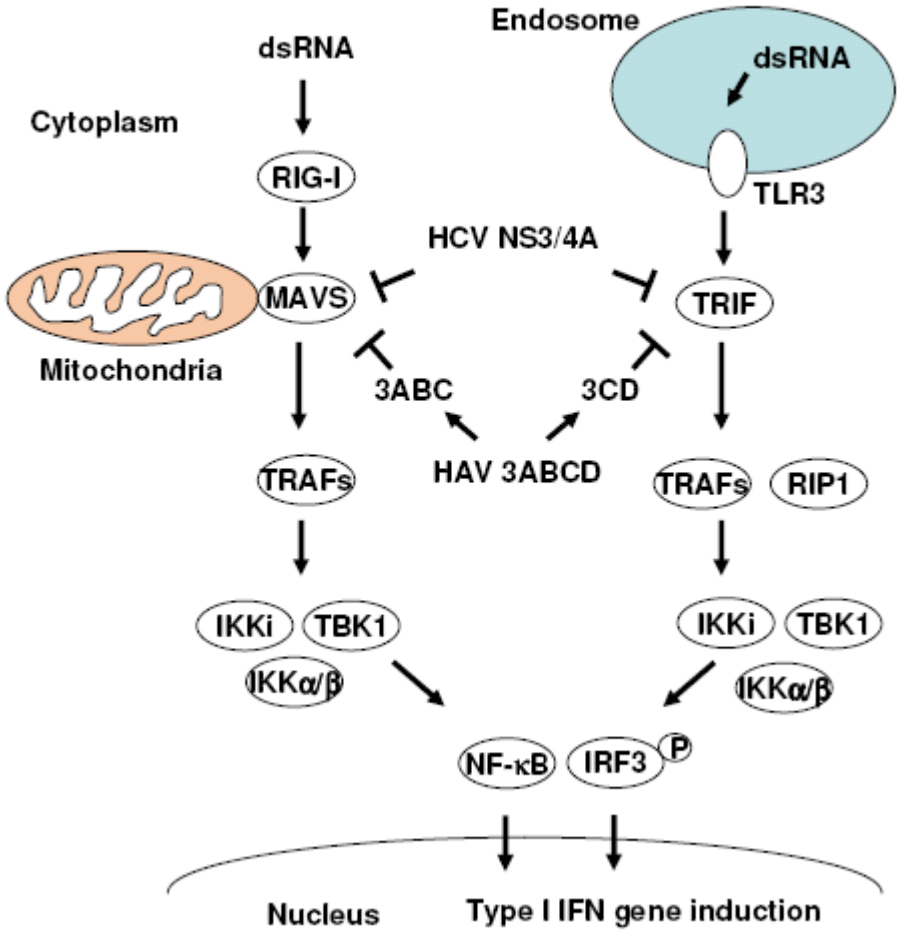

References

1. **Akira, S.** 2003. Toll-like receptor signaling. J Biol Chem **278:**38105-38108.
2. **Akira, S., and S. Sato.** 2003. Toll-like receptors and their signaling mechanisms. Scand J Infect Dis **35:**555-562.
3. **Akira, S., and K. Takeda.** 2004. Toll-like receptor signalling. Nat Rev Immunol **4:**499-511.
4. **Akira, S., K. Takeda, and T. Kaisho.** 2001. Toll-like receptors: critical proteins linking innate and acquired immunity. Nat Immunol **2:**675-680.
5. **Alexopoulou, L., A. C. Holt, R. Medzhitov, and R. A. Flavell.** 2001. Recognition of double-stranded RNA and activation of NF-kappaB by Toll-like receptor 3. Nature **413:**732-738.
6. **Anderson, K. V., L. Bokla, and C. Nusslein-Volhard.** 1985. Establishment of dorsal-ventral polarity in the Drosophila embryo: the induction of polarity by the Toll gene product. Cell **42:**791-798.
7. **Andrejeva, J., K. S. Childs, D. F. Young, T. S. Carlos, N. Stock, S. Goodbourn, and R. E. Randall.** 2004. The V proteins of paramyxoviruses bind the IFN-inducible RNA helicase, mda-5, and inhibit its activation of the IFN-beta promoter. Proc Natl Acad Sci U S A **101:**17264-17269.
8. **Bakhshesh, M., E. Groppelli, M. M. Willcocks, E. Royall, G. J. Belsham, and L. O. Roberts.** 2008. The picornavirus avian encephalomyelitis virus possesses a hepatitis C virus-like internal ribosome entry site element. J Virol **82:**1993-2003.
9. **Bauhofer, O., A. Summerfield, Y. Sakoda, J. D. Tratschin, M. A. Hofmann, and N. Ruggli.** 2007. Classical swine fever virus Npro interacts with interferon

regulatory factor 3 and induces its proteasomal degradation. J Virol **81:**3087-3096.

10. **Bell, J. K., J. Askins, P. R. Hall, D. R. Davies, and D. M. Segal.** 2006. The dsRNA binding site of human Toll-like receptor 3. Proc Natl Acad Sci U S A **103:**8792-8797.

11. **Bell, J. K., I. Botos, P. R. Hall, J. Askins, J. Shiloach, D. M. Segal, and D. R. Davies.** 2005. The molecular structure of the Toll-like receptor 3 ligand-binding domain. Proc Natl Acad Sci U S A **102:**10976-10980.

12. **Beneduce, F., A. Ciervo, Y. Kusov, V. Gauss-Muller, and G. Morace.** 1999. Mapping of protein domains of hepatitis A virus 3AB essential for interaction with 3CD and viral RNA. Virology **264:**410-421.

13. **Beneduce, F., A. Ciervo, and G. Morace.** 1997. Site-directed mutagenesis of hepatitis A virus protein 3A: effects on membrane interaction. Biochim Biophys Acta **1326:**157-165.

14. **Bergmann, E. M., S. C. Mosimann, M. M. Chernaia, B. A. Malcolm, and M. N. James.** 1997. The refined crystal structure of the 3C gene product from hepatitis A virus: specific proteinase activity and RNA recognition. J Virol **71:**2436-2448.

15. **Bishop, N. E., and D. A. Anderson.** 1993. RNA-dependent cleavage of VP0 capsid protein in provirions of hepatitis A virus. Virology **197:**616-623.

16. **Blight, K. J., A. A. Kolykhalov, K. E. Reed, E. V. Agapov, and C. M. Rice.** 1998. Molecular virology of hepatitis C virus: an update with respect to potential antiviral targets. Antivir Ther **3:**71-81.

17. **Bowie, A., E. Kiss-Toth, J. A. Symons, G. L. Smith, S. K. Dower, and L. A. O'Neill.** 2000. A46R and A52R from vaccinia virus are antagonists of host IL-1 and toll-like receptor signaling. Proc Natl Acad Sci U S A **97:**10162-10167.

18. **Bowie, A., and L. A. O'Neill.** 2000. The interleukin-1 receptor/Toll-like receptor superfamily: signal generators for pro-inflammatory interleukins and microbial products. J Leukoc Biol **67:**508-514.

19. **Brack, K., I. Berk, T. Magulski, J. Lederer, A. Dotzauer, and A. Vallbracht.** 2002. Hepatitis A virus inhibits cellular antiviral defense mechanisms induced by double-stranded RNA. J Virol **76:**11920-11930.

20. **Brown, E. A., S. P. Day, R. W. Jansen, and S. M. Lemon.** 1991. The 5' nontranslated region of hepatitis A virus RNA: secondary structure and elements required for translation in vitro. J Virol **65:**5828-5838.

21. **Bryant, C., and K. A. Fitzgerald.** 2009. Molecular mechanisms involved in inflammasome activation. Trends Cell Biol **19:**455-464.

22. **Carty, M., R. Goodbody, M. Schroder, J. Stack, P. N. Moynagh, and A. G. Bowie.** 2006. The human adaptor SARM negatively regulates adaptor protein TRIF-dependent Toll-like receptor signaling. Nat Immunol **7:**1074-1081.

23. **Chang, K. H., E. A. Brown, and S. M. Lemon.** 1993. Cell type-specific proteins which interact with the 5' nontranslated region of hepatitis A virus RNA. J Virol **67:**6716-6725.

24. **Chen, Z., Y. Benureau, R. Rijnbrand, J. Yi, T. Wang, L. Warter, R. E. Lanford, S. A. Weinman, S. M. Lemon, A. Martin, and K. Li.** 2007. GB virus B disrupts RIG-I signaling by NS3/4A-mediated cleavage of the adaptor protein MAVS. J Virol **81:**964-976.

25. **Chen, Z., R. Rijnbrand, R. K. Jangra, S. G. Devaraj, L. Qu, Y. Ma, S. M. Lemon, and K. Li.** 2007. Ubiquitination and proteasomal degradation of interferon regulatory factor-3 induced by Npro from a cytopathic bovine viral diarrhea virus. Virology **366:**277-292.

26. **Chen, Z. J.** 2005. Ubiquitin signalling in the NF-kappaB pathway. Nat Cell Biol **7:**758-765.

27. **Childs, K., N. Stock, C. Ross, J. Andrejeva, L. Hilton, M. Skinner, R. Randall, and S. Goodbourn.** 2007. mda-5, but not RIG-I, is a common target for paramyxovirus V proteins. Virology **359:**190-200.

28. **Choe, J., M. S. Kelker, and I. A. Wilson.** 2005. Crystal structure of human toll-like receptor 3 (TLR3) ectodomain. Science **309:**581-585.

29. **Choe, S. S., D. A. Dodd, and K. Kirkegaard.** 2005. Inhibition of cellular protein secretion by picornaviral 3A proteins. Virology **337:**18-29.

30. **Chuang, T., and R. J. Ulevitch.** 2001. Identification of hTLR10: a novel human Toll-like receptor preferentially expressed in immune cells. Biochim Biophys Acta **1518:**157-161.

31. **Chuang, T. H., and R. J. Ulevitch.** 2000. Cloning and characterization of a sub-family of human toll-like receptors: hTLR7, hTLR8 and hTLR9. Eur Cytokine Netw **11:**372-378.

32. **Ciervo, A., F. Beneduce, and G. Morace.** 1998. Polypeptide 3AB of hepatitis A virus is a transmembrane protein. Biochem Biophys Res Commun **249:**266-274.

33. **de Bouteiller, O., E. Merck, U. A. Hasan, S. Hubac, B. Benguigui, G. Trinchieri, E. E. Bates, and C. Caux.** 2005. Recognition of double-stranded RNA by human toll-like receptor 3 and downstream receptor signaling requires multimerization and an acidic pH. J Biol Chem **280:**38133-38145.

34. **Deng, L., C. Wang, E. Spencer, L. Yang, A. Braun, J. You, C. Slaughter, C. Pickart, and Z. J. Chen.** 2000. Activation of the IkappaB kinase complex by TRAF6 requires a dimeric ubiquitin-conjugating enzyme complex and a unique polyubiquitin chain. Cell **103:**351-361.

35. **Didcock, L., D. F. Young, S. Goodbourn, and R. E. Randall.** 1999. The V protein of simian virus 5 inhibits interferon signalling by targeting STAT1 for proteasome-mediated degradation. J Virol **73:**9928-9933.

36. **Diebold, S. S., T. Kaisho, H. Hemmi, S. Akira, and C. Reis e Sousa.** 2004. Innate antiviral responses by means of TLR7-mediated recognition of single-stranded RNA. Science **303:**1529-1531.

37. **Du, X., A. Poltorak, Y. Wei, and B. Beutler.** 2000. Three novel mammalian toll-like receptors: gene structure, expression, and evolution. Eur Cytokine Netw **11:**362-371.

38. **Edelmann, K. H., S. Richardson-Burns, L. Alexopoulou, K. L. Tyler, R. A. Flavell, and M. B. Oldstone.** 2004. Does Toll-like receptor 3 play a biological role in virus infections? Virology **322:**231-238.

39. **Egger, D., and K. Bienz.** 2005. Intracellular location and translocation of silent and active poliovirus replication complexes. J Gen Virol **86:**707-718.

40. **Emerson, S. U., Y. K. Huang, C. McRill, M. Lewis, and R. H. Purcell.** 1992. Mutations in both the 2B and 2C genes of hepatitis A virus are involved in adaptation to growth in cell culture. J Virol **66:**650-654.

41. **Emerson, S. U., Y. K. Huang, and R. H. Purcell.** 1993. 2B and 2C mutations are essential but mutations throughout the genome of HAV contribute to adaptation to cell culture. Virology **194:**475-480.

42. **Feigelstock, D., P. Thompson, P. Mattoo, Y. Zhang, and G. G. Kaplan.** 1998. The human homolog of HAVcr-1 codes for a hepatitis A virus cellular receptor. J Virol **72:**6621-6628.

43. **Fensterl, V., D. Grotheer, I. Berk, S. Schlemminger, A. Vallbracht, and A. Dotzauer.** 2005. Hepatitis A virus suppresses RIG-I-mediated IRF-3 activation to block induction of beta interferon. J Virol **79:**10968-10977.

44. **Ferreon, J. C., A. C. Ferreon, K. Li, and S. M. Lemon.** 2005. Molecular determinants of TRIF proteolysis mediated by the hepatitis C virus NS3/4A protease. J Biol Chem **280:**20483-20492.

45. **Fiore, A. E.** 2004. Hepatitis A transmitted by food. Clin Infect Dis **38:**705-15.

46. **Fitzgerald, K. A., E. M. Palsson-McDermott, A. G. Bowie, C. A. Jefferies, A. S. Mansell, G. Brady, E. Brint, A. Dunne, P. Gray, M. T. Harte, D. McMurray, D. E. Smith, J. E. Sims, T. A. Bird, and L. A. O'Neill.** 2001. Mal (MyD88-adapter-like) is required for Toll-like receptor-4 signal transduction. Nature **413:**78-83.

47. **Franchi, L., C. McDonald, T. D. Kanneganti, A. Amer, and G. Nunez.** 2006. Nucleotide-binding oligomerization domain-like receptors: intracellular pattern recognition molecules for pathogen detection and host defense. J Immunol **177:**3507-3513.

48. **Funami, K., M. Matsumoto, H. Oshiumi, T. Akazawa, A. Yamamoto, and T. Seya.** 2004. The cytoplasmic 'linker region' in Toll-like receptor 3 controls receptor localization and signaling. Int Immunol **16:**1143-1154.

49. **Funami, K., M. Sasai, H. Oshiumi, T. Seya, and M. Matsumoto.** 2008. Homo-oligomerization is essential for Toll/interleukin-1 receptor domain-containing

adaptor molecule-1-mediated NF-kappaB and interferon regulatory factor-3 activation. J Biol Chem **283:**18283-18291.

50. **Gale, M., Jr., and E. M. Foy.** 2005. Evasion of intracellular host defence by hepatitis C virus. Nature **436:**939-945.

51. **Garcin, D., J. Curran, M. Itoh, and D. Kolakofsky.** 2001. Longer and shorter forms of Sendai virus C proteins play different roles in modulating the cellular antiviral response. J Virol **75:**6800-6807.

52. **Garcin, D., P. Latorre, and D. Kolakofsky.** 1999. Sendai virus C proteins counteract the interferon-mediated induction of an antiviral state. J Virol **73:**6559-6565.

53. **Gitlin, L., W. Barchet, S. Gilfillan, M. Cella, B. Beutler, R. A. Flavell, M. S. Diamond, and M. Colonna.** 2006. Essential role of mda-5 in type I IFN responses to polyriboinosinic:polyribocytidylic acid and encephalomyocarditis picornavirus. Proc Natl Acad Sci U S A **103:**8459-8464.

54. **Gitlin, L., L. Benoit, C. Song, M. Cella, S. Gilfillan, M. J. Holtzman, and M. Colonna.** 2010. Melanoma differentiation-associated gene 5 (MDA5) is involved in the innate immune response to Paramyxoviridae infection in vivo. PLoS Pathog **6:**e1000734.

55. **Gordon, S.** 2002. Pattern recognition receptors: doubling up for the innate immune response. Cell **111:**927-930.

56. **Gotoh, B., T. Komatsu, K. Takeuchi, and J. Yokoo.** 2002. Paramyxovirus strategies for evading the interferon response. Rev Med Virol **12:**337-357.

57. **Grakoui, A., N. H. Shoukry, D. J. Woollard, J. H. Han, H. L. Hanson, J. Ghrayeb, K. K. Murthy, C. M. Rice, and C. M. Walker.** 2003. HCV

persistence and immune evasion in the absence of memory T cell help. Science **302:**659-662.

58. **Grimm, S., B. Z. Stanger, and P. Leder.** 1996. RIP and FADD: two "death domain"-containing proteins can induce apoptosis by convergent, but dissociable, pathways. Proc Natl Acad Sci U S A **93:**10923-10927.

59. **Han, K. J., X. Su, L. G. Xu, L. H. Bin, J. Zhang, and H. B. Shu.** 2004. Mechanisms of the TRIF-induced interferon-stimulated response element and NF-kappaB activation and apoptosis pathways. J Biol Chem **279:**15652-15661.

60. **Hayashi, F., K. D. Smith, A. Ozinsky, T. R. Hawn, E. C. Yi, D. R. Goodlett, J. K. Eng, S. Akira, D. M. Underhill, and A. Aderem.** 2001. The innate immune response to bacterial flagellin is mediated by Toll-like receptor 5. Nature **410:**1099-1103.

61. **Heil, F., H. Hemmi, H. Hochrein, F. Ampenberger, C. Kirschning, S. Akira, G. Lipford, H. Wagner, and S. Bauer.** 2004. Species-specific recognition of single-stranded RNA via toll-like receptor 7 and 8. Science **303:**1526-1529.

62. **Hemmi, H., O. Takeuchi, T. Kawai, T. Kaisho, S. Sato, H. Sanjo, M. Matsumoto, K. Hoshino, H. Wagner, K. Takeda, and S. Akira.** 2000. A Toll-like receptor recognizes bacterial DNA. Nature **408:**740-745.

63. **Hoebe, K., X. Du, P. Georgel, E. Janssen, K. Tabeta, S. O. Kim, J. Goode, P. Lin, N. Mann, S. Mudd, K. Crozat, S. Sovath, J. Han, and B. Beutler.** 2003. Identification of Lps2 as a key transducer of MyD88-independent TIR signalling. Nature **424:**743-748.

64. **Honda, K., A. Takaoka, and T. Taniguchi.** 2006. Type I interferon [corrected] gene induction by the interferon regulatory factor family of transcription factors. Immunity **25:**349-360.

65. **Hornung, V., J. Ellegast, S. Kim, K. Brzozka, A. Jung, H. Kato, H. Poeck, S. Akira, K. K. Conzelmann, M. Schlee, S. Endres, and G. Hartmann.** 2006. 5'-Triphosphate RNA is the ligand for RIG-I. Science **314:**994-997.

66. **Hoshino, K., O. Takeuchi, T. Kawai, H. Sanjo, T. Ogawa, Y. Takeda, K. Takeda, and S. Akira.** 1999. Cutting edge: Toll-like receptor 4 (TLR4)-deficient mice are hyporesponsive to lipopolysaccharide: evidence for TLR4 as the Lps gene product. J Immunol **162:**3749-3752.

67. **Jacobs, B. L., and J. O. Langland.** 1996. When two strands are better than one: the mediators and modulators of the cellular responses to double-stranded RNA. Virology **219:**339-349.

68. **James, M. N.** 2006. The peptidases from fungi and viruses. Biol Chem **387:**1023-1029.

69. **Jecht, M., C. Probst, and V. Gauss-Muller.** 1998. Membrane permeability induced by hepatitis A virus proteins 2B and 2BC and proteolytic processing of HAV 2BC. Virology **252:**218-227.

70. **Jewell, D. A., W. Swietnicki, B. M. Dunn, and B. A. Malcolm.** 1992. Hepatitis A virus 3C proteinase substrate specificity. Biochemistry **31:**7862-7869.

71. **Jiang, Z., T. W. Mak, G. Sen, and X. Li.** 2004. Toll-like receptor 3-mediated activation of NF-kappaB and IRF3 diverges at Toll-IL-1 receptor domain-containing adapter inducing IFN-beta. Proc Natl Acad Sci U S A **101:**3533-3538.

72. **Johnson, C. L., and M. Gale, Jr.** 2006. CARD games between virus and host get a new player. Trends Immunol **27:**1-4.

73. **Jurgensen, D., Y. Y. Kusov, M. Facke, H. G. Krausslich, and V. Gauss-Muller.** 1993. Cell-free translation and proteolytic processing of the hepatitis A virus polyprotein. J Gen Virol **74 (Pt 4):**677-683.

74. **Kaiser, W. J., and M. K. Offermann.** 2005. Apoptosis induced by the toll-like receptor adaptor TRIF is dependent on its receptor interacting protein homotypic interaction motif. J Immunol **174:**4942-4952.

75. **Kaisho, T., and S. Akira.** 2000. Critical roles of Toll-like receptors in host defense. Crit Rev Immunol **20:**393-405.

76. **Kang, D. C., R. V. Gopalkrishnan, Q. Wu, E. Jankowsky, A. M. Pyle, and P. B. Fisher.** 2002. mda-5: An interferon-inducible putative RNA helicase with double-stranded RNA-dependent ATPase activity and melanoma growth-suppressive properties. Proc Natl Acad Sci U S A **99:**637-642.

77. **Kato, H., O. Takeuchi, E. Mikamo-Satoh, R. Hirai, T. Kawai, K. Matsushita, A. Hiiragi, T. S. Dermody, T. Fujita, and S. Akira.** 2008. Length-dependent recognition of double-stranded ribonucleic acids by retinoic acid-inducible gene-I and melanoma differentiation-associated gene 5. J Exp Med **205:**1601-1610.

78. **Kato, H., O. Takeuchi, S. Sato, M. Yoneyama, M. Yamamoto, K. Matsui, S. Uematsu, A. Jung, T. Kawai, K. J. Ishii, O. Yamaguchi, K. Otsu, T. Tsujimura, C. S. Koh, C. Reis e Sousa, Y. Matsuura, T. Fujita, and S. Akira.** 2006. Differential roles of MDA5 and RIG-I helicases in the recognition of RNA viruses. Nature **441:**101-105.

79. **Kawai, T., and S. Akira.** 2008. Toll-like receptor and RIG-I-like receptor signaling. Ann N Y Acad Sci **1143:**1-20.

80. **Kawai, T., K. Takahashi, S. Sato, C. Coban, H. Kumar, H. Kato, K. J. Ishii, O. Takeuchi, and S. Akira.** 2005. IPS-1, an adaptor triggering RIG-I- and Mda5-mediated type I interferon induction. Nat Immunol **6:**981-988.

81. **Kemmer, N. M., and E. P. Miskovsky.** 2000. Hepatitis A. Infect Dis Clin North Am **14:**605-615.

82. **Koff, R. S.** 1992. Clinical manifestations and diagnosis of hepatitis A virus infection. Vaccine **10 Suppl 1:**S15-17.

83. **Konduru, K., and G. G. Kaplan.** 2010. Determinants in 3Dpol modulate the rate of growth of Hepatitis A Virus. J Virol. **84:**8342-8347.

84. **Konduru, K., and G. G. Kaplan.** 2006. Stable growth of wild-type hepatitis A virus in cell culture. J Virol **80:**1352-1360.

85. **Kovacsovics, M., F. Martinon, O. Micheau, J. L. Bodmer, K. Hofmann, and J. Tschopp.** 2002. Overexpression of Helicard, a CARD-containing helicase cleaved during apoptosis, accelerates DNA degradation. Curr Biol **12:**838-843.

86. **Kusov, Y., and V. Gauss-Muller.** 1999. Improving proteolytic cleavage at the 3A/3B site of the hepatitis A virus polyprotein impairs processing and particle formation, and the impairment can be complemented in trans by 3AB and 3ABC. J Virol **73:**9867-9878.

87. **Kusov, Y. Y., G. Morace, C. Probst, and V. Gauss-Muller.** 1997. Interaction of hepatitis A virus (HAV) precursor proteins 3AB and 3ABC with the 5' and 3' termini of the HAV RNA. Virus Res **51:**151-157.

88. **Kwong, A. D., J. L. Kim, G. Rao, D. Lipovsek, and S. A. Raybuck.** 1999. Hepatitis C virus NS3/4A protease. Antiviral Res **41:**67-84.

89. **La Rocca, S. A., R. J. Herbert, H. Crooke, T. W. Drew, T. E. Wileman, and P. P. Powell.** 2005. Loss of interferon regulatory factor 3 in cells infected with classical swine fever virus involves the N-terminal protease, Npro. J Virol **79:**7239-7247.

90. **Lamothe, B., A. D. Campos, W. K. Webster, A. Gopinathan, L. Hur, and B. G. Darnay.** 2008. The RING domain and first zinc finger of TRAF6 coordinate

signaling by interleukin-1, lipopolysaccharide, and RANKL. J Biol Chem **283:**24871-24880.

91. **Le Goffic, R., V. Balloy, M. Lagranderie, L. Alexopoulou, N. Escriou, R. Flavell, M. Chignard, and M. Si-Tahar.** 2006. Detrimental contribution of the Toll-like receptor (TLR)3 to influenza A virus-induced acute pneumonia. PLoS Pathog **2:**e53.

92. **Lemon, S. M., L. N. Binn, R. Marchwicki, P. C. Murphy, L. H. Ping, R. W. Jansen, L. V. Asher, J. T. Stapleton, D. G. Taylor, and J. W. LeDuc.** 1990. In vivo replication and reversion to wild type of a neutralization-resistant antigenic variant of hepatitis A virus. J Infect Dis **161:**7-13.

93. **Lemon, S. M., P. C. Murphy, P. A. Shields, L. H. Ping, S. M. Feinstone, T. Cromeans, and R. W. Jansen.** 1991. Antigenic and genetic variation in cytopathic hepatitis A virus variants arising during persistent infection: evidence for genetic recombination. J Virol **65:**2056-2065.

94. **Li, K., Z. Chen, N. Kato, M. Gale, Jr., and S. M. Lemon.** 2005. Distinct poly(I-C) and virus-activated signaling pathways leading to interferon-beta production in hepatocytes. J Biol Chem **280:**16739-16747.

95. **Li, K., E. Foy, J. C. Ferreon, M. Nakamura, A. C. Ferreon, M. Ikeda, S. C. Ray, M. Gale, Jr., and S. M. Lemon.** 2005. Immune evasion by hepatitis C virus NS3/4A protease-mediated cleavage of the Toll-like receptor 3 adaptor protein TRIF. Proc Natl Acad Sci U S A **102:**2992-2997.

96. **Li, X. D., L. Sun, R. B. Seth, G. Pineda, and Z. J. Chen.** 2005. Hepatitis C virus protease NS3/4A cleaves mitochondrial antiviral signaling protein off the mitochondria to evade innate immunity. Proc Natl Acad Sci U S A **102:**17717-17722.

97. **Liang, Y., H. Ishida, O. Lenz, T. I. Lin, O. Nyanguile, K. Simmen, R. B. Pyles, N. Bourne, M. Yi, K. Li, and S. M. Lemon.** 2008. Antiviral suppression vs restoration of RIG-I signaling by hepatitis C protease and polymerase inhibitors. Gastroenterology **135:**1710-1718 e2.

98. **Lien, E., T. K. Means, H. Heine, A. Yoshimura, S. Kusumoto, K. Fukase, M. J. Fenton, M. Oikawa, N. Qureshi, B. Monks, R. W. Finberg, R. R. Ingalls, and D. T. Golenbock.** 2000. Toll-like receptor 4 imparts ligand-specific recognition of bacterial lipopolysaccharide. J Clin Invest **105:**497-504.

99. **Ling, Z., K. C. Tran, and M. N. Teng.** 2009. Human respiratory syncytial virus nonstructural protein NS2 antagonizes the activation of beta interferon transcription by interacting with RIG-I. J Virol **83:**3734-3742.

100. **Liu, J., T. Wei, and J. Kwang.** 2002. Avian encephalomyelitis virus induces apoptosis via major structural protein VP3. Virology **300:**39-49.

101. **Lo, M. S., R. M. Brazas, and M. J. Holtzman.** 2005. Respiratory syncytial virus nonstructural proteins NS1 and NS2 mediate inhibition of Stat2 expression and alpha/beta interferon responsiveness. J Virol **79:**9315-9319.

102. **Loo, Y. M., J. Fornek, N. Crochet, G. Bajwa, O. Perwitasari, L. Martinez-Sobrido, S. Akira, M. A. Gill, A. Garcia-Sastre, M. G. Katze, and M. Gale, Jr.** 2008. Distinct RIG-I and MDA5 signaling by RNA viruses in innate immunity. J Virol **82:**335-345.

103. **Loo, Y. M., D. M. Owen, K. Li, A. K. Erickson, C. L. Johnson, P. M. Fish, D. S. Carney, T. Wang, H. Ishida, M. Yoneyama, T. Fujita, T. Saito, W. M. Lee, C. H. Hagedorn, D. T. Lau, S. A. Weinman, S. M. Lemon, and M. Gale, Jr.** 2006. Viral and therapeutic control of IFN-beta promoter stimulator 1 during hepatitis C virus infection. Proc Natl Acad Sci U S A **103:**6001-6006.

104. **Losick, V. P., P. E. Schlax, R. A. Emmons, and T. G. Lawson.** 2003. Signals in hepatitis A virus P3 region proteins recognized by the ubiquitin-mediated proteolytic system. Virology **309:**306-319.

105. **Lu, L. L., M. Puri, C. M. Horvath, and G. C. Sen.** 2008. Select paramyxoviral V proteins inhibit IRF3 activation by acting as alternative substrates for inhibitor of kappaB kinase epsilon (IKKe)/TBK1. J Biol Chem **283:**14269-14276.

106. **Lund, J. M., L. Alexopoulou, A. Sato, M. Karow, N. C. Adams, N. W. Gale, A. Iwasaki, and R. A. Flavell.** 2004. Recognition of single-stranded RNA viruses by Toll-like receptor 7. Proc Natl Acad Sci U S A **101:**5598-5603.

107. **Martin, A., D. Benichou, S. F. Chao, L. M. Cohen, and S. M. Lemon.** 1999. Maturation of the hepatitis A virus capsid protein VP1 is not dependent on processing by the 3Cpro proteinase. J Virol **73:**6220-6227.

108. **Martin, A., and S. M. Lemon.** 2006. Hepatitis A virus: from discovery to vaccines. Hepatology **43:**S164-172.

109. **Marvil, P., N. J. Knowles, A. P. Mockett, P. Britton, T. D. Brown, and D. Cavanagh.** 1999. Avian encephalomyelitis virus is a picornavirus and is most closely related to hepatitis A virus. J Gen Virol **80 (Pt 3):**653-662.

110. **Matsumoto, M., K. Funami, M. Tanabe, H. Oshiumi, M. Shingai, Y. Seto, A. Yamamoto, and T. Seya.** 2003. Subcellular localization of Toll-like receptor 3 in human dendritic cells. J Immunol **171:**3154-3162.

111. **McCartney, S. A., L. B. Thackray, L. Gitlin, S. Gilfillan, H. W. Virgin, and M. Colonna.** 2008. MDA-5 recognition of a murine norovirus. PLoS Pathog **4:**e1000108.

112. **Medzhitov, R., and C. A. Janeway, Jr.** 2002. Decoding the patterns of self and nonself by the innate immune system. Science **296:**298-300.

113. **Medzhitov, R., P. Preston-Hurlburt, and C. A. Janeway, Jr.** 1997. A human homologue of the Drosophila Toll protein signals activation of adaptive immunity. Nature **388:**394-397.

114. **Meylan, E., K. Burns, K. Hofmann, V. Blancheteau, F. Martinon, M. Kelliher, and J. Tschopp.** 2004. RIP1 is an essential mediator of Toll-like receptor 3-induced NF-kappa B activation. Nat Immunol **5:**503-507.

115. **Meylan, E., J. Curran, K. Hofmann, D. Moradpour, M. Binder, R. Bartenschlager, and J. Tschopp.** 2005. Cardif is an adaptor protein in the RIG-I antiviral pathway and is targeted by hepatitis C virus. Nature **437:**1167-1172.

116. **Meylan, E., and J. Tschopp.** 2005. The RIP kinases: crucial integrators of cellular stress. Trends Biochem Sci **30:**151-159.

117. **Meylan, E., and J. Tschopp.** 2006. Toll-like receptors and RNA helicases: two parallel ways to trigger antiviral responses. Mol Cell **22:**561-569.

118. **Meylan, E., J. Tschopp, and M. Karin.** 2006. Intracellular pattern recognition receptors in the host response. Nature **442:**39-44.

119. **Miller, D. J., M. D. Schwartz, and P. Ahlquist.** 2001. Flock house virus RNA replicates on outer mitochondrial membranes in Drosophila cells. J Virol **75:**11664-11676.

120. **Misaghi, S., G. A. Korbel, B. Kessler, E. Spooner, and H. L. Ploegh.** 2006. z-VAD-fmk inhibits peptide:N-glycanase and may result in ER stress. Cell Death Differ **13:**163-165.

121. **Muzio, M., G. Natoli, S. Saccani, M. Levrero, and A. Mantovani.** 1998. The human toll signaling pathway: divergence of nuclear factor kappaB and JNK/SAPK activation upstream of tumor necrosis factor receptor-associated factor 6 (TRAF6). J Exp Med **187:**2097-2101.

122. **Muzio, M., J. Ni, P. Feng, and V. M. Dixit.** 1997. IRAK (Pelle) family member IRAK-2 and MyD88 as proximal mediators of IL-1 signaling. Science **278:**1612-1615.

123. **O'Neill, L. A., and A. G. Bowie.** 2007. The family of five: TIR-domain-containing adaptors in Toll-like receptor signalling. Nat Rev Immunol **7:**353-364.

124. **O'Neill, L. A., K. A. Fitzgerald, and A. G. Bowie.** 2003. The Toll-IL-1 receptor adaptor family grows to five members. Trends Immunol **24:**286-290.

125. **Oganesyan, G., S. K. Saha, B. Guo, J. Q. He, A. Shahangian, B. Zarnegar, A. Perry, and G. Cheng.** 2006. Critical role of TRAF3 in the Toll-like receptor-dependent and -independent antiviral response. Nature **439:**208-211.

126. **Okahira, S., F. Nishikawa, S. Nishikawa, T. Akazawa, T. Seya, and M. Matsumoto.** 2005. Interferon-beta induction through toll-like receptor 3 depends on double-stranded RNA structure. DNA Cell Biol **24:**614-623.

127. **Oshiumi, H., M. Matsumoto, K. Funami, T. Akazawa, and T. Seya.** 2003. TICAM-1, an adaptor molecule that participates in Toll-like receptor 3-mediated interferon-beta induction. Nat Immunol **4:**161-167.

128. **Parsley, T. B., C. T. Cornell, and B. L. Semler.** 1999. Modulation of the RNA binding and protein processing activities of poliovirus polypeptide 3CD by the viral RNA polymerase domain. J Biol Chem **274:**12867-12876.

129. **Pathak, H. B., H. S. Oh, I. G. Goodfellow, J. J. Arnold, and C. E. Cameron.** 2008. Picornavirus genome replication: roles of precursor proteins and rate-limiting steps in oriI-dependent VPg uridylylation. J Biol Chem **283:**30677-30688.

130. **Pichlmair, A., O. Schulz, C. P. Tan, T. I. Naslund, P. Liljestrom, F. Weber, and C. Reis e Sousa.** 2006. RIG-I-mediated antiviral responses to single-stranded RNA bearing 5'-phosphates. Science **314:**997-1001.

131. **Pisani, G., F. Beneduce, V. Gauss-Muller, and G. Morace.** 1995. Recombinant expression of hepatitis A virus protein 3A: interaction with membranes. Biochem Biophys Res Commun **211:**627-638.

132. **Plumet, S., F. Herschke, J. M. Bourhis, H. Valentin, S. Longhi, and D. Gerlier.** 2007. Cytosolic 5'-triphosphate ended viral leader transcript of measles virus as activator of the RIG I-mediated interferon response. PLoS One **2:**e279.

133. **Poltorak, A., X. He, I. Smirnova, M. Y. Liu, C. Van Huffel, X. Du, D. Birdwell, E. Alejos, M. Silva, C. Galanos, M. Freudenberg, P. Ricciardi-Castagnoli, B. Layton, and B. Beutler.** 1998. Defective LPS signaling in C3H/HeJ and C57BL/10ScCr mice: mutations in Tlr4 gene. Science **282:**2085-2088.

134. **Probst, C., M. Jecht, and V. Gauss-Muller.** 1999. Intrinsic signals for the assembly of hepatitis A virus particles. Role of structural proteins VP4 and 2A. J Biol Chem **274:**4527-4531.

135. **Probst, C., M. Jecht, and V. Gauss-Muller.** 1998. Processing of proteinase precursors and their effect on hepatitis A virus particle formation. J Virol **72:**8013-8020.

136. **Racanelli, V., and B. Rehermann.** 2003. Hepatitis C virus infection: when silence is deception. Trends Immunol **24:**456-464.

137. **Rakela, J., and H. E. Vargas.** 2002. Hepatitis C: magnitude of the problem. Liver Transpl **8:**S3-6.

138. **Ramaswamy, M., L. Shi, M. M. Monick, G. W. Hunninghake, and D. C. Look.** 2004. Specific inhibition of type I interferon signal transduction by respiratory syncytial virus. Am J Respir Cell Mol Biol **30:**893-900.

139. **Ramaswamy, M., L. Shi, S. M. Varga, S. Barik, M. A. Behlke, and D. C. Look.** 2006. Respiratory syncytial virus nonstructural protein 2 specifically inhibits type I interferon signal transduction. Virology **344:**328-339.

140. **Ray Kim, W.** 2002. Global epidemiology and burden of hepatitis C. Microbes Infect **4:**1219-1225.

141. **Rebsamen, M., E. Meylan, J. Curran, and J. Tschopp.** 2008. The antiviral adaptor proteins Cardif and Trif are processed and inactivated by caspases. Cell Death Differ **15:**1804-1811.

142. **Reshetnyak, V. I., T. I. Karlovich, and L. U. Ilchenko.** 2008. Hepatitis G virus. World J Gastroenterol **14:**4725-4734.

143. **Rock, F. L., G. Hardiman, J. C. Timans, R. A. Kastelein, and J. F. Bazan.** 1998. A family of human receptors structurally related to Drosophila Toll. Proc Natl Acad Sci U S A **95:**588-593.

144. **Rowe, D. C., A. F. McGettrick, E. Latz, B. G. Monks, N. J. Gay, M. Yamamoto, S. Akira, L. A. O'Neill, K. A. Fitzgerald, and D. T. Golenbock.** 2006. The myristoylation of TRIF-related adaptor molecule is essential for Toll-like receptor 4 signal transduction. Proc Natl Acad Sci U S A **103:**6299-6304.

145. **Rust, R. C., L. Landmann, R. Gosert, B. L. Tang, W. Hong, H. P. Hauri, D. Egger, and K. Bienz.** 2001. Cellular COPII proteins are involved in production of the vesicles that form the poliovirus replication complex. J Virol **75:**9808-9818.

146. **Saito, T., and M. Gale, Jr.** 2008. Differential recognition of double-stranded RNA by RIG-I-like receptors in antiviral immunity. J Exp Med **205:**1523-1527.

147. **Saito, T., R. Hirai, Y. M. Loo, D. Owen, C. L. Johnson, S. C. Sinha, S. Akira, T. Fujita, and M. Gale, Jr.** 2007. Regulation of innate antiviral defenses through a shared repressor domain in RIG-I and LGP2. Proc Natl Acad Sci U S A **104:**582-587.

148. **Saito, T., D. M. Owen, F. Jiang, J. Marcotrigiano, and M. Gale, Jr.** 2008. Innate immunity induced by composition-dependent RIG-I recognition of hepatitis C virus RNA. Nature **454:**523-527.

149. **Sasai, M., M. Tatematsu, H. Oshiumi, K. Funami, M. Matsumoto, S. Hatakeyama, and T. Seya.** 2010. Direct binding of TRAF2 and TRAF6 to TICAM-1/TRIF adaptor participates in activation of the Toll-like receptor 3/4 pathway. Mol Immunol **47:**1283-1291.

150. **Sato, S., M. Sugiyama, M. Yamamoto, Y. Watanabe, T. Kawai, K. Takeda, and S. Akira.** 2003. Toll/IL-1 receptor domain-containing adaptor inducing IFN-beta (TRIF) associates with TNF receptor-associated factor 6 and TANK-binding kinase 1, and activates two distinct transcription factors, NF-kappa B and IFN-regulatory factor-3, in the Toll-like receptor signaling. J Immunol **171:**4304-4310.

151. **Satoh, T., H. Kato, Y. Kumagai, M. Yoneyama, S. Sato, K. Matsushita, T. Tsujimura, T. Fujita, S. Akira, and O. Takeuchi.** 2010. LGP2 is a positive regulator of RIG-I- and MDA5-mediated antiviral responses. Proc Natl Acad Sci U S A **107:**1512-1517.

152. **Schaffner, F., J. L. Dienstag, R. H. Purcell, and H. Popper.** 1977. Chimpanzee livers after infection with human hepatitis viruses A and B: Ultrastructural studies. Arch Pathol Lab Med **101:**113-117.

153. **Schultheiss, T., Y. Y. Kusov, and V. Gauss-Muller.** 1994. Proteinase 3C of hepatitis A virus (HAV) cleaves the HAV polyprotein P2-P3 at all sites including VP1/2A and 2A/2B. Virology **198:**275-281.

154. **Schwandner, R., R. Dziarski, H. Wesche, M. Rothe, and C. J. Kirschning.** 1999. Peptidoglycan- and lipoteichoic acid-induced cell activation is mediated by toll-like receptor 2. J Biol Chem **274:**17406-17409.

155. **Seipelt, J., A. Guarne, E. Bergmann, M. James, W. Sommergruber, I. Fita, and T. Skern.** 1999. The structures of picornaviral proteinases. Virus Res **62:**159-168.

156. **Seth, R. B., L. Sun, C. K. Ea, and Z. J. Chen.** 2005. Identification and characterization of MAVS, a mitochondrial antiviral signaling protein that activates NF-kappaB and IRF 3. Cell **122:**669-682.

157. **Shoukry, N. H., A. Grakoui, M. Houghton, D. Y. Chien, J. Ghrayeb, K. A. Reimann, and C. M. Walker.** 2003. Memory CD8+ T cells are required for protection from persistent hepatitis C virus infection. J Exp Med **197:**1645-1655.

158. **Silberstein, E., K. Konduru, and G. G. Kaplan.** 2009. The interaction of hepatitis A virus (HAV) with soluble forms of its cellular receptor 1 (HAVCR1) share the physiological requirements of infectivity in cell culture. Virol J **6:**175.

159. **Spann, K. M., K. C. Tran, B. Chi, R. L. Rabin, and P. L. Collins.** 2004. Suppression of the induction of alpha, beta, and lambda interferons by the NS1 and NS2 proteins of human respiratory syncytial virus in human epithelial cells and macrophages [corrected]. J Virol **78:**4363-4369.

160. **Stack, J., I. R. Haga, M. Schroder, N. W. Bartlett, G. Maloney, P. C. Reading, K. A. Fitzgerald, G. L. Smith, and A. G. Bowie.** 2005. Vaccinia virus

protein A46R targets multiple Toll-like-interleukin-1 receptor adaptors and contributes to virulence. J Exp Med **201:**1007-1018.

161. **Suhy, D. A., T. H. Giddings, Jr., and K. Kirkegaard.** 2000. Remodeling the endoplasmic reticulum by poliovirus infection and by individual viral proteins: an autophagy-like origin for virus-induced vesicles. J Virol **74:**8953-8965.

162. **Sui, L., W. Zhang, Y. Chen, Y. Zheng, T. Wan, Y. Yang, G. Fang, J. Mao, and X. Cao.** 2006. Human membrane protein Tim-3 facilitates hepatitis A virus entry into target cells. Int J Mol Med **17:**1093-1099.

163. **Sumpter, R., Jr., Y. M. Loo, E. Foy, K. Li, M. Yoneyama, T. Fujita, S. M. Lemon, and M. Gale, Jr.** 2005. Regulating intracellular antiviral defense and permissiveness to hepatitis C virus RNA replication through a cellular RNA helicase, RIG-I. J Virol **79:**2689-2699.

164. **Sun, X., J. Lee, T. Navas, D. T. Baldwin, T. A. Stewart, and V. M. Dixit.** 1999. RIP3, a novel apoptosis-inducing kinase. J Biol Chem **274:**16871-16875.

165. **Tabeta, K., P. Georgel, E. Janssen, X. Du, K. Hoebe, K. Crozat, S. Mudd, L. Shamel, S. Sovath, J. Goode, L. Alexopoulou, R. A. Flavell, and B. Beutler.** 2004. Toll-like receptors 9 and 3 as essential components of innate immune defense against mouse cytomegalovirus infection. Proc Natl Acad Sci U S A **101:**3516-3521.

166. **Takeuchi, O., and S. Akira.** 2008. MDA5/RIG-I and virus recognition. Curr Opin Immunol **20:**17-22.

167. **Takeuchi, O., and S. Akira.** 2002. MyD88 as a bottle neck in Toll/IL-1 signaling. Curr Top Microbiol Immunol **270:**155-167.

168. **Takeuchi, O., K. Hoshino, T. Kawai, H. Sanjo, H. Takada, T. Ogawa, K. Takeda, and S. Akira.** 1999. Differential roles of TLR2 and TLR4 in recognition

of gram-negative and gram-positive bacterial cell wall components. Immunity **11:**443-451.

169. **Takeuchi, O., T. Kawai, P. F. Muhlradt, M. Morr, J. D. Radolf, A. Zychlinsky, K. Takeda, and S. Akira.** 2001. Discrimination of bacterial lipoproteins by Toll-like receptor 6. Int Immunol **13:**933-940.

170. **Takeuchi, O., T. Kawai, H. Sanjo, N. G. Copeland, D. J. Gilbert, N. A. Jenkins, K. Takeda, and S. Akira.** 1999. TLR6: A novel member of an expanding toll-like receptor family. Gene **231:**59-65.

171. **Takeuchi, O., S. Sato, T. Horiuchi, K. Hoshino, K. Takeda, Z. Dong, R. L. Modlin, and S. Akira.** 2002. Cutting edge: role of Toll-like receptor 1 in mediating immune response to microbial lipoproteins. J Immunol **169:**10-14.

172. **Tami, C., E. Silberstein, M. Manangeeswaran, G. J. Freeman, S. E. Umetsu, R. H. DeKruyff, D. T. Umetsu, and G. G. Kaplan.** 2007. Immunoglobulin A (IgA) is a natural ligand of hepatitis A virus cellular receptor 1 (HAVCR1), and the association of IgA with HAVCR1 enhances virus-receptor interactions. J Virol **81:**3437-3446.

173. **Tesar, M., I. Pak, X. Y. Jia, O. C. Richards, D. F. Summers, and E. Ehrenfeld.** 1994. Expression of hepatitis A virus precursor protein P3 in vivo and in vitro: polyprotein processing of the 3CD cleavage site. Virology **198:**524-533.

174. **Teterina, N. L., K. Bienz, D. Egger, A. E. Gorbalenya, and E. Ehrenfeld.** 1997. Induction of intracellular membrane rearrangements by HAV proteins 2C and 2BC. Virology **237:**66-77.

175. **Thompson, P., J. Lu, and G. G. Kaplan.** 1998. The Cys-rich region of hepatitis A virus cellular receptor 1 is required for binding of hepatitis A virus and protective monoclonal antibody 190/4. J Virol **72:**3751-3761.

176. **Venkataraman, T., M. Valdes, R. Elsby, S. Kakuta, G. Caceres, S. Saijo, Y. Iwakura, and G. N. Barber.** 2007. Loss of DExD/H box RNA helicase LGP2 manifests disparate antiviral responses. J Immunol **178:**6444-6455.

177. **Wajant, H., F. Henkler, and P. Scheurich.** 2001. The TNF-receptor-associated factor family: scaffold molecules for cytokine receptors, kinases and their regulators. Cell Signal **13:**389-400.

178. **Walsh, D. E., C. M. Greene, T. P. Carroll, C. C. Taggart, P. M. Gallagher, S. J. O'Neill, and N. G. McElvaney.** 2001. Interleukin-8 up-regulation by neutrophil elastase is mediated by MyD88/IRAK/TRAF-6 in human bronchial epithelium. J Biol Chem **276:**35494-35499.

179. **Wang, N., Y. Liang, S. Devaraj, J. Wang, S. M. Lemon, and K. Li.** 2009. Toll-like receptor 3 mediates establishment of an antiviral state against hepatitis C virus in hepatoma cells. J Virol **83:**9824-9834.

180. **Weitz, M., B. M. Baroudy, W. L. Maloy, J. R. Ticehurst, and R. H. Purcell.** 1986. Detection of a genome-linked protein (VPg) of hepatitis A virus and its comparison with other picornaviral VPgs. J Virol **60:**124-130.

181. **Wessels, E., D. Duijsings, K. H. Lanke, S. H. van Dooren, C. L. Jackson, W. J. Melchers, and F. J. van Kuppeveld.** 2006. Effects of picornavirus 3A Proteins on Protein Transport and GBF1-dependent COP-I recruitment. J Virol **80:**11852-11860.

182. **Wieland, S. F., and F. V. Chisari.** 2005. Stealth and cunning: hepatitis B and hepatitis C viruses. J Virol **79:**9369-9380.

183. **Xiang, W., A. Cuconati, A. V. Paul, X. Cao, and E. Wimmer.** 1995. Molecular dissection of the multifunctional poliovirus RNA-binding protein 3AB. RNA **1:**892-904.

184. **Xu, L. G., Y. Y. Wang, K. J. Han, L. Y. Li, Z. Zhai, and H. B. Shu.** 2005. VISA is an adapter protein required for virus-triggered IFN-beta signaling. Mol Cell **19:**727-740.

185. **Xu, Y., X. Tao, B. Shen, T. Horng, R. Medzhitov, J. L. Manley, and L. Tong.** 2000. Structural basis for signal transduction by the Toll/interleukin-1 receptor domains. Nature **408:**111-115.

186. **Yamamoto, M., S. Sato, H. Hemmi, K. Hoshino, T. Kaisho, H. Sanjo, O. Takeuchi, M. Sugiyama, M. Okabe, K. Takeda, and S. Akira.** 2003. Role of adaptor TRIF in the MyD88-independent toll-like receptor signaling pathway. Science **301:**640-643.

187. **Yamamoto, M., S. Sato, H. Hemmi, H. Sanjo, S. Uematsu, T. Kaisho, K. Hoshino, O. Takeuchi, M. Kobayashi, T. Fujita, K. Takeda, and S. Akira.** 2002. Essential role for TIRAP in activation of the signalling cascade shared by TLR2 and TLR4. Nature **420:**324-329.

188. **Yamamoto, M., S. Sato, H. Hemmi, S. Uematsu, K. Hoshino, T. Kaisho, O. Takeuchi, K. Takeda, and S. Akira.** 2003. TRAM is specifically involved in the Toll-like receptor 4-mediated MyD88-independent signaling pathway. Nat Immunol **4:**1144-1150.

189. **Yamamoto, M., S. Sato, K. Mori, K. Hoshino, O. Takeuchi, K. Takeda, and S. Akira.** 2002. Cutting edge: a novel Toll/IL-1 receptor domain-containing adapter that preferentially activates the IFN-beta promoter in the Toll-like receptor signaling. J Immunol **169:**6668-6672.

190. **Yang, Y., Y. Liang, L. Qu, Z. Chen, M. Yi, K. Li, and S. M. Lemon.** 2007. Disruption of innate immunity due to mitochondrial targeting of a picornaviral protease precursor. Proc Natl Acad Sci U S A **104:**7253-7258.

191. **Yi, M., F. Bodola, and S. M. Lemon.** 2002. Subgenomic hepatitis C virus replicons inducing expression of a secreted enzymatic reporter protein. Virology **304:**197-210.

192. **Yi, M., and S. M. Lemon.** 2002. Replication of subgenomic hepatitis A virus RNAs expressing firefly luciferase is enhanced by mutations associated with adaptation of virus to growth in cultured cells. J Virol **76:**1171-1180.

193. **Yoneyama, M., M. Kikuchi, K. Matsumoto, T. Imaizumi, M. Miyagishi, K. Taira, E. Foy, Y. M. Loo, M. Gale, Jr., S. Akira, S. Yonehara, A. Kato, and T. Fujita.** 2005. Shared and unique functions of the DExD/H-box helicases RIG-I, MDA5, and LGP2 in antiviral innate immunity. J Immunol **175:**2851-2858.

194. **Yoneyama, M., M. Kikuchi, T. Natsukawa, N. Shinobu, T. Imaizumi, M. Miyagishi, K. Taira, S. Akira, and T. Fujita.** 2004. The RNA helicase RIG-I has an essential function in double-stranded RNA-induced innate antiviral responses. Nat Immunol **5:**730-737.

195. **Yoshimura, A., E. Lien, R. R. Ingalls, E. Tuomanen, R. Dziarski, and D. Golenbock.** 1999. Cutting edge: recognition of Gram-positive bacterial cell wall components by the innate immune system occurs via Toll-like receptor 2. J Immunol **163:**1-5.

196. **Ypma-Wong, M. F., P. G. Dewalt, V. H. Johnson, J. G. Lamb, and B. L. Semler.** 1988. Protein 3CD is the major poliovirus proteinase responsible for cleavage of the P1 capsid precursor. Virology **166:**265-270.

197. **Zeng, W., L. Sun, X. Jiang, X. Chen, F. Hou, A. Adhikari, M. Xu, and Z. J. Chen.** 2010. Reconstitution of the RIG-I pathway reveals a signaling role of unanchored polyubiquitin chains in innate immunity. Cell **141:**315-330.

198. **Zhang, H., S. F. Chao, L. H. Ping, K. Grace, B. Clarke, and S. M. Lemon.** 1995. An infectious cDNA clone of a cytopathic hepatitis A virus: genomic regions associated with rapid replication and cytopathic effect. Virology **212:**686-697.

199. **Zheng, D., G. Chen, B. Guo, G. Cheng, and H. Tang.** 2008. PLP2, a potent deubiquitinase from murine hepatitis virus, strongly inhibits cellular type I interferon production. Cell Res **18:**1105-1113.

Vita

Permanent address:

Lin Qu

7950 N. Stadium Dr, Apt 222

Houston, TX 77030

Phone: 617-794-2938

E-mail: liqu@utmb.edu

Education:

M.A. in Molecular Microbiology, 1999, Washington University, St. Louis, MO

M.S. in Biochemistry, 1996, Peking University, Beijing, China

B.S. in Biochemistry, 1993, Nankai University, Tianjin, China

Experience:

8/05-8/10, University of Texas Medical Branch, Galveston, TX

Ph.D. Graduate Student, Lab of Prof. Stanley M. Lemon

Ph.D. Dissertation: Evasion of RIG-I/MDA5 and TLR3-Mediated Innate Immunity by Hepatitis A Virus.

12/00-8/05, Idenix Pharmaceuticals, Boston, MA

Research Associate

Worked on discovery and development of HCV antiviral drugs.

10/00-12/00, Anadys Pharmaceuticals, Waltham, MA

Research Associate

Participated in development and implementation of HCV replicon system.

8/96-9/00, Washington University, St. Louis, MO

M.A. Graduate Student, Lab of Prof. Charles M. Rice

M.A. Thesis: Isolation and Characterization of Noncytopathic Mutants of Bovine Viral Diarrhea Virus (BVDV) Strain NADL Reveal A Role for NS4B in Viral Cytopathogenicity.

8/93-7/96, Peking University, Beijing, China

M.S. Graduate Student, Lab of Zhangliang Chen

M.S. Thesis: Cloning and Expression in *E. coli* of Rice Dwarf Virus (RDV) Genome Segments.

Publications:

Chen Z, Rijnbrand R, Jangra RK, Devaraj SG, **Qu L**, Ma Y, Lemon SM, Li K. (2007) Ubiquitination and proteasomal degradation of interferon regulatory factor-3 induced by Npro from a cytopathic bovine viral diarrhea virus. **Virology** 366:277-292

Yang Y*, Liang Y*, **Qu L***, Chen Z, Yi M, Li K, Lemon SM. (2007) Disruption of innate immunity due to mitochondrial targeting of a picornaviral protease precursor. **Proc Natl Acad Sci USA** 104:7253-7258 * Equal contributing authors.

Agapov EV, Murray CL, Frolov I, **Qu L**, Myers TM, Rice CM. (2004) Uncleaved NS2-NS3 is required for production of infectious bovine viral diarrhea virus. **Journal of Virology** 78:2414-2425

Qu L, McMullan LK, Rice CM. (2001) Isolation and characterization of noncytopathic pestivirus mutants reveals a role for nonstructural protein NS4B in viral cytopathogenicity. **Journal of Virology** 75:10651-10662

Xu H, Li Y, Mao Z, Li Y, Wu Z, **Qu L**, An C, Ming X, Schiemann J, Casper R, Chen Z. (1998) Rice dwarf phytoreovirus segment S11 encodes a nucleic acid binding protein. **Virology** 240:267-272

Qu L, Li Y, Quan S, Ding S, Suzuki N, Chen Z. (1996) Nucleotide sequence analysis and expression in *E. coli* of rice dwarf virus genome segment S7. **Acta Microbiologica Sinica** 36:335-343 (in Chinese)

Qu L, Li Y, Zhu Y, Chen Z. (1995) cDNA cloning and sequence analysis of rice dwarf virus genome segment S9. **Chinese Journal of Virology** 11:271-275 (in Chinese)

Presentation:

Qu L, Feng Z, Liang Y, Wang N, Li K, Lemon SM. (2009) Inhibition of TLR3 antiviral signaling by hepatitis A virus. **AASLD Basic Research Single Topic Conference**. Atlanta, GA.

Qu L, Liang Y, Yang Y, Yi M, Li K, Lemon SM. (2007) Cleavage of MAVS by mitochondrial targeting of a hepatitis A virus (HAV) protease precursor. **The 8th International Symposium on Positive-Strand RNA Viruses.** Washington, DC.

Bichko V, Tausek M, **Qu L**, La Colla M, Pierra C, Storer R, Gosselin G, Sommadossi J-P, Standring DN. (2004) Enhanced antiviral activity of NM107 in combination with interferon alfa. **The 11th International Symposium on HCV and Related Viruses**. Heidelberg, Germany.

Standring DN, Lanford R, Wright T, Chung RT, Bichko V, Cretton-Scott E, Pan-Zhou X, Bergelson S, **Qu L**, Tausek M, Bridges E, Moussa A, Storer R, Pierra C, Benzaria S, Gosselin G, La Colla P, Sommadossi J-P. (2003) NM283 has potent antiviral activity against chronic hepatitis C virus genotype 1 infection in the chimpanzee. **The 11th Triennial Symposium on Viral Hepatitis and Liver Disease.** Sydney, Australia.

Qu L, Rice CM. (2000) Isolation and characterization of noncytopathic mutants of bovine viral diarrhea virus reveal a role for NS4B in viral cytopathogenicity. **American Society for Virology 19th Annual Meeting**. Ft. Collins, CO.

Patent:

Sommadossi J-P, Standring DN, Bichko V, **Qu L.** (2002) Flaviviridae Mutation Caused by 2'-Branched Nucleosides. U.S. Provisional Patent Application Serial No. 60/426,675.

This dissertation was typed by Lin Qu.